

WATER
WATER
WATER
WATER
WATER
WATER
WATER
WATER
WATER
WATER
WATER
WATER

PROJECT COMPLETION
REPORT NO. 401-X

Electromagnetic
Pulse Sounding
For Surveying
Underground Water

By

R. Caldecott
D. A. Irons, Jr.
D. L. Moffatt
L. Peters, Jr.
R. J. Puskar
J. F. Toth
J. D. Young

United States Department
of the Interior

CONTRACT NO.
B-028-OHIO
14-01-0001-3629



**ELECTROMAGNETIC PULSE SOUNDING
FOR SURVEYING UNDERGROUND WATER**

**R. Caldecott
D. A. Irons, Jr.
D. L. Moffatt
L. Peters, Jr.
R. J. Puskar
J. F. Toth
J. D. Young**

**The Ohio State University ElectroScience Laboratory
Department of Electrical Engineering
Columbus, Ohio**

**This project supported in part by the
Office of Water Resources Research
U. S. Department of the Interior
Washington, D. C.**

Project B-028-OHIO

October, 1972

ABSTRACT

A number of approaches have been explored for measuring the water content of soil electrically. In contrast with traditional measurements, which utilize electric currents at DC or at specific frequencies, our techniques have been based on the transmission and reflection of sharp, regularly repeated pulses. Such pulse measurements can be shown to be equivalent to measuring the electrical properties at all frequencies in a very wide band, and therefore the possibility of extracting the desired information is much greater than with single-frequency measurements.

Because the information content of the signal is great, data processing can be used to extract those features which relate most directly to moisture content and reject those which appear to depend more on soil inhomogenieties. For example, it was found that the attenuation in the frequency band of approximately 10 to 20 MHz had a much higher correlation with soil moisture than that in other frequency bands for the actual field conditions under which our measurements were made.

This information content increase is obtained by means of sophisticated research equipment. The measurements reported herein were made and processed under real-time computer control. They include the signal scattered from known buried targets, transmission measurements through the ground, and the measurement of reflections in a coaxial test cell, all with pulses containing very wide frequency bands. The results are encouraging in that definite correlations with moisture were found. Unfortunately the one-year time limitation of this effort, much of it spent in instrumentation development, was insufficient to allow testing these correlations quantitatively over extended time periods or in a variety of locations. Thus the techniques must be evaluated at present as promising, but not fully proven.

It should be noted that, while the research system to obtain this information is complex, field equipment based on these techniques need not be unduly complicated or expensive. Once the features relating to moisture content under the greatest variety of field conditions are identified, means for extracting this information more simply should be devised. This is proposed as the objective for continuation of this effort.

CONTENTS

	Page
SUMMARY	1
INTRODUCTION	3
1. <u>The Measuring System</u>	4
2. <u>Data Processing</u>	6
3. <u>Underground Moisture Content Monitoring by Measurement of Buried Target Signatures</u>	7
4. <u>Sampled Moisture Conditions</u>	19
5. <u>Underground Propagation Experiment</u>	20
6. <u>Reflection Measurements on Soil Samples in a Vertical Coaxial Test Cell</u>	34
7. <u>Propagation Calculations</u>	48
CONCLUSIONS	56
RECOMMENDATIONS	58
REFERENCES	59
APPENDIX I - TRANSMISSION MEASUREMENTS USING A BURIED ANTENNA	60

SUMMARY

From the beginning of this program it was known that the electrical properties of soils depend strongly, but not at all simply, on moisture content. It has been customary to measure the ground conductivity at DC and low frequencies in order to predict radio propagation phenomena, and maps constructed from such measurements show some correlation with mean annual rainfall contours. Also the electrical properties of some "typical" soil samples (e.g., "sand", "beach sand", "clay") have been measured in the laboratory and shown to depend on moisture content. Despite this known interrelationship of electrical properties and moisture content, no instrument is presently available for measuring the moisture content of soils in the field electrically. The reason is that many other factors also affect the electrical behavior of soil, such as its mechanical condition, physical structure, and chemical constituents. For example, the low-frequency conductivity is known to depend not only on the moisture content, but also strongly on the presence of soluble salts which combine with the moisture to form an electrolyte (ionized conducting medium), and on the porosity which allows electrolyte retention. At higher frequencies, which produce waves of smaller length in the ground, inhomogenities which have dimensions of the order of the wavelength also produce pronounced effects. It is clearly not possible to extract the parameter of interest, soil moisture, from these complicated interactions by a single-frequency measurement. More information is needed.

This effort addressed itself to the task of demonstrating that this information can be obtained by using not single frequencies, but repetitive pulses which are equivalent to a very wide band of frequencies transmitted simultaneously. This method yields a vastly greater amount of information, which can then be processed to extract the desired features. The present effort has been successful in demonstrating that suitably processed data correlate much more closely with moisture content variations under field conditions than either unprocessed data or single-frequency measurements. However, since much of the one-year period had to be devoted to developing the needed instrumentation, measurements had to be restricted to a single site, a few months, and two basic measurement approaches. While it was possible to demonstrate the validity of the pulse approach qualitatively within the time and funding scope of this effort, direct quantitative readout, optimization of the approaches, and design of a field-usable instrument are tasks yet to be accomplished.

One of the two basic measurement techniques employed consisted of illuminating a long, thin metallic cylinder buried in the ground with pulses radiated from the surface. The frequencies at which a cylinder of given dimensions reradiates maximum signal toward the surface (called the resonant frequencies) can be shown to depend on the electrical properties of the ground, and hence on the ground

moisture. The difficulty with this method is that the cylinder-scattered signal is attenuated (reduced) in the two-way passage through the ground and can be masked easily by scattering from inhomogenities of the surface and in the ground. In fact, with the unprocessed data it is not at all easy to see the effect of the cylinders. However, it was found that when the data is suitably processed, waveforms which appear characteristic of the cylinders can be obtained. The processing consists of first isolating the time period corresponding to the depth from which the cylinder reradiated, then selecting from this signal the frequency band in which the resonances are known to occur, and finally reconstituting the signal as a time-varying function. This is a good illustration of the superiority of the pulse approach compared to DC or single-frequency measurements which do not allow this sort of processing.

The second basic measurement consisted of measuring the attenuation (reduction) of pulsed signals transmitted between a buried antenna and antennas located on the ground. The pulsed signals were processed by resolving them into their frequency components, and comparison of these components between antenna pairs allowed the elimination of effects of the antennas themselves. The interesting result was that the attenuation curves obtained in this manner not only correlated well with moisture trends but were sufficiently sensitive to obtain a measure of the moisture content for certain frequency ranges which can be selected out of the total frequencies available in the pulses.

The same antenna installation also allowed the measurement of the impedance of the antenna (the ratio of the voltage to the current at its terminals), which also depends on the ground constants. However, no simple correlation between the measured impedances and moisture was obtained.

In addition to these two field-measurement approaches, a laboratory technique was instrumented for measuring the electrical characteristics of soil samples. It consists of a coaxial transmission line (two coaxial cylinders between which energy is allowed to propagate) and is similar in geometry to devices used with single-frequency measurements, but the source of energy consisted of pulses, just as in the field measurements. The satisfactory operation of the device was verified, but time did not allow the quantitative evaluation of more than a few soil samples.

INTRODUCTION

The objectives of this program have been twofold: to adapt and further develop existing electromagnetic pulse techniques for the measurement of underground water, and to evaluate the resulting system, using buried targets, as a potential tool for surveying underground water.

Pulse, or time domain, techniques have a number of distinct advantages over methods employing one or more discrete radio frequencies. Most important is the fact that it is possible to obtain range information by observing the transit time of the pulse when it is transmitted from an antenna, reflected off some object or ground feature, and received by the same or another antenna. Alternatively, when the reflection is from an object at known range, this same measurement may be used to obtain information about the propagation velocity and hence indirectly the water content of the intervening medium. The second major advantage of the time domain technique is that the pulse spectrum contains a wide range of frequencies. Thus, in a single measurement, it provides information which would require a considerable number of discrete frequency measurements. The spectrum is limited at the upper end by the rise time of the pulse generator or, more usually, by the attenuation rate of the ground, which increases with frequency. The low frequency limit of the spectrum is determined by the repetition rate of the pulse generated. In theory this may be made indefinitely low. However, since it is usually necessary to average a number of pulses in order to minimise the effects of stray noise in the measuring system, there is a practical limit if the measurement time is not to become prohibitively long.

On completion of the system development phase of this program three types of experiment were performed. One of these was the measurement of the reflection characteristics of a number of targets of known size and shape buried at known depths. The original intention was to use metal spheres as the targets. However, cylinders were used in practice because firstly they are simpler to fabricate, and secondly they have two characteristic dimensions: length and diameter, with potentially identifiable resonance characteristics. At the same time that the cylinders were buried a long dipole antenna was also buried. This formed the basis for a companion experiment. The long dipole antenna experiment provided the most successful correlation of the measured curves with moisture content trends. Wires from the center of this dipole were brought up to the surface. It was thus possible to measure the impedance of this buried antenna under changing ground conditions and also to make transmission measurements between it and a similar antenna on the surface. The third experiment was devised late in the program to provide more controlled moisture conditions than it was possible to obtain outside under natural conditions. It employed a coaxial transmission line, mounted vertically and short circuited at the lower end, which could be filled with various types of soil. Water could be added in various amounts and reflection measurements performed from the upper end of the line.

The measuring and data processing system and the three experiments performed with it are described in the following pages.

1. The Measuring System

The system is shown schematically in Fig. 1. The radio frequency portion consists of a pulse generator, a sampling oscilloscope and the antenna system or test cell associated with the particular experiment being performed. Two modes of operation were used. For most of the buried target measurements a pair of antennas was used, arranged orthogonally to minimize direct coupling between the antennas. One of these was used to transmit, being connected directly to the pulse generator. The other, the receiver, was connected to the sampling oscilloscope. The same arrangement was used when transmitting from the buried dipole to one on the surface. For some tests, including impedance measurements on the buried dipole and reflection measurements in the coaxial test cell, a single connection to the test system was employed, the pulse generator being connected via a feed through provision in the sampling oscilloscope (inset, Fig. 1). Three different pulse generators were used on occasion having various pulse length, amplitude and repetition rate characteristics. All the pulse generators were free running and a trigger connection was provided for synchronization of the oscilloscope sampling circuits. Actual sweeping of the oscilloscope time base was, however, controlled by computer.

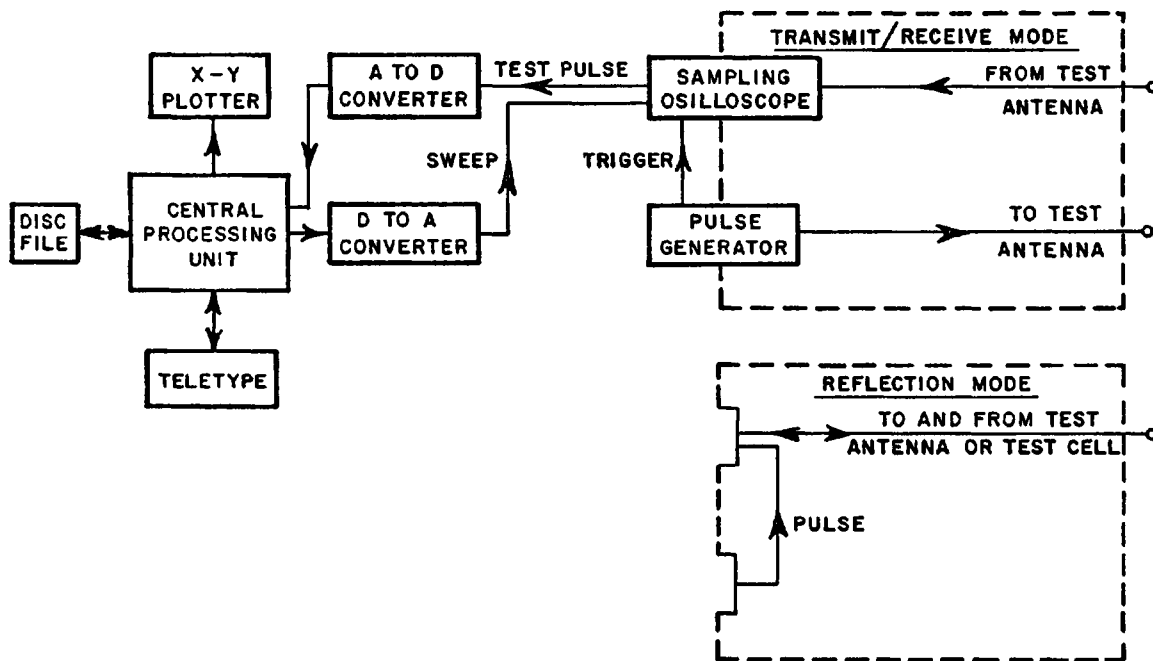


Fig. 1. Computer controlled, time domain, measuring and data processing system.

The computer is in effect the heart of the system. It makes possible the collection, processing, storage and comparison of an amount of data which would otherwise be prohibitively time consuming. Programming has been arranged to provide a high degree of operator interaction thus giving great flexibility to the way in which data are recorded and processed. All operations are performed on command from the teletype and the computer currently recognizes in excess of twenty five separate commands (Fig. 2). Because of the relatively small core size of this computer (4000 words) core swapping has been used to extend the effective program length.

SLOW. Sets slow sweep for Ikor pulser.
FAST. Sets fast sweep for other pulsers.
SWEep. Sweeps 'scope 12 min. or until break. Destroys buffer.
REStore. Recovers calibration and data from previous file.
CALibrate. High and low limits on 'scope are set and recorded
RECORD. Data are recorded from 'scope into program buffer.
WRite. Data are written from buffer onto disc file.
REAd. Reads a file from the disc into core buffer.
DEScription. Prints out the current file description.
WHAt is? Prints a file description without affecting buffer.
PLOt. Plots current contents of buffer.
XSHift. Rotates buffer by specified amount.
YSHift. Moves buffer up or down by specified amount.
GRId. Draws a grid on the plotter.
ADVance. Moves the plotter forward to next page.
REVerse. Moves the plotter back one page.
COMbine. Sums a number of files with individual real multipliers.
USER. Changes the current user name.
FFT. Takes the fast Fourier transform of the core buffer.
IFFt. Takes the inverse Fourier transform of the buffer.
FILter. Bandpass filters a time domain waveform.
GATE. Passes a time domain waveform through a trapezoidal gate.
PRInt. Prints all or part of the core buffer.
LABel. Draws current description and file name on plotter.
SMIth. Draws a Smith chart on the plotter.
RHO. Plots frequency domain data on the Smith chart.
LINE. Replaces part of core buffer with straight line.

Fig. 2. List of commands recognized by the time domain data recording and processing program.

Before recording data a "calibrate" command is first issued and the upper and lower scale limits of the sampling oscilloscope are recorded by the computer. During data recording the oscilloscope time base is swept by the computer in 256 steps, one data point being recorded for each position. In practice the time base is swept any desired number of times, usually either 50 or 200, and the average signal level saved. This greatly reduces background noise level, particularly due to 60 cycles, which is apt to be picked up in ground measurements.

2. Data Processing

Once the data are stored in the computer memory a number of courses of action are possible. It may be plotted directly on the X-Y plotter to provide a permanent paper record, the result being an enlarged, smoothed version of the waveform seen on the sampling oscilloscope; the smoothing results from the averaging performed during the recording process. The data may also be written on the magnetic disc file from which it may be recovered at any time for further processing.

Probably the single most important processing capability is that of taking a fast Fourier transform (FFT) of a time domain waveform. The 256 time domain points are replaced in core by 128 complex harmonic amplitudes. The period of the first harmonic is simply the length of the original time base sweep when the data were recorded. The other harmonics are of course simply integral multiples of this frequency. The program provides for plotting the spectrum represented by the first hundred of these harmonics (the higher harmonics usually contain only noise) on the X-Y plotter, the amplitudes being shown on a decibel scale. This form of presentation makes it possible to see at a glance what characteristic or resonant frequencies are present in the response of the target or medium under test. This procedure may also be used for bandpass filtering of a time domain waveform. In this case only those harmonics within the passband, whose limits are entered via the teletype, are retained, all others being set to zero. An inverse Fourier transform is then performed which results in a new time domain waveform, the result of passing the original waveform through a bandpass filter. This has the advantage of emphasising certain frequency characteristics in the waveform while still retaining most of the range information.

It is sometimes helpful, when measuring reflected signals from a single antenna or test cell, to be able to present the data on a reflection coefficient plane or Smith Chart, where the magnitude of the reflection is proportional to distance from the center of the chart and direction is indicative of phase angle. The data processing procedures include provision for making this sort of presentation on the X-Y plotter using the frequency domain data obtained from a Fourier transformation.

One of the major problems in this type of work is in distinguishing the relatively weak response, from say a buried target, from the frequently stronger responses due to ground anomalies. This was often found to be

the case in the present program when target responses were masked by those from the trenches in which the targets had been buried. As an aid to resolving such problems provision was included for averaging and differencing time domain waveforms. Averaging of waveforms obtained from a number of similar targets helps to smooth out irregularities due to ground surface roughness. Taking a difference between waveforms obtained from a target buried in a trench and a similar empty trench helps to isolate the response due to the target itself.

Another feature of the data processing is the provision for range gating. It often happens that a strong response is obtained by direct coupling or by reflection from the ground surface. If a Fourier transform were performed on this waveform this strong response would tend to mask a weaker target response separated from it in time. By range gating the time domain waveform the large unwanted response may be removed before transforming to the frequency domain.

Provision has thus been included for manipulating data in a variety of ways on command. If during an experiment the operator observes some new feature in the data it is possible for him to examine the characteristics of that feature immediately or to save the data on the disc file for later study.

3. Underground Moisture Content Monitoring by Measurement of Buried Target Signatures

It is known that the time domain scattering signature of an object is dependent not only on the objects geometrical parameters, but also on the constitutive parameters of the medium in which it is immersed. The goal of the experimental effort to be described in this section was to find out if time domain target signature measurements could be used to determine the moisture dependent variations in μ and ϵ (the magnetic permeability and dielectric permittivity) of the ground in the vicinity of a buried target. To test this idea, a series of metal cylinders was buried at various depths, a system for signature measurements was developed, and then a set of signatures was measured over a two-month springtime period.

The cylinder targets were lengths of 4 inch diameter galvanized pipe. Four lengths were chosen 1, 3, 5, and 10 ft. Pipe sections of each length were buried (lying horizontally) at three depths 1, 3 and 5 ft., in a grass lawn behind the Laboratory building. The twelve buried targets were arranged in a grid pattern, with sufficient spacing between targets to assure that the probe antenna only senses one target at a time. In addition, a 5 ft. deep "dummy trench" was dug and refilled. A sketch of the buried target field is shown in Fig. 3. The dirt was compacted in all trenches as they were refilled, and all were covered with sod. The target burying phase was completed in early October, 1971.

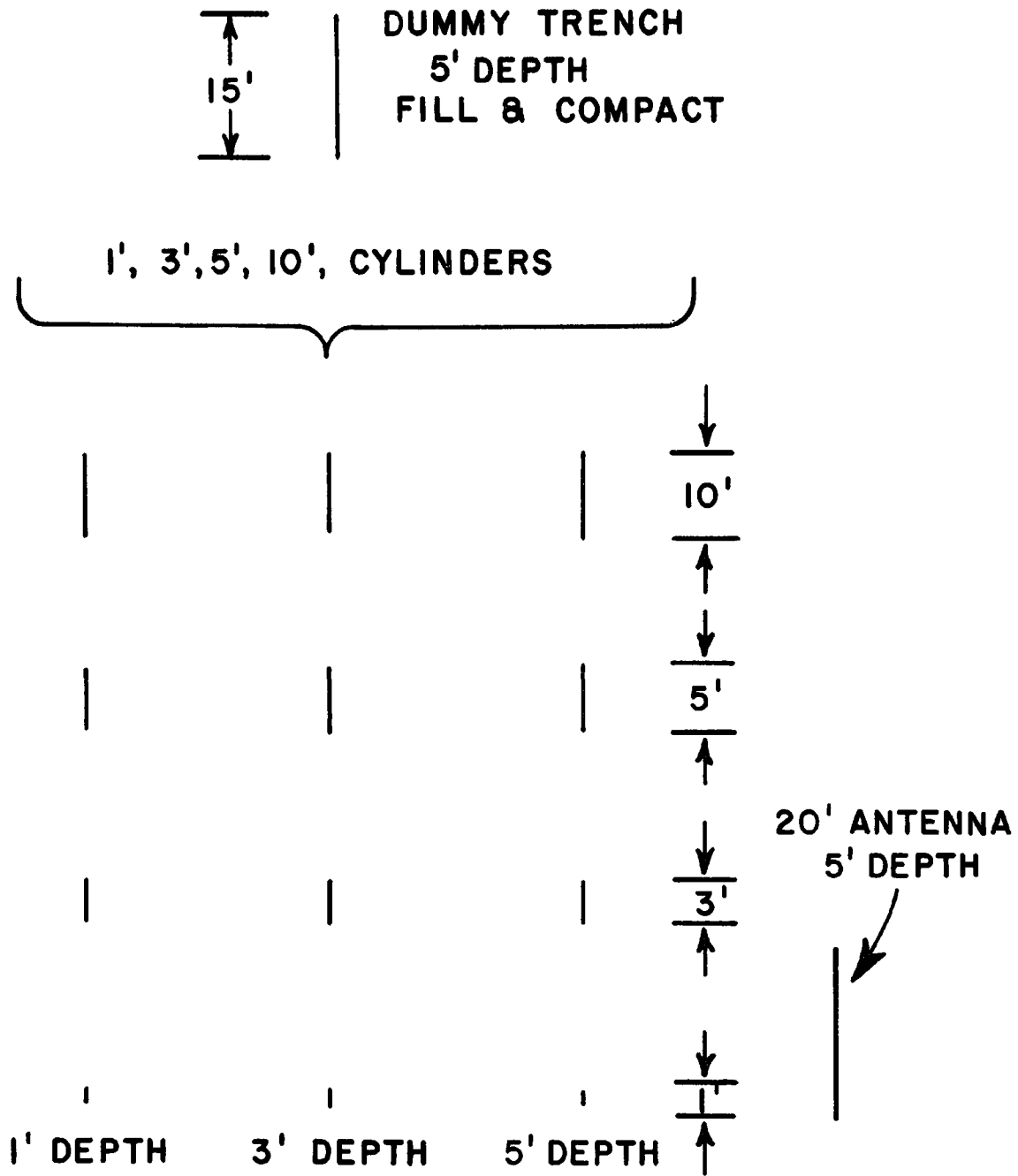


Fig. 3. Layout of buried targets.

A block diagram of the measurement system is shown in Fig. 1. The pulse generator used was an IKOR unit which puts out a 1 Kv, ~ 300 psec video pulse at a repetition rate of approximately 250 pps. The probe antennas transmit this video pulse and receive the backscattered signature waveforms of the targets. A computer-controlled Tektronix sampling oscilloscope records the data. This basic system has been used before for detection of shallow buried targets. Only a different pulse generator and antenna probe set were added for this application.

The principal development efforts on this system were spent on design and construction of a satisfactory probe antenna set. Some of the difficult requirements for this unit include:

1. Bandwidth

The frequency spectrum of the transmitted pulse is almost flat from 250 Hz to about 10 GHz. To obtain the impulse response signatures of the buried targets directly, all system performance parameters, including antenna gains, impedance, etc. must remain constant over that total bandwidth! As a compromise requirement, it was desired that system performance vary as little and as smoothly as possible over a 1 MHz to 100 MHz frequency band. Such performance could be compensated for if necessary by calibrating the system using a set of reference targets.

2. Sensitivity to Buried Targets

At the frequencies specified above, it is difficult to get a portable antenna set which achieves any measurable focusing of energy into a small underground target region. Furthermore, the air-ground interface reflects most of the energy radiated from a normal above-ground antenna.

3. Transmit-receive Isolation

The transmit and receive antennas must both occupy the region directly above the buried target in order to obtain satisfactory target sensitivity. Yet the average isolation over the 100:1 operating band must be about 40 dB to keep direct coupled energy from the transmitting antenna from swamping out the received target signature waveform.

The probe antenna set developed for this system is sketched in Fig. 4. This optimally shaped crossed bow-tie configuration lays on the ground over the buried target region. It has the following desirable properties.

1. The lossy nature of the grass and turf which the probe antenna set lays on makes each element behave like a heavily loaded bow-tie antenna. The antenna impedance and its radiation properties in the

region directly beneath the probe set, vary slowly over the 1-100 MHz region.

2. Although the probe system has little far field directivity, its sensitivity to buried targets is comparatively good, mainly due to its nearness to the ground-air interface. Energy transfer through the air-ground interface seems exceptional for this geometry.

3. The orthogonal arrangement of the transmit-receive antennas provides approximately 40-50 dB isolation over the whole frequency range of interest.

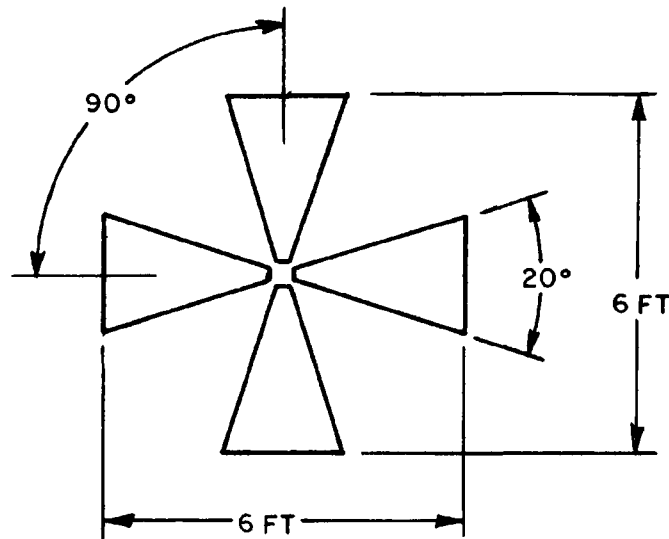


Fig. 4. Crossed bow-tie antenna probe set.

The system and the probe antenna set just described were completed in time to begin buried target measurements in the spring of 1972. As will be seen, the targets are visible to the system, and this in itself is a considerable improvement over initial measurement attempts on this contract. More effort on time-domain probe design, in particular, could probably improve present performance considerably.

A typical time-domain waveform measured by the buried target system is shown in Fig. 5. Portions of this waveform can be identified with scattering obstacles at certain distances if the electromagnetic propagation velocity is known. Thus, for example, a distortionless scatterer located 6 ft away from a distortionless antenna should yield an impulse in the return waveform which is delayed by a time proportional to the 12 ft. round trip, from an assumed reference point which is the instant when the impulse was radiated (t_0). Target signatures, using our dispersive system, will no longer be replicas of the incident impulse, but can still be identified on the basis of the transit time expected for the target, whose range is approximately known.

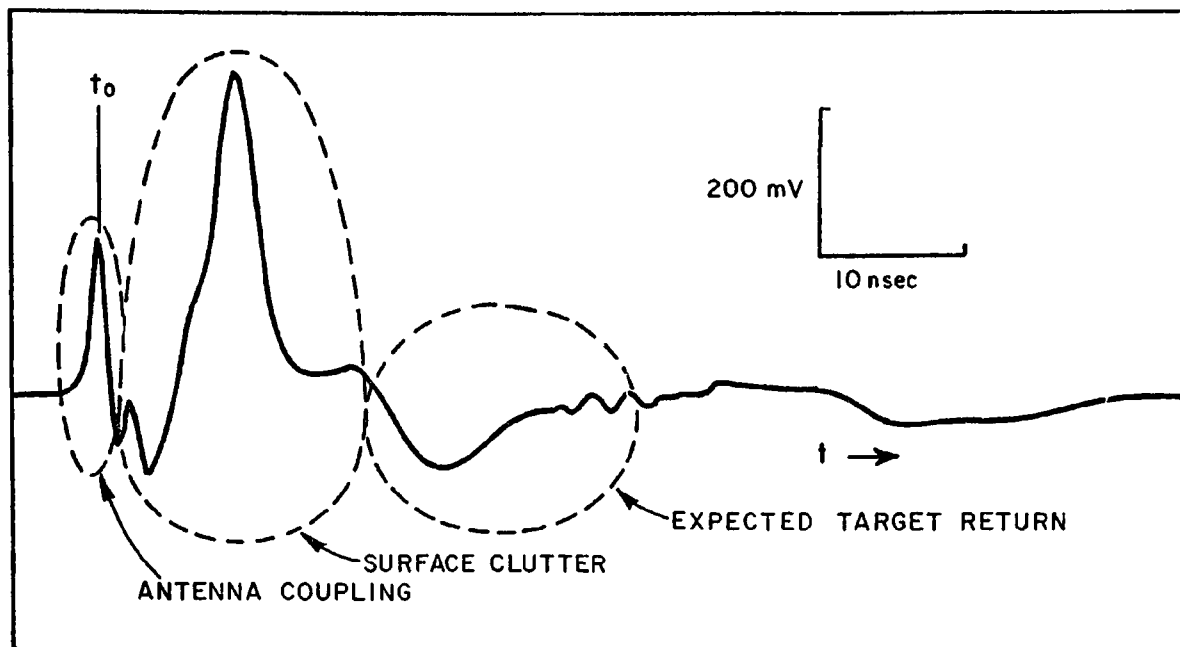


Fig. 5. Typical time domain return waveform.

Some of the salient features of the waveform in Fig. 5 are circled. The first sharp pulse is essentially a marker for the time t_0 referred to earlier. The transmit and receive antennas are not perfectly isolated in the small feed region at the center of the structure. Hence a portion of the incident impulse is coupled to the receiving antenna at almost the exact instant that the transmission of the pulse begins. The delay of all subsequent waveform features are referenced to this pulse.

The second region circled is a "clutter return" feature, which will be seen in following waveforms to vary considerably from trial to trial. This portion is attributed to ground surface irregularities in the vicinity of the antenna probe set. For "no target" measurements over undisturbed ground, this feature has relatively small amplitude. However, there are slight humps or depressions on the surface where the trenches were filled up and resodded, so this feature is usually stronger on the buried target trials. In order to delay the buried target returns so they are not submerged in this clutter, only the 3 and 5 ft. deep cylinders were measured.

The third waveform region circled in Fig. 5 is the expected target return area. For an electromagnetic index of refraction of ~ 3 , the returns from the 3 and 5 ft. deep targets should be about 15-20 and 25-30 nsec following t_0 , respectively.

In Figs. 6 and 7, the returns of an undisturbed ground (no target) location, of the dummy trench, and of the 3 and 5 ft cylinders at 3 and 5 ft depth are shown. All of these data were taken on March 24, 1972. There are certainly differences in these raw waveforms, but interpretation is difficult. Further computer processing produced a more meaningful data set. The antenna response portion of the waveforms was eliminated by range gating, an average no target return was subtracted, and the resulting waveforms were band-pass filtered. A "3 ft" or "5 ft" filter was used. Each of these filters passed a 20% frequency band centered at the expected resonant frequency of the appropriate buried target.

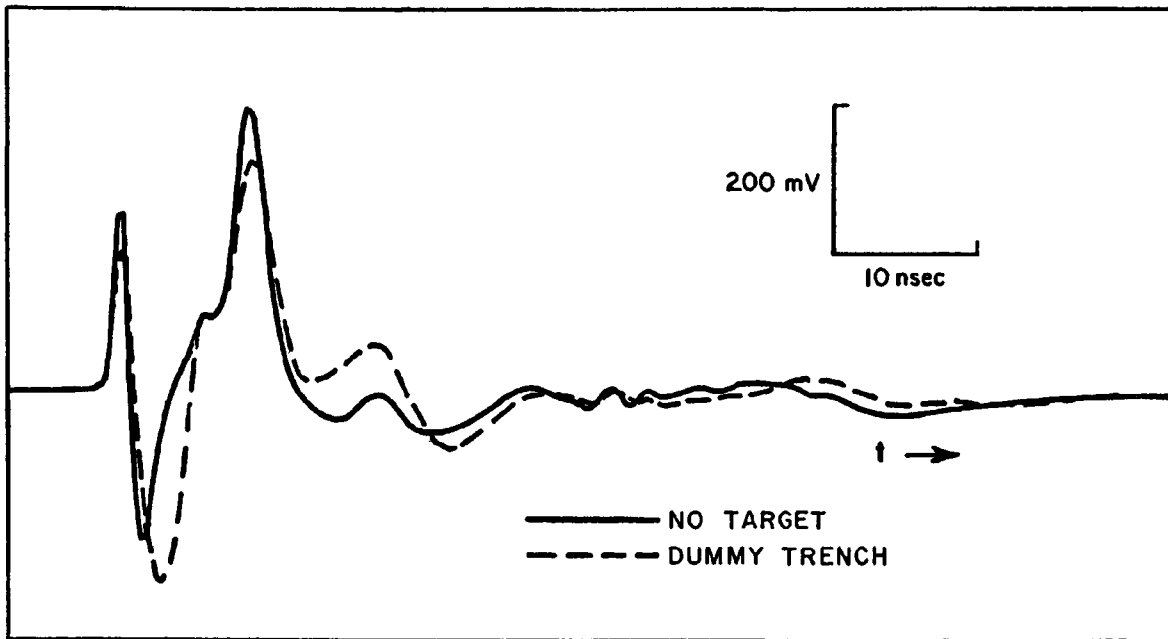


Fig. 6. "No target" and "Dummy trench" return waveforms (3-24-72).

Figures 8 and 9 represent the results of such processing. A relatively strong return is observed when a cylinder length and filter characteristic match, and the position of the return in time is proportional to the depth of the target.

Measurements of the 3 and 5 ft. cylinders at 3 and 5 ft. depths were continued through June 7, 1972. Five measurement sets were made. Some general characteristics of these waveforms became evident.

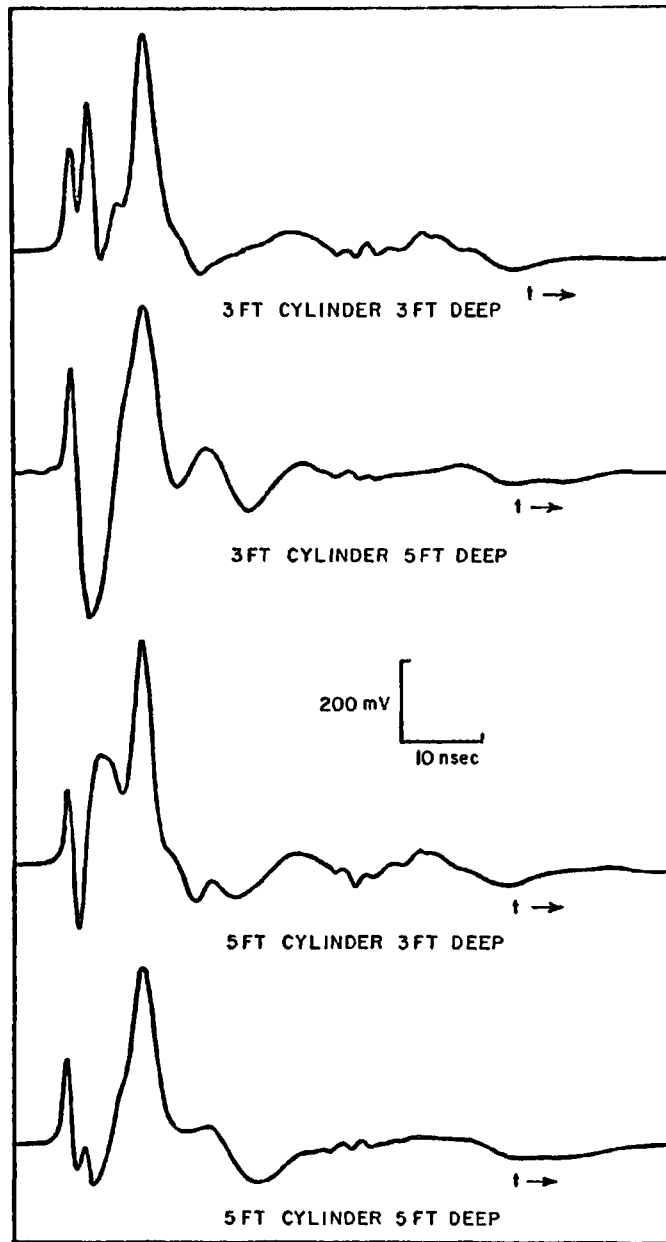
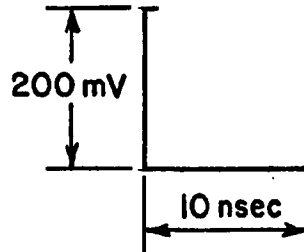


Fig. 7. 3 ft and 5 ft cylinder return waveforms (3-24-72).

**"MATCHED FILTERED" RETURN WAVEFORMS
3 FT. CYLINDER FILTER**

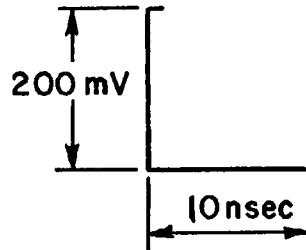


NO TARGET AND 5FT. CYLINDER, 5FT. DEEP

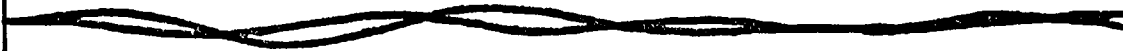
NO TARGET AND 3FT. CYLINDER, 5FT. DEEP

Fig. 8. 5 ft depth return waveforms after filtering for 3 ft cylinder.

**"MATCHED FILTERED" RETURN WAVEFORMS
5 FT. CYLINDER FILTER**



NO TARGET AND 5 FT. CYLINDER, 5 FT. DEEP



NO TARGET AND 3 FT. CYLINDER, 5 FT. DEEP

Fig. 9. 5 ft depth return waveforms after filtering for 5 ft cylinder.

1. The signature waveforms were dependent on the characteristics of the grass or possibly of surface moisture changes. For example, in Fig. 10 the return waveforms of the two cylinders at 5 ft. depths taken on May 12, following a rainy period so that the grass was tall and lush, show that the 3 ft. cylinder is almost invisible. In fact, virtually all portions of the waveforms are attenuated compared to those of late March.

2. There appeared to be a rather smooth, long-term variation in the relative delay of the target response region. Comparing 5 ft. deep, 5 ft. long returns of late March and early June, in Fig. 11, this difference can be seen. This change may be due to a gradual decrease of the average soil moisture content at the surface. More measurements and also independent soil moisture content measurements are needed to test this hypothesis.

3. There were no discernable changes in the resonances of these targets which could be correlated to moisture content in the immediate vicinity (within 1 ft. of the surface and laterally) of the buried cylinders. Part of this fact was due to the difficulty in measuring accurately the period of the sinusoidal cylinder returns due to the clutter and their damped nature. The two waveforms in Fig. 11 adequately illustrate this problem. Some frequency spectra for 5 ft. cylinder, 5 ft. deep returns are shown in Fig. 12. Because of ground losses, only the lowest 50-60 MHz of these spectra are considered significant as far as buried target returns are concerned. It is seen that the peak of the spectrum is about 40 MHz for all three trials. This is the expected resonance frequency of the 5 ft. cylinder assuming $\sqrt{|\mu_r \epsilon_r|} \sim 3$. But no variation in this peak is discernable from these measurements.

It could be that the moisture content at ~5 ft. depth did not change through April and May and that such a change would have been seen. Again, more measurements and independent moisture content measurements would have answered this question. Measurements from soil samples taken at a 2 ft. depth to be discussed later indicate this to be the case.

The presence of the sinusoidal patterns which correlate well with the length and depth of the cylinders lends support to the idea that this technique will be useful for measuring subsurface moisture, but the lack of control over moisture conditions in the field does not allow a clear-cut positive evaluation at this point. Measurements over at least a one-year interval should be continued, with independent monitoring of ground moisture in the target vicinity, if possible. Calculations of target returns from cylinders imbedded in a lossy medium and laboratory measurements under controlled conditions should also be compared with the field measurements to enable quantitative interpretation of these data.

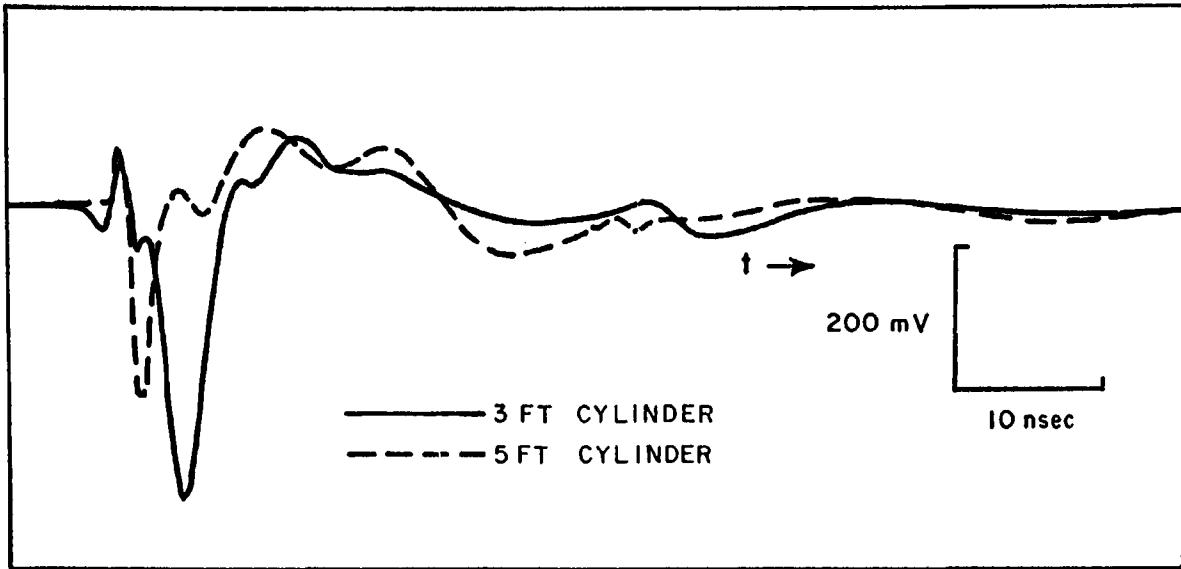


Fig. 10. Cylinder target returns at 5 ft depth after rain (5-12-72).

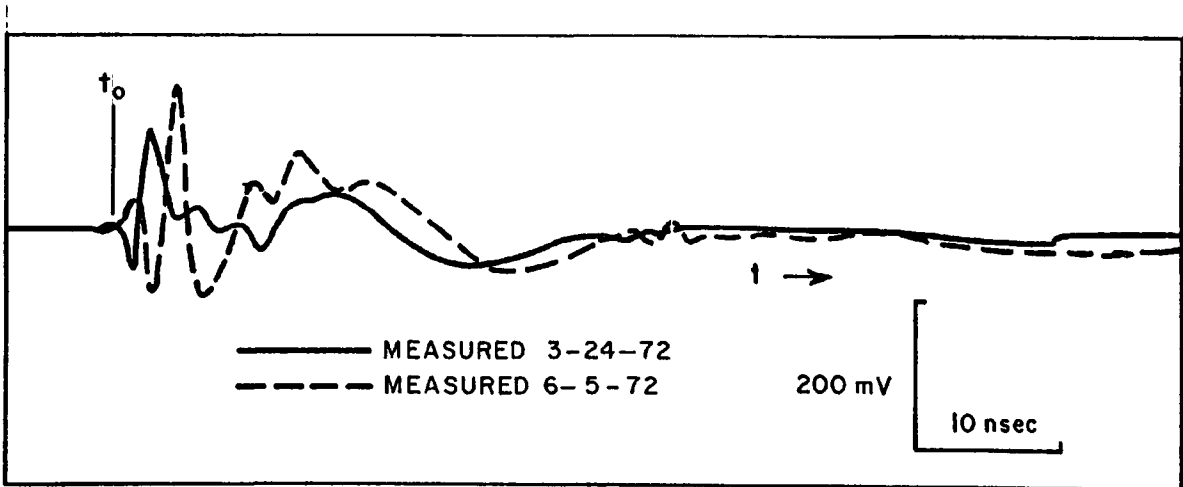


Fig. 11. 5 ft deep, 5 ft long cylinder return waveform.

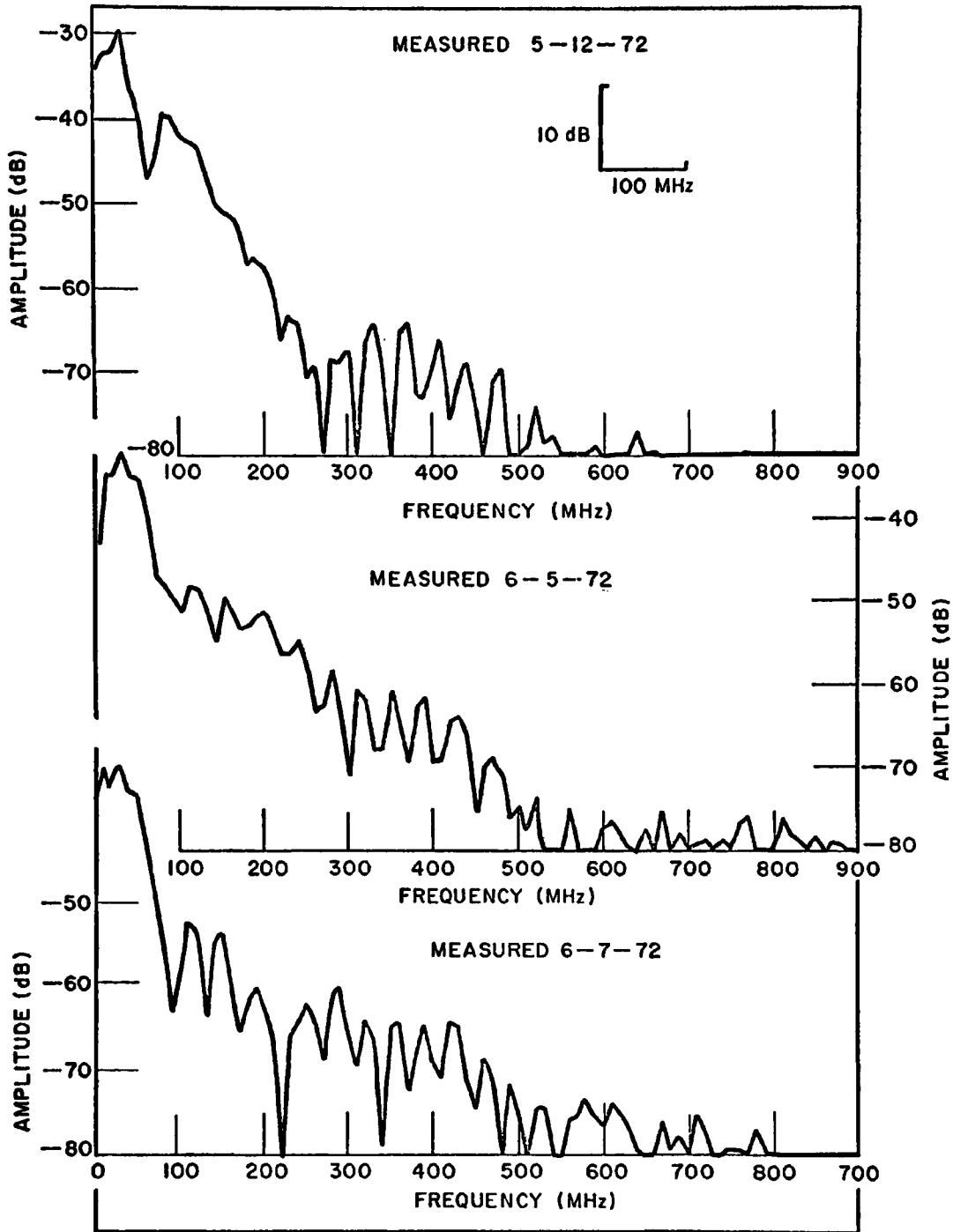


Fig. 12. Frequency spectra of the returns from the 5 ft long 5 ft deep cylinder.

4. Sampled Moisture Conditions

The transmission measurements were initiated in November 1971 and ended in June 1972. Initially only the transmission measurements were performed; the impedance measurements were added in February 1972. In March it was decided to try and obtain some correlation between the measured data and known soil conditions. Thus a sample of the soil in the vicinity of the antenna site was taken at a depth of 6 in. at the time of each measurement. This sample was weighed, baked over night at approximately 100°C to drive out moisture, and reweighed. The percentage decrease in weight of the sample after baking is taken to be the relative moisture content of the soil as given in Table I. Because of the low loss behavior of the transmission measurements taken in June and also because of the lack of sensitivity of the resonant frequency of the scattered fields of cylinders discussed previously, a sample was taken on 6-15-72 at a two foot depth. Its moisture content was 22% consistent with the highest values measured at the 1 ft. depth even though the surface was completely dry and the 1 ft. depth moisture content obtained on 6-6-72 had decreased to 13.1%.

Table I.
Surface Moisture Content

Date	% Surface Moisture (by weight)
3-20-72	17.8
3-22-72	22.4
3-28-72	21.5
3-31-72	20.2
4-12-72	15.6
4-20-72	20.3
4-24-72	21.5
4-28-72	21.3
5-9-72	25.7
5-12-72	22.4
5-19-72	21.6
5-22-72	19.5
6-1-72	17.0
6-6-72	13.1

The available accumulated 30 day rainfall is given in Table II for reference. These data are intended merely to provide the reader with an additional input for the moisture available in the Columbus area.

Table II.
Accumulated 30 Day Rainfall

Date	Accum. Rainfall (Previous 30 days)
11-10-71	1.48 inches
11-12-71	1.20
11-16-71	1.47
11-17-71	1.47
11-23-71	0.90
12-11-71	2.73
12-17-71	3.81
1-1-72	4.51
1-15-72	2.94
2-1-72	1.13
2-15-72	1.93
3-7-72	2.00
3-20-72	2.08
3-22-72	2.56
3-28-72	2.73
3-31-72	2.48

5. Underground Propagation Experiment

This experiment was designed to obtain data on propagation through the overburden on a long term basis, to observe any variations which are caused by changes of moisture content. The experiment geometry is illustrated in Fig. 13. Four antennas are used in the experiment, three on the surface and one buried to a depth of five feet. All antennas are simple 20 ft. parallel dipoles with co-planar feed points.

The three surface antennas are insulated number 12 gauge copper wire. Each end is terminated by an aluminum rod driven eight inches into the ground. This was done to match the ends of the dipole into the ground and minimize end reflection. The feed network for a surface antenna is shown in Fig. 14. The signal is converted from the unbalanced mode to the balanced mode via the Vari-L transformer which has a pass band of 10 KHz-100 MHz. The antenna is connected to the secondary (balanced) side of the transformer by ordinary 300 ohm twin lead.

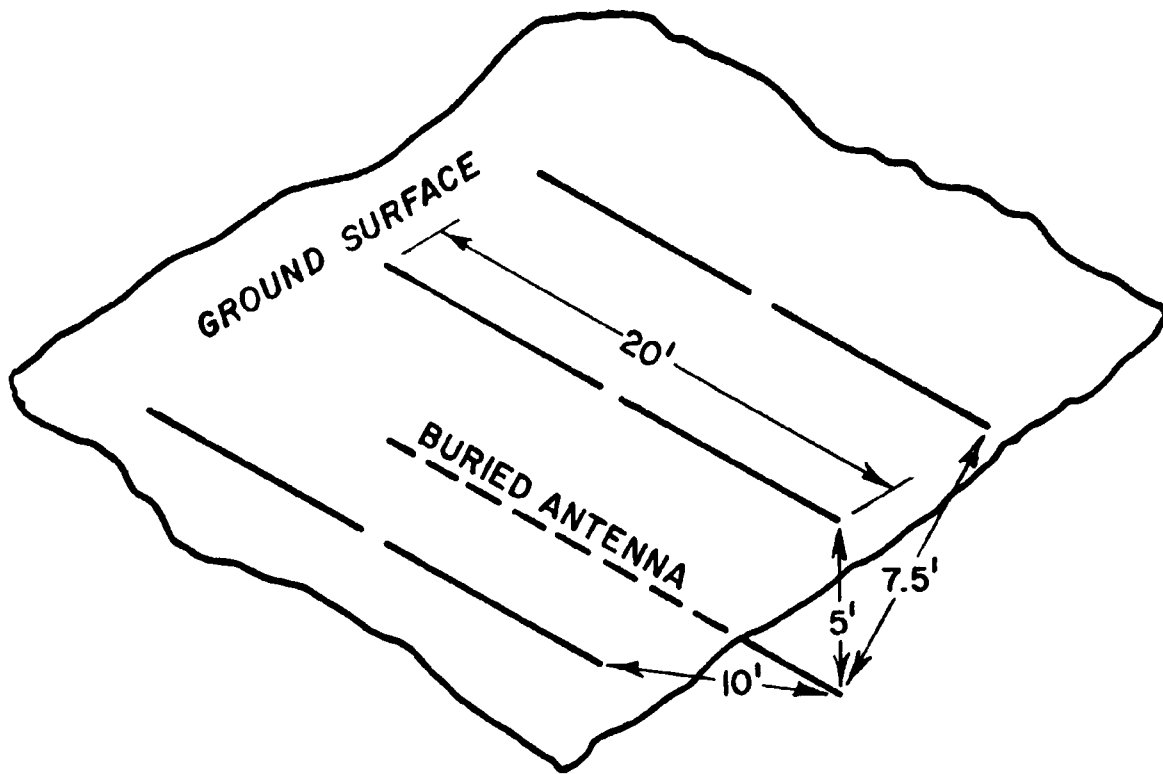


Fig. 13. Propagation experiment geometry.

The feed network for the underground antenna is shown in Fig. 15. The impedance of this antenna was calculated assuming an infinite medium with conductivity of 0.01 mho/meter and relative dielectric constant of 15. Over the frequency range of interest the theoretical impedance was found to be 55 ohm. Thus it was decided to feed the antenna with a 50 ohm cable. Because the antenna is below ground, shielded balanced cable was required to feed the antenna from a balanced to unbalanced transformer located above ground. Standard cable with 50 ohm impedance was not available so a cable was fashioned from coaxial RG-8A/U as shown. Each side of the balanced line was formed from two 15 ft. lengths of RG-8A/U coaxial cable with their center conductors in parallel. The shields are all connected together at both ends to form a true shielded cable and the shield is returned through the transformer to ground as shown in Fig. 15.

Measurements were made of this antenna system at approximately one week intervals during the winter-spring season of 1972. Each measurement consisted of the following:

1. Direct reflection from the buried antenna
2. Direct reflection from a reference short circuit in place of the buried antenna
3. Direct reflection from each surface antenna
4. Direct reflection from a reference short circuit in place of the surface antenna
5. Pulse transmission from the buried antenna to each surface antenna.

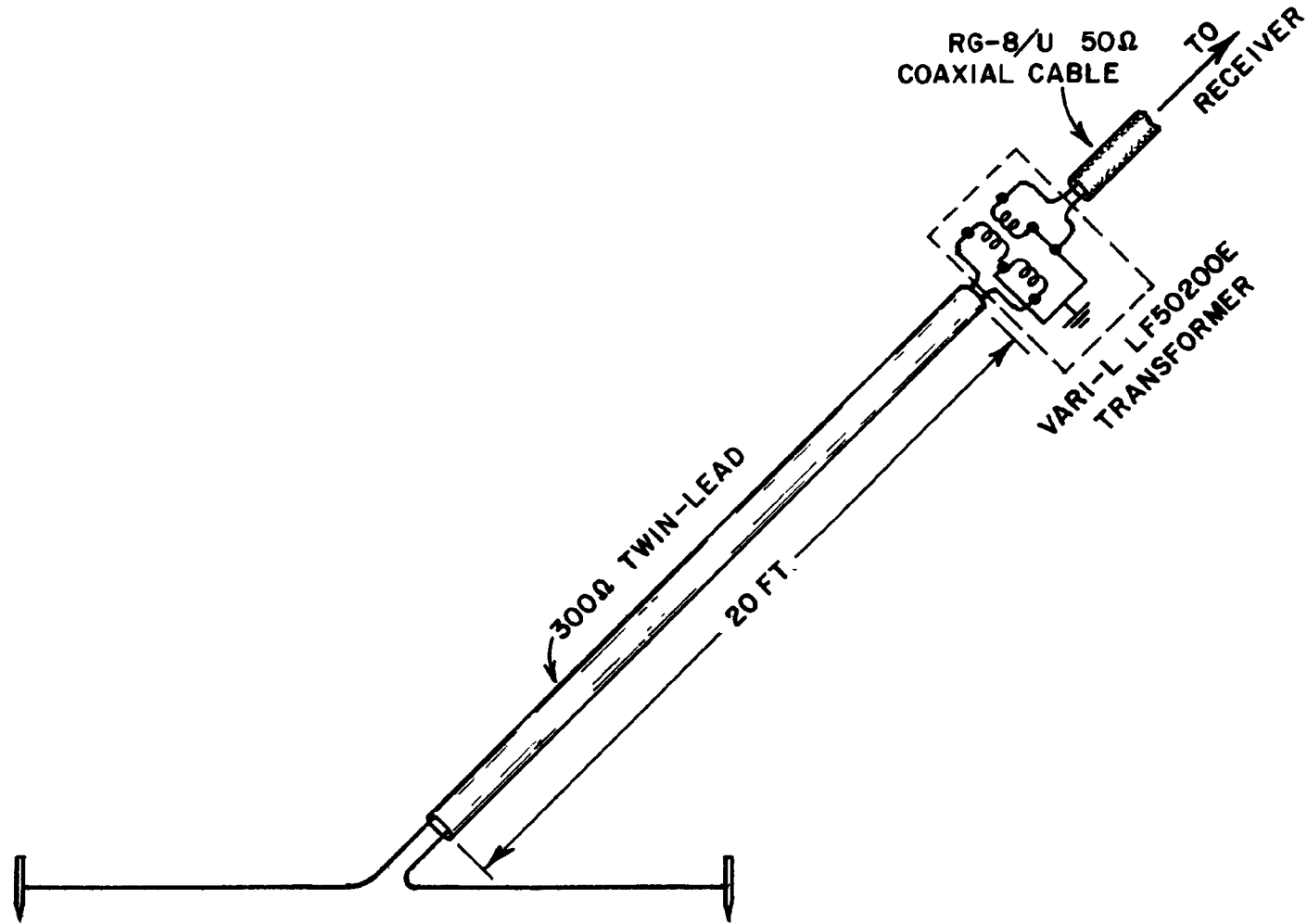


Fig. 14. Feed network for surface antenna.

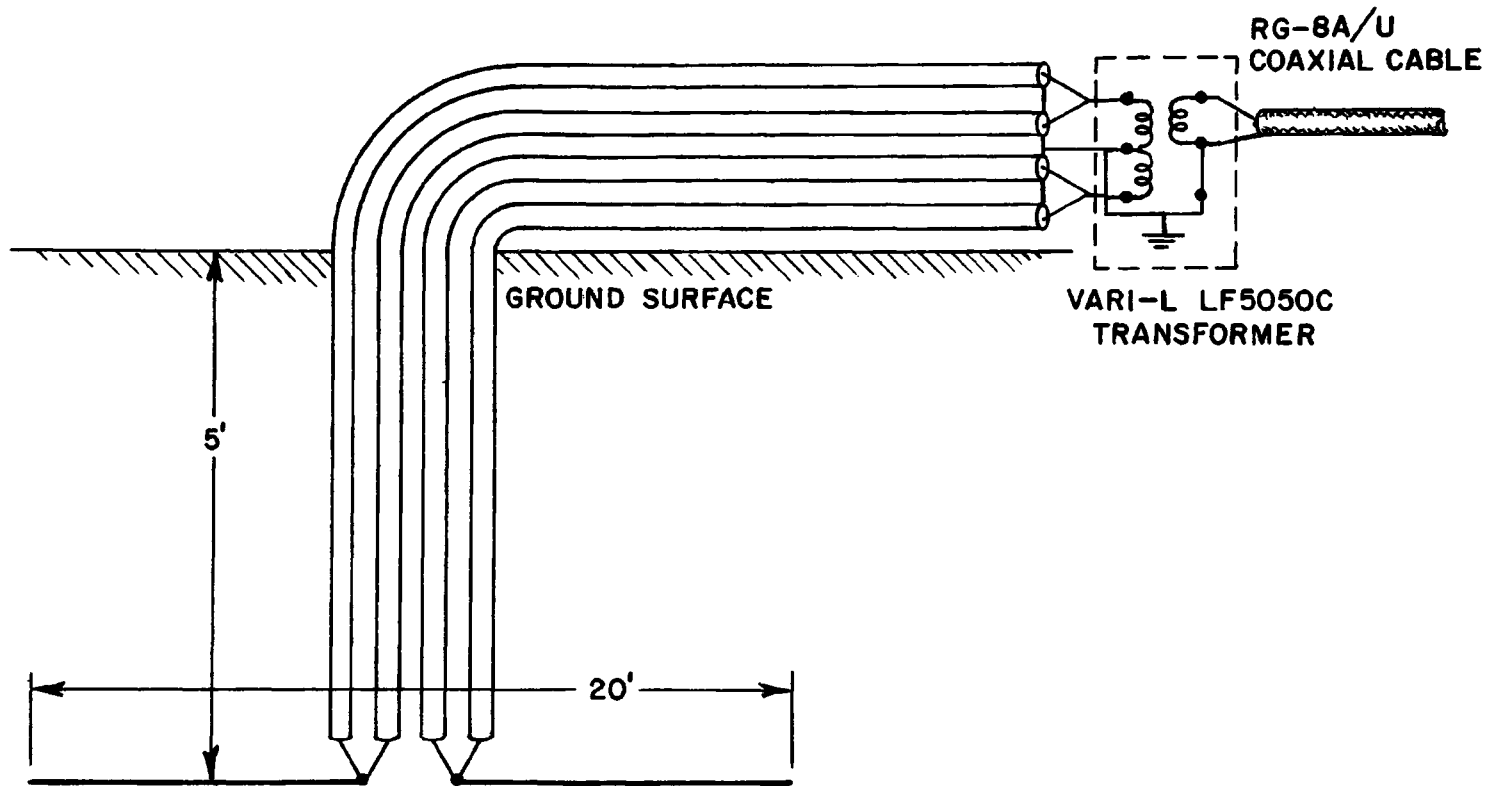


Fig. 15. Feed network for underground antenna.

The basic measurement procedures and the raw data are given in Appendix I. The data reported in this section were obtained by the following process. The buried antenna is excited by the pulse generator and a received pulse is recorded at each of the surface antennas. The Fourier transform of these received pulses is obtained by means of the Fast Fourier Transform program available in the instrumentation computer. The loss per unit path length is computed at each frequency by dividing the signal obtained for the shortest path by that obtained over the longer path lengths and then dividing by the change in path length. One should realize that it would be impossible to accumulate this vast amount of data by more conventional techniques and that the instrumentation computer and this data process is essential. It should also be noted that the processing drastically improves the accuracy of the measurements by essentially eliminating all sources of problems common to the different antenna pairs, i.e., the characteristics of the antennas, the sources, the transmission lines, and the baluns are all calibrated out of the system by the division process. Of this series of five measurements, only the last measurement just discussed could be made with the accuracy required to obtain valid correlation with the moisture content in the soil. It will be seen later that by measuring the difference in attenuation over two paths, a very consistent correlation of the loss per unit path length with the moisture content emerges.

Figure 16 shows the most promising set of data obtained. Here, there is a consistent increase in the attenuation of the high frequency data taken in November and December. This is related to the time period when growth of the grass has slowed and the ground water is being recharged. Unfortunately, no measurements of soil samples were taken so no comparison can be made, because our efforts were, at this time, still being directed toward refining the equipment and the measurement techniques.

Measurements were resumed in March with the measured data given in Fig. 17. Again significant trends are noted. First, the attenuation per foot for the low frequencies appears to be at the same level as noted in December. The established trend of increased attenuation for the high frequency data appears to continue until the soil is saturated toward the end of March and the beginning of April. The data of April 12 seem to represent an exception. However this is associated with the driest 1 ft. soil sample in this period (15.6%). The April 20 data appear similar but here the deep soil sample contained 20.3% moisture. One might conclude that the electromagnetic measurement is more reliable than is the soil sample. Here, apparently, the top level has a higher moisture content but the price is being paid for the dry spell of April 12 at a lower level. The anomalous behavior of May 9 shown in Fig. 18 resulted in the highest attenuation of the high frequency data but this occurred on the day of the most moist 6 in. deep sample (25.7%). It is suggested that the lower frequency data would contain information about the overall moisture content since the wavelength is larger and it should be less influenced by minor perturbations

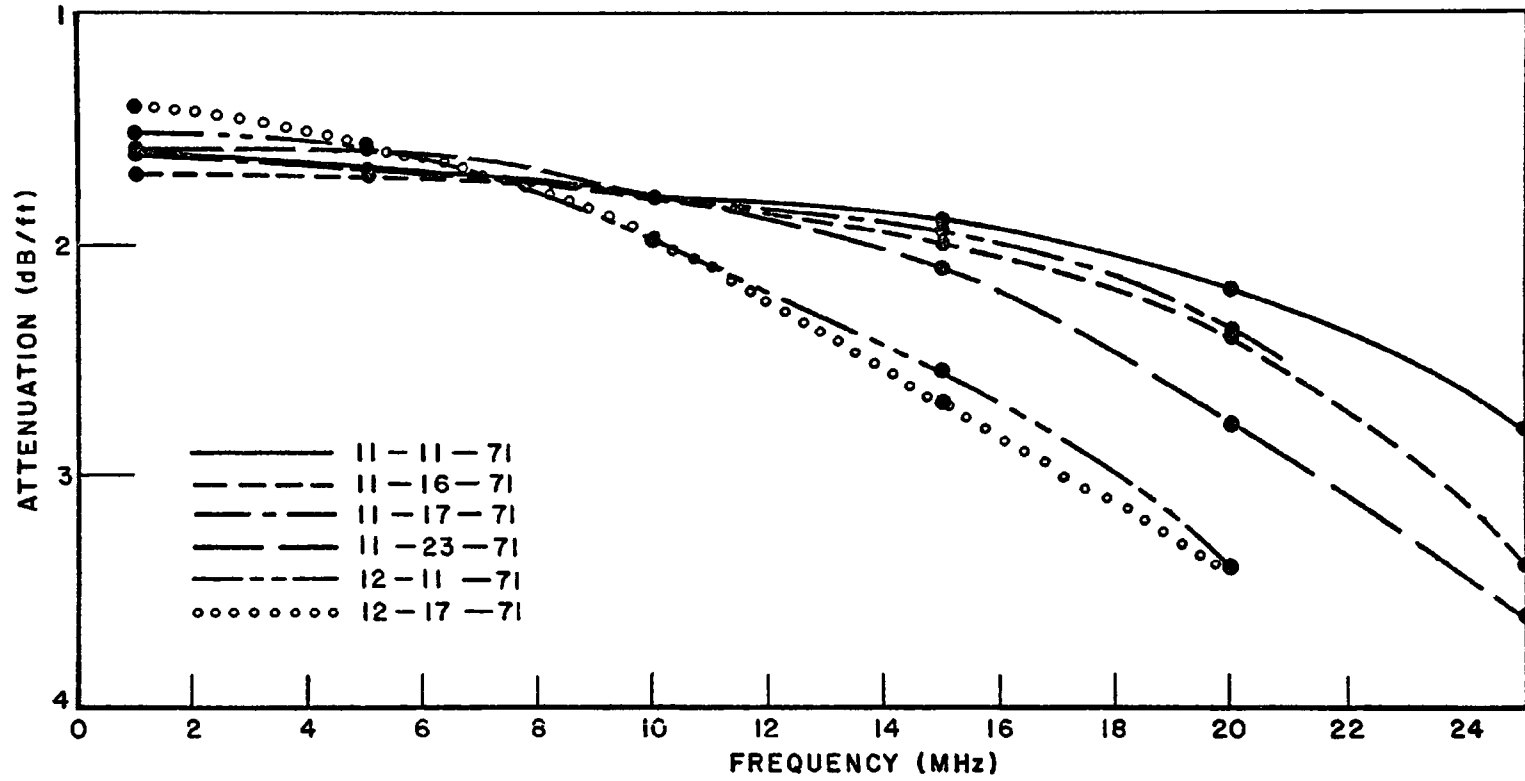


Fig. 16. Ground attenuation (dB/ft), Nov.-Dec., high frequency.

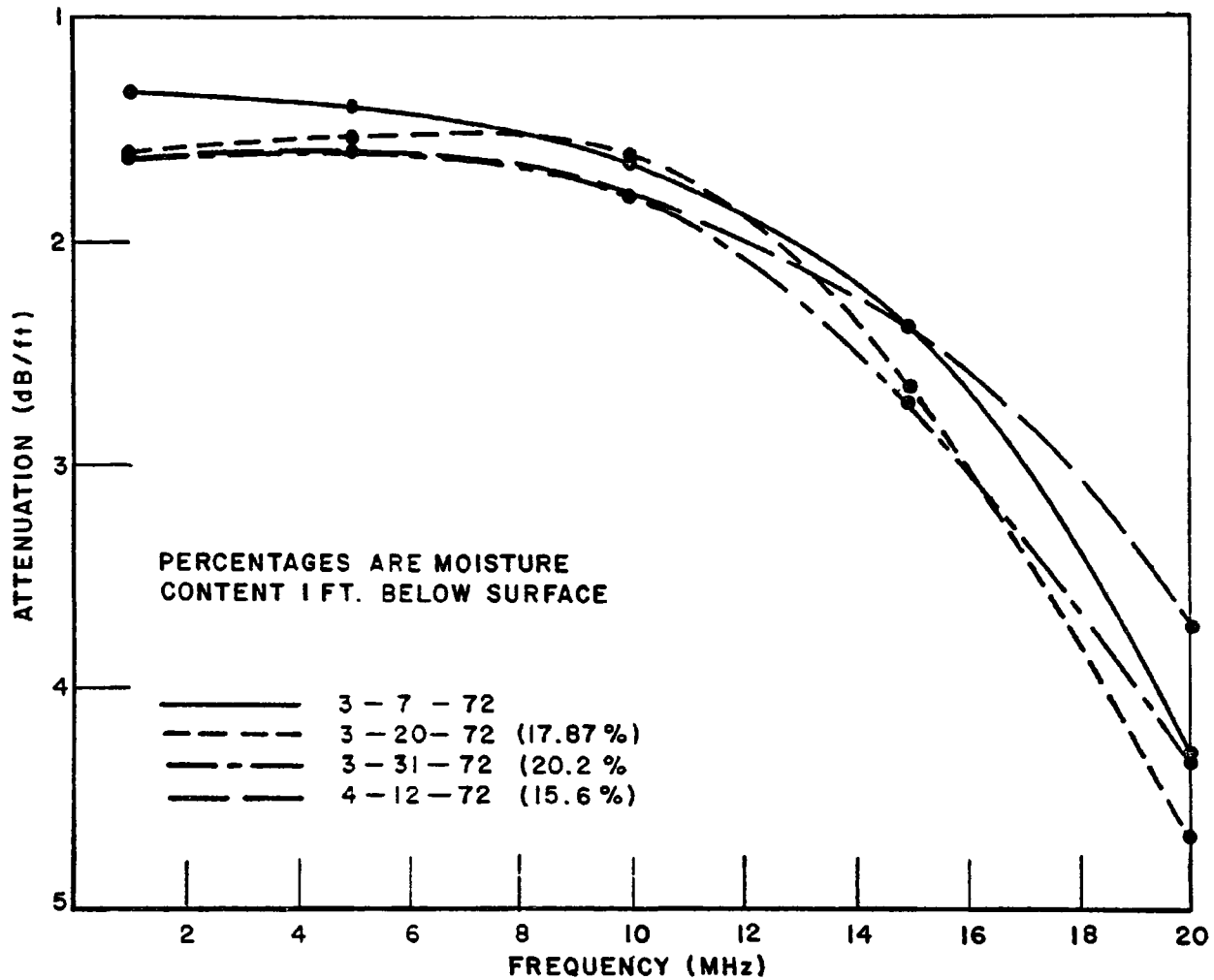


Fig. 17. Ground attenuation (dB/ft), March-April, high frequency.

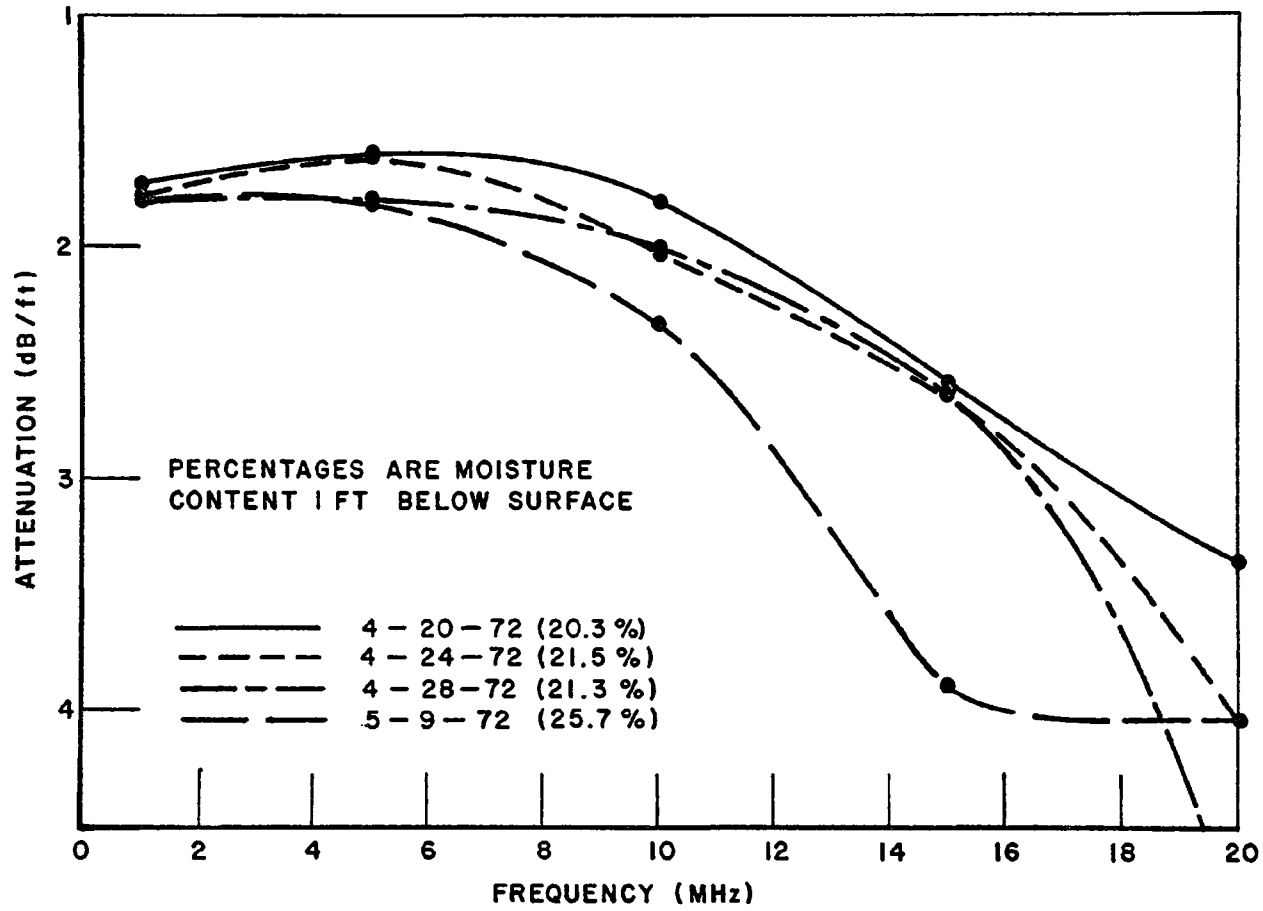


Fig. 18. Ground attenuation (dB/ft), April-May, high frequency.

of the moisture content. Such trends do appear to exist at 1 MHz in the data of Figs. 16-18 but they represent small changes. Finally data taken during May and early June shown in Fig. 19 seem to indicate that the total moisture content between the transmitting and receiving antenna is increasing even though the 1 ft deep soil sample indicated that the ground was drying out and the surface conditions had changed from soggy to hard dry ground. Again one must conclude that the electromagnetic measurements are providing a very realistic qualitative measure of the moisture content.

The lower frequency data are plotted in Figs. 20-23. The dates are the same as for the high frequency data. These data exhibit a more rapid variation with frequency than the higher frequency data, and no significant long term trends were discernable. The data appear to oscillate randomly and even measurements on consecutive days vary widely as can be seen in Fig. 20 (Nov. 16 and Nov. 17). Thus this frequency range does not appear to be particularly useful in monitoring long term trends in ground conditions at least with the current experimental setup. Several possible explanations could be offered for this erratic behavior in this frequency band. The most likely is that the antennas are now short in terms of wavelengths and are hence subject to detuning caused by variations in the moisture content.

It seems clear that significant changes in the measured transmission of electromagnetic energy through the soil as the moisture content changes have indeed been observed. Reduction of the data to moisture content, however, remains difficult because it is not distributed uniformly through the soil. A new set of experiments that are carefully designed based on the extensive knowledge gained under this grant would alleviate these difficulties. A proposed experiment is shown in Fig. 24. Here a source at the transmitting antenna would produce a signal at various receiving antennas. Correlation of data would then produce the desired attenuation per unit distance. This would be compared with a moisture content vs attenuation curve measured, using soil obtained at various depths, using the system outlined in the next section. Note also that the attenuation measurements using the buried antennas would involve almost no propagation path in the region perturbed by burying those antennas.

A scatterer is also shown in Fig. 24 for the purpose of performing those measurements outlined in the previous section. This would be a cylindrical scatterer with a pronounced resonance and its frequency response curve can be measured much more precisely by the calibration that would now be available. Here, receiving antenna B would be used as a transmitting antenna and the resonance curve would be measured at the surface.

Various combinations of measurements would provide a series of cross checks and also produce information concerning any vertical layering of the ground water.

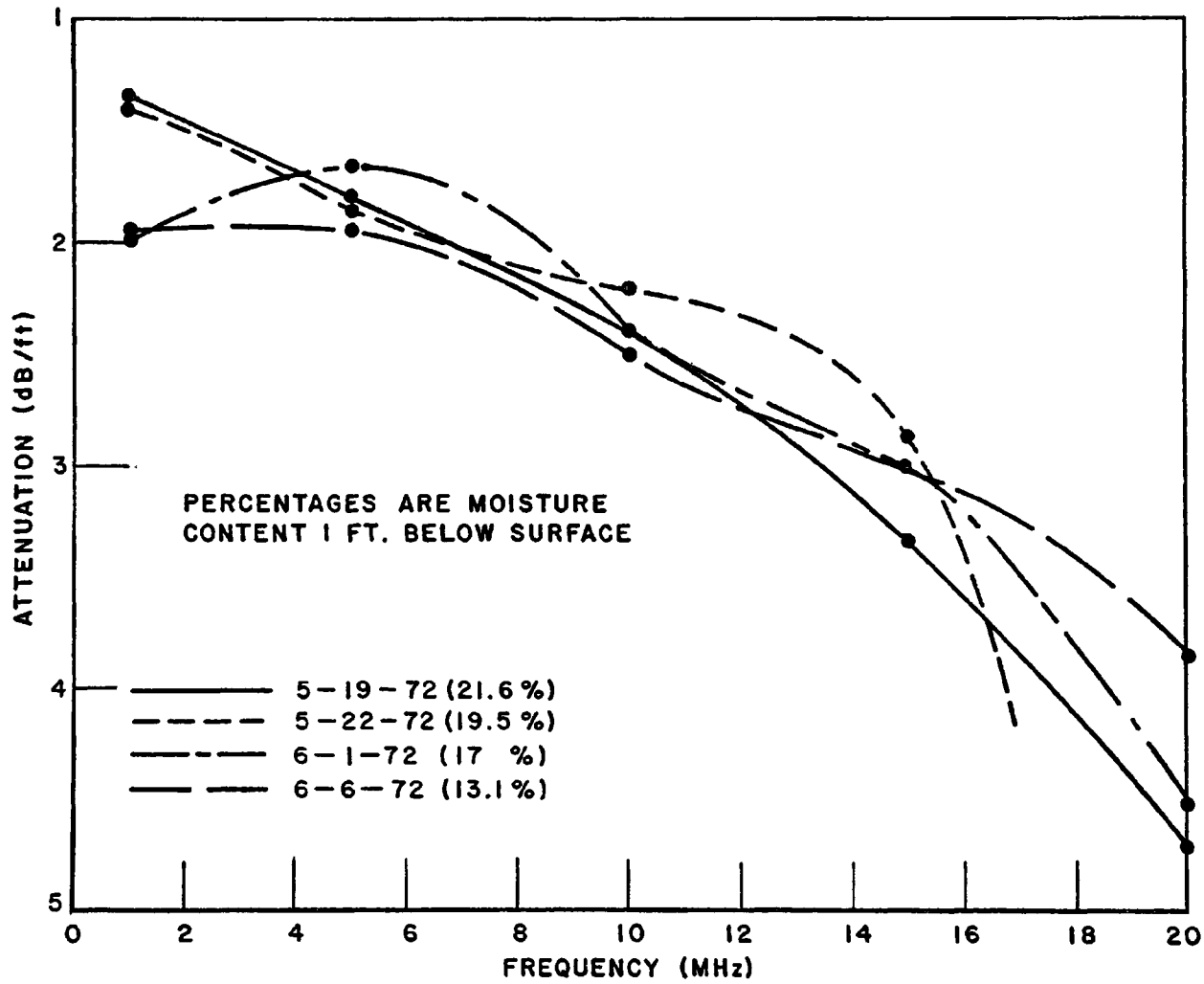


Fig. 19. Ground attenuation (dB/ft), May-June, high frequency.

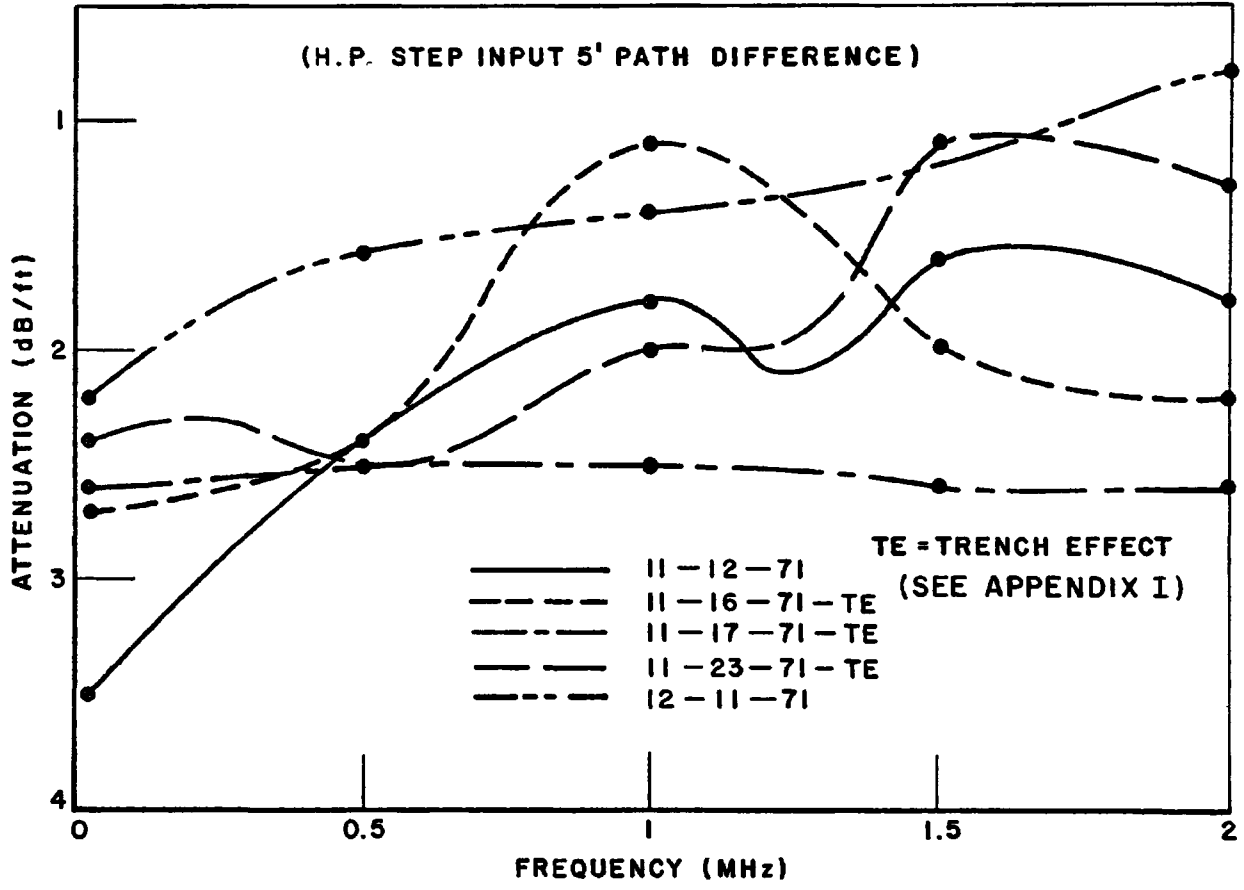


Fig. 20. Attenuation (dB/ft), Nov.-Dec., low frequency.

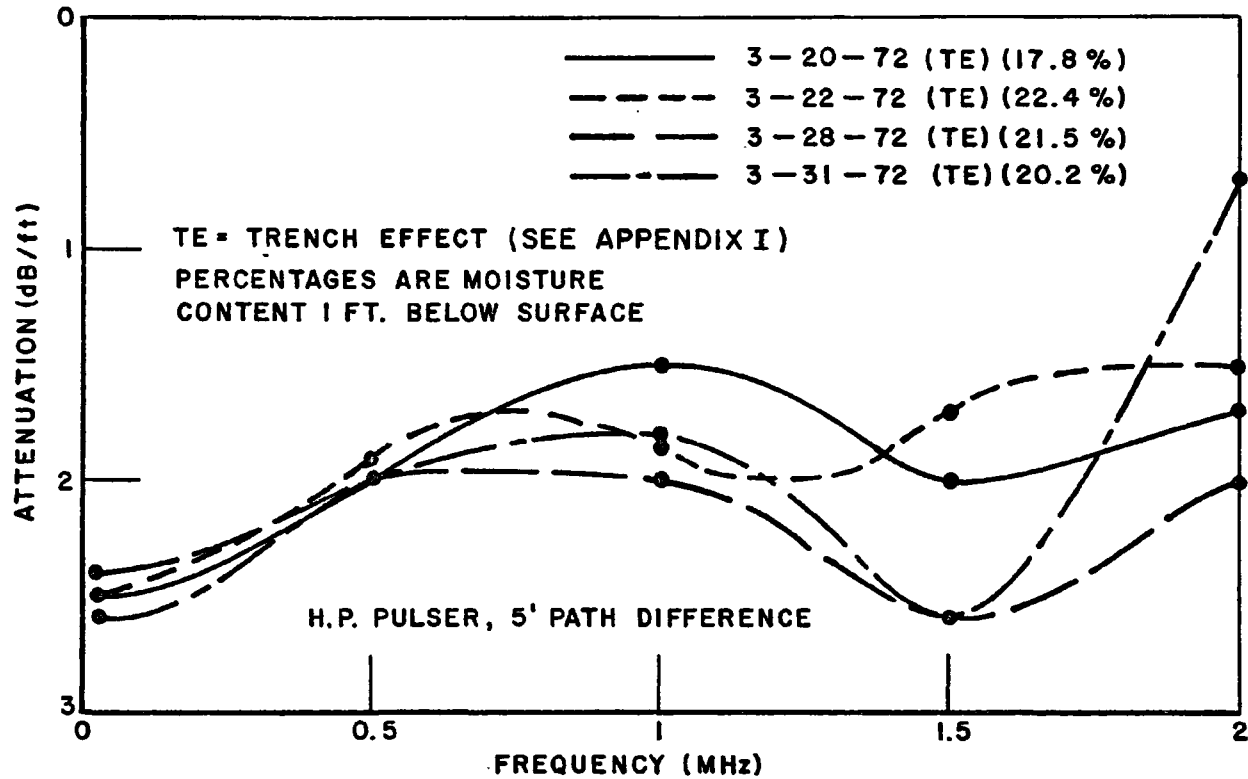


Fig. 21. Attenuation (dB/ft), March, low frequency.

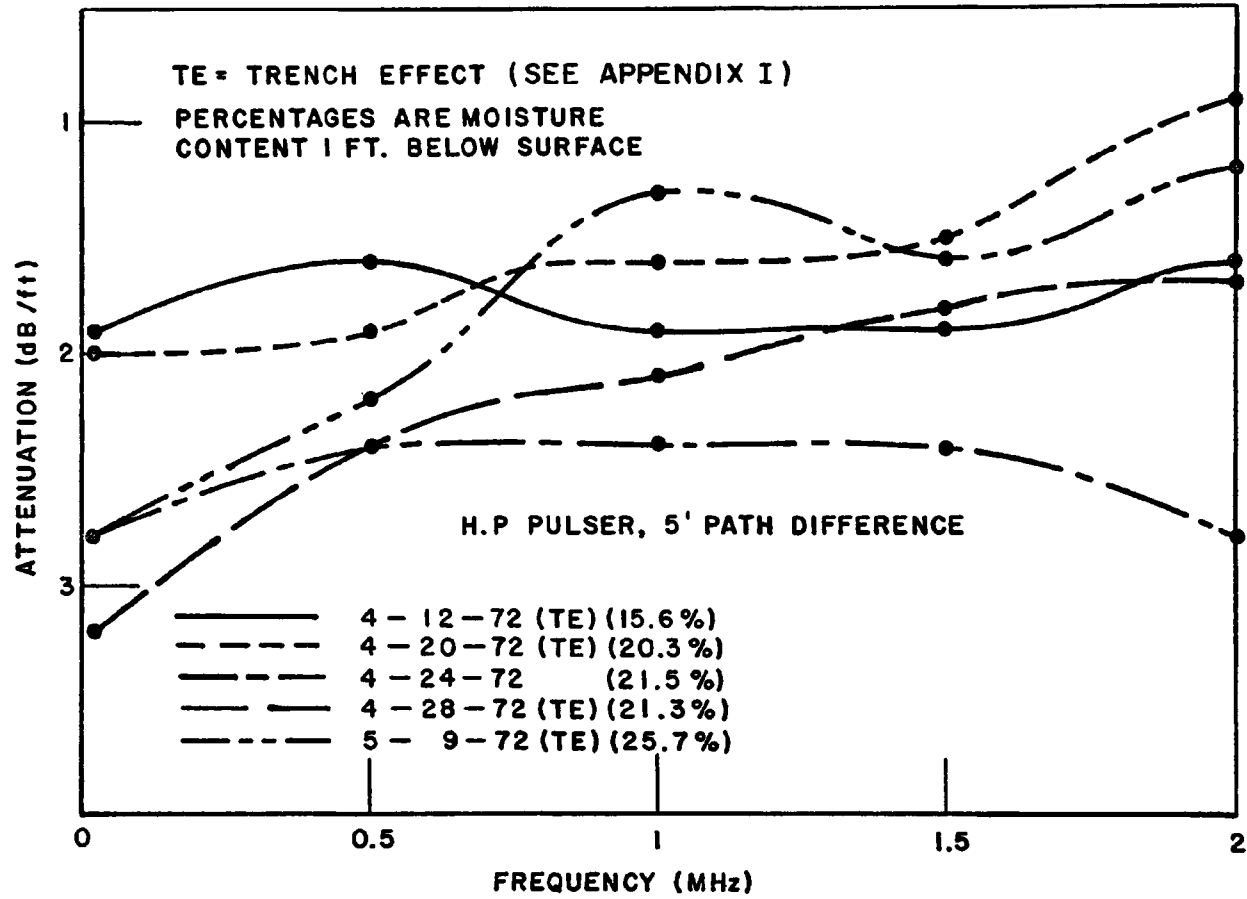


Fig. 22. Attenuation (dB/ft), April, low frequency.

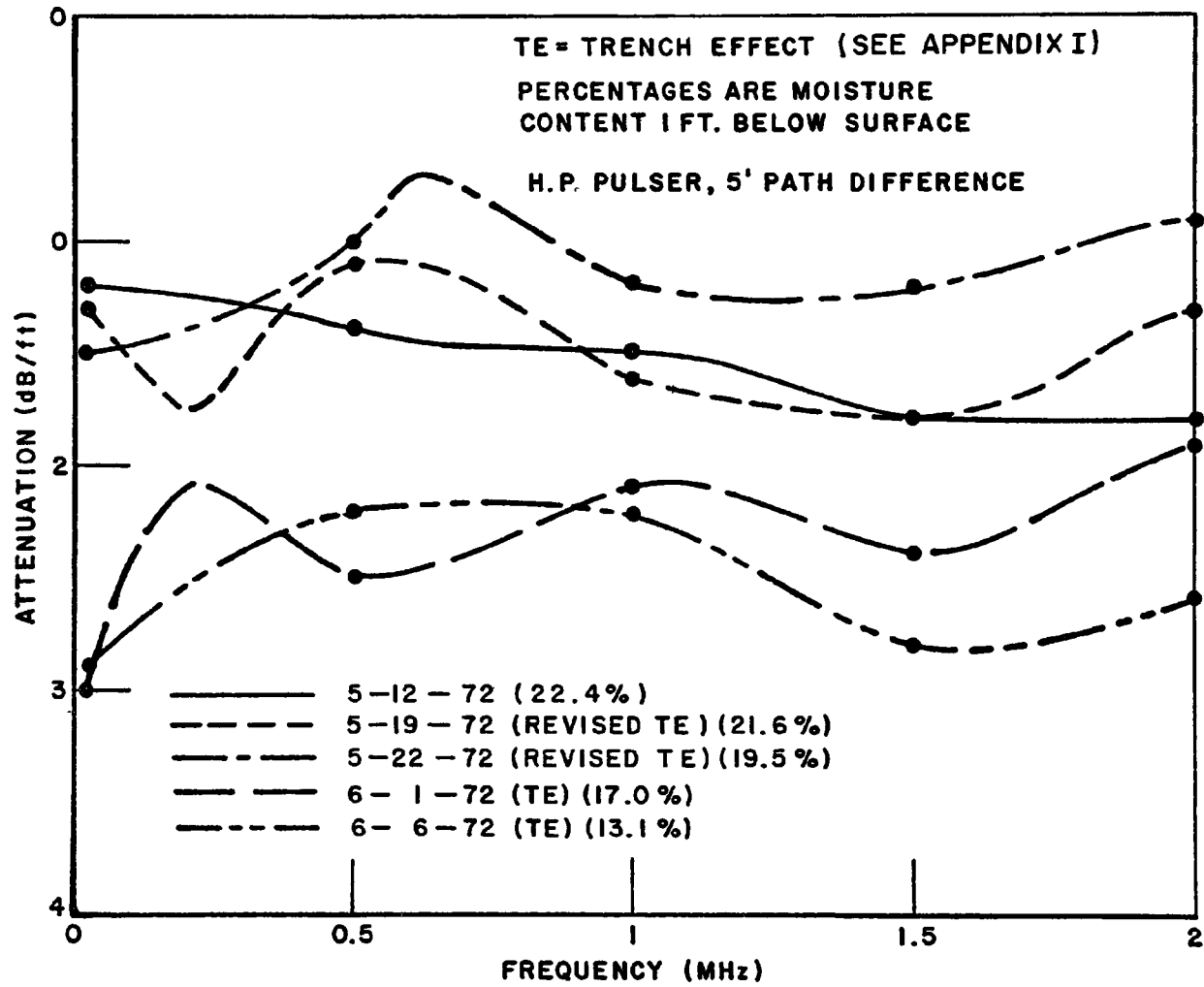


Fig. 23. Attenuation (dB/ft), May-June, low frequency.

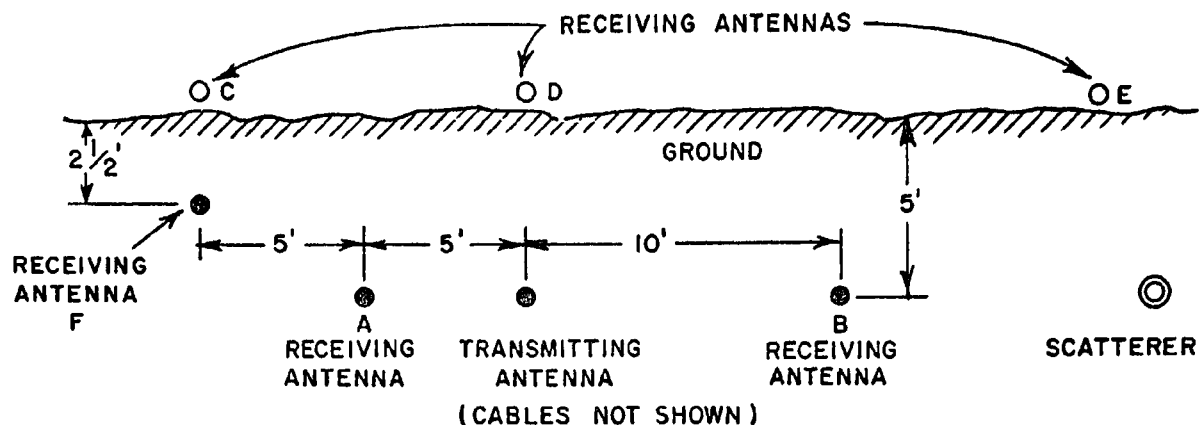


Fig. 24. Proposed electromagnetic transmission moisture measurement.

6. Reflection Measurements on Soil Samples in a Vertical Coaxial Test Cell

The coaxial tube shown in Fig. 25 was used as a test line to obtain data for determining the attenuation per foot and reflection coefficient of a number of soil samples. A cable extending from the sampling head of the sampling oscilloscope is connected to the tube via a UG-23-D/U coaxial connector, and a brass shorting plate is used to terminate the test line at the lower end. In order to reduce the amount of reflection at the connection, the tube was designed to match the characteristic impedance of a 50 ohm coaxial cable (RG-9/U). Mounted in a vertical position, the coaxial tube is partially filled with the material to be measured. Valves and removable end plates are provided at both ends of the tube for filling and draining the soil sample. Although the tube was constructed from standard sizes of copper pipe, the mismatch at the cable connection was small. A quarter-inch synthane washer was included for centering the inner conductor. The effect of this centering washer was negligible.

Using the pulse system described elsewhere, samples of the following materials were tested in the tube; distilled water, tap water, sand, finely sifted dirt (potting soil) and unsifted dirt. A pulse incident on the empty test cell will give the required information on the short circuit reflection. When one of the samples is present in the tube, there will be two reflected pulses. The first reflection occurs at the top surface of the sample and contains the information necessary for calculating the reflection coefficient and hence the refractive index of the material. The other reflection occurs at the shorting plate, and information from this reflection is used to calculate the attenuation of the sample.

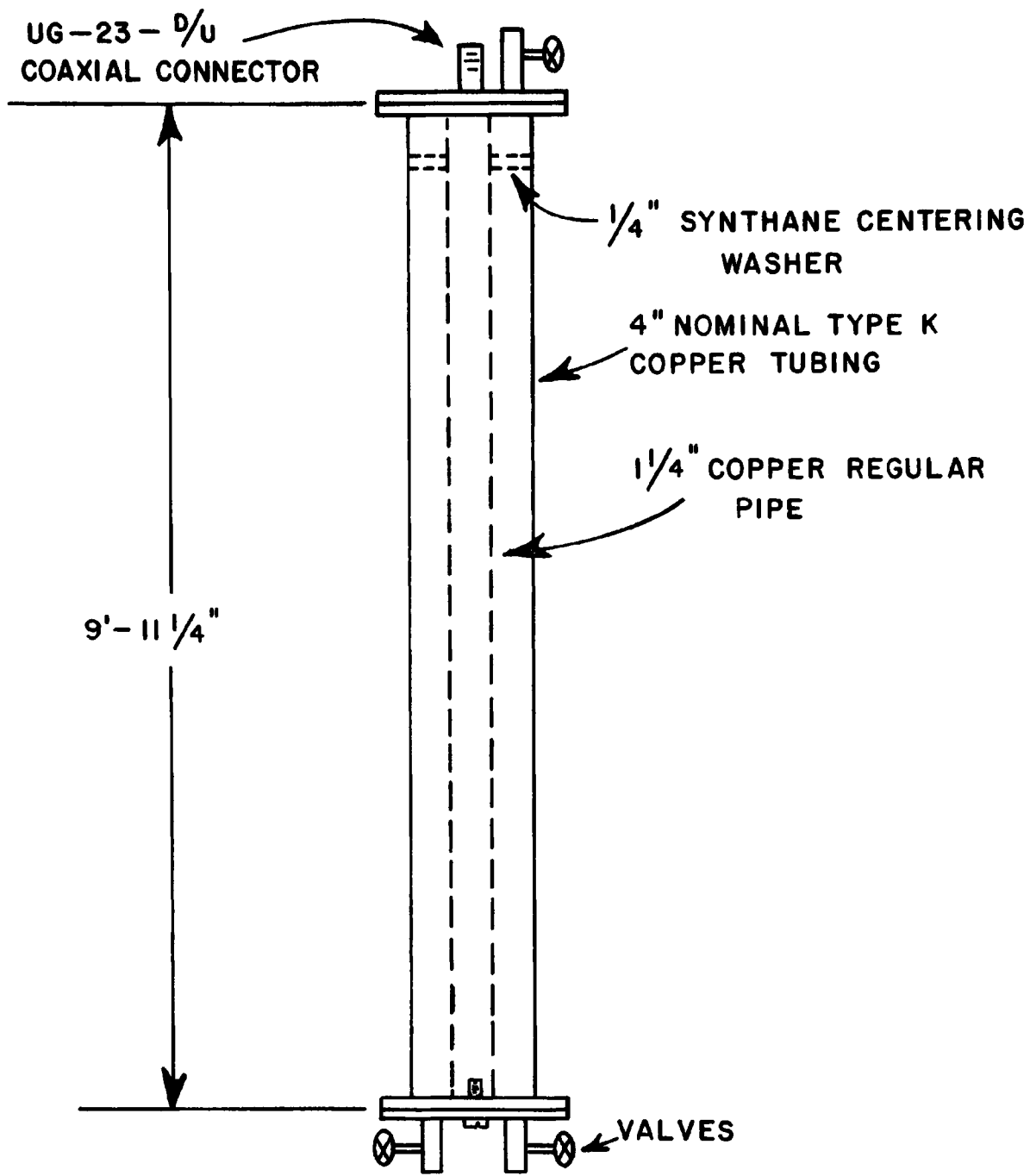


Fig. 25. The coaxial test cell.

Since it is necessary to isolate the primary reflection from either surface, the reflected pulses must be sufficiently separated in time so that each can be identified. Also both pulses must be separated in time from any secondary reflections which occur. As an example, the time-domain waveform for a 1 ft column of distilled water is shown in Fig. 26. Once the reflected pulses can be isolated by the range-gating operation, the reflection coefficient and attenuation of the sample can be determined.

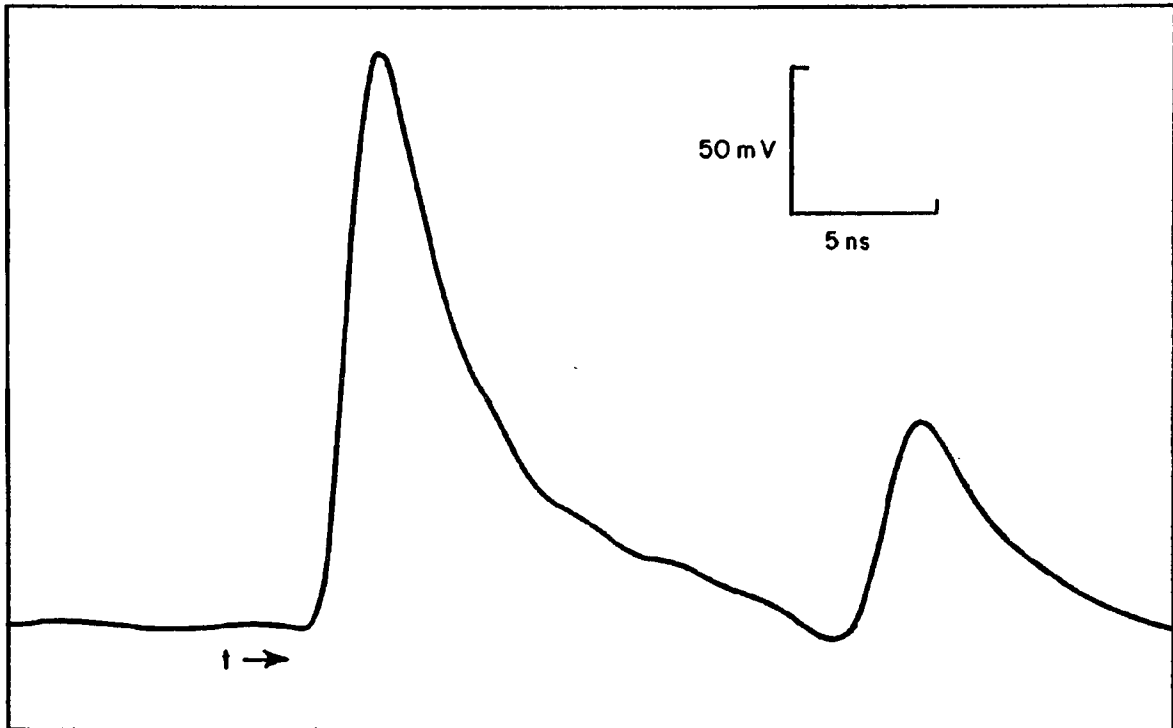


Fig. 26. Reflected pulses from a 1 ft sample of distilled water in the test cell.

The reflection coefficient is determined from the frequency spectra of the short circuit reflected pulse in the empty line and the reflected pulse from the top surface of the sample. Having obtained the necessary frequency data, the frequency spectrum of the reflected pulse from the top surface of the sample is divided by the short circuit reflection frequency spectrum (harmonic by harmonic). This produces the reflection coefficient as a function of frequency which is plotted on a Smith Chart.

The attenuation of a material is determined from the frequency spectra of the shorted-end reflections of two different column lengths of the material under consideration. The frequency spectrum of the

shorted-end reflected pulse for the shorter sample column is divided (harmonic by harmonic) by the frequency spectrum of the shorted-end reflected pulse for the longer sample column. To obtain the attenuation per foot, the resulting spectrum must be divided by twice the difference in column lengths. This takes account of the two way transit through the sample of the energy in the pulse reflected from the shorting plate. The attenuation is then presented in decibels per foot as a function of frequency.

A typical time-domain waveform for a 1 ft column of distilled water is shown in Fig. 26. The relatively large reflection from the top surface indicates the magnitude of the reflection coefficient is near unity. The average magnitude of the reflection coefficient in the 20-500 MHz range is nearly constant at 0.795. Figure 27 shows the shorted-end reflection for column lengths of 1, 2, and 5 ft of distilled water. The attenuation was found to be negligible over the 20-500 MHz range using the procedure described previously. This is as expected since the three reflected pulses in Fig. 27 are similar.

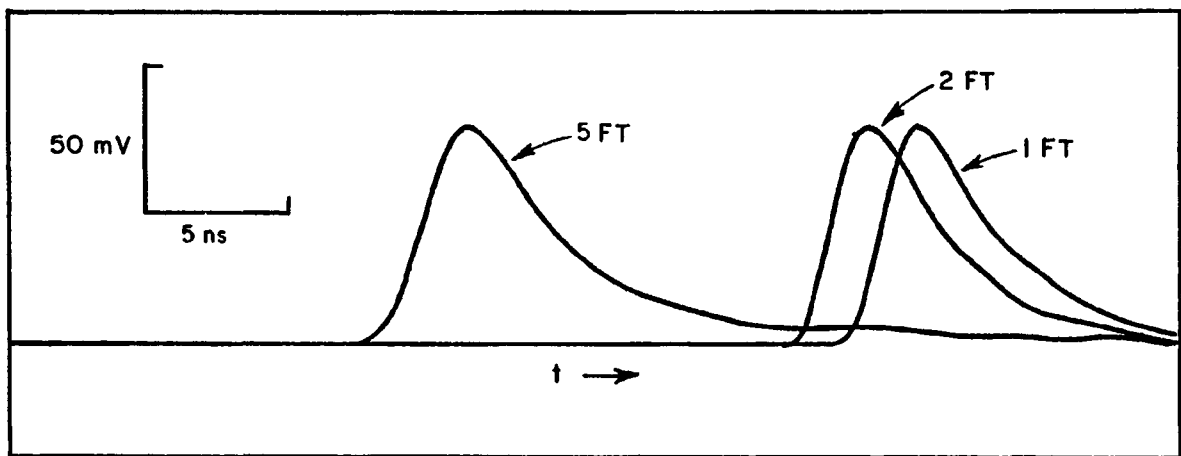


Fig. 27. Reflections from the end of the test cell seen through distilled water columns of length 1 ft, 2 ft and 5 ft.

For comparison, Fig. 28 presents the time-domain waveform for a 1 ft sample of tap water. The reflection from the top surface is similar to that shown in Fig. 26 for distilled water but the shorted-end reflection is significantly reduced. This indicates that the reflection coefficient for tap water is not greatly different from that of distilled water, but the tap water attenuates the signal considerably. The effect of the attenuation of tap water is even more markedly shown in Fig. 29 which presents the shorted-end reflections with 1, 2, and 5 ft samples of tap water. The 5 ft sample even shows substantial pulse spreading caused by dispersion. Employing the required frequency-domain procedures, the

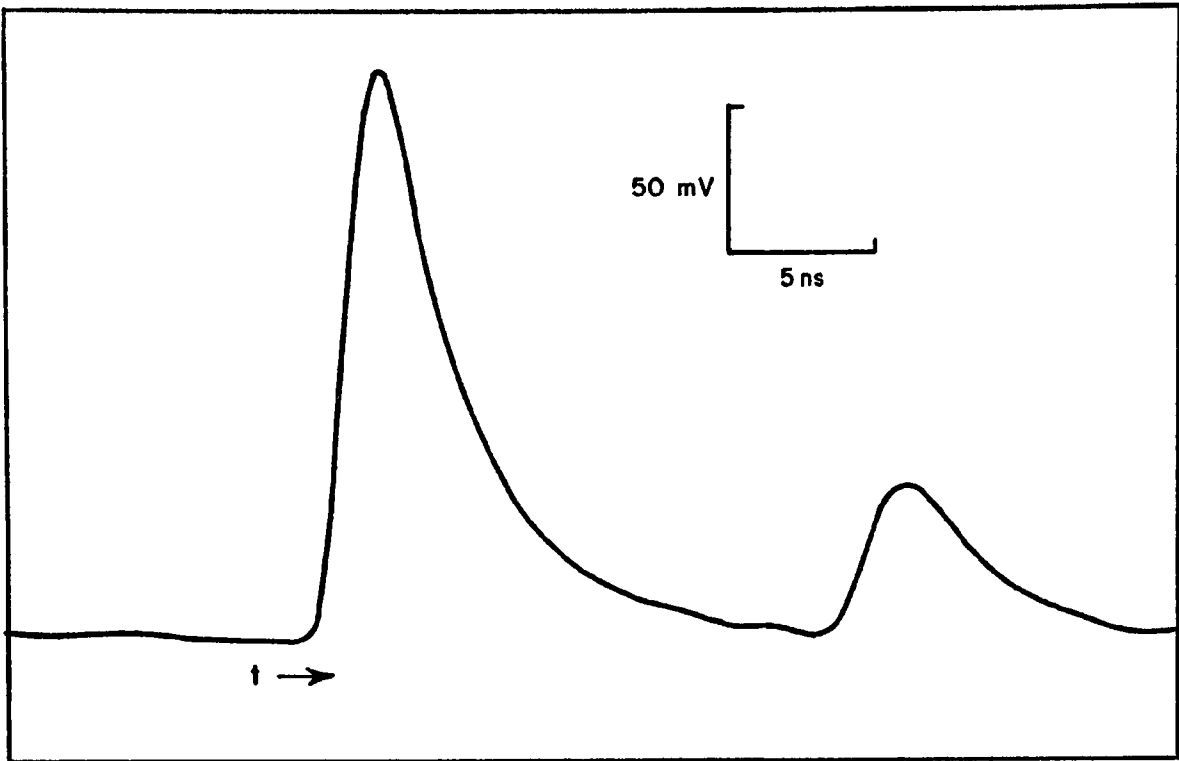


Fig. 28. Reflected pulses from a 1 ft sample of tap water in the test cell.

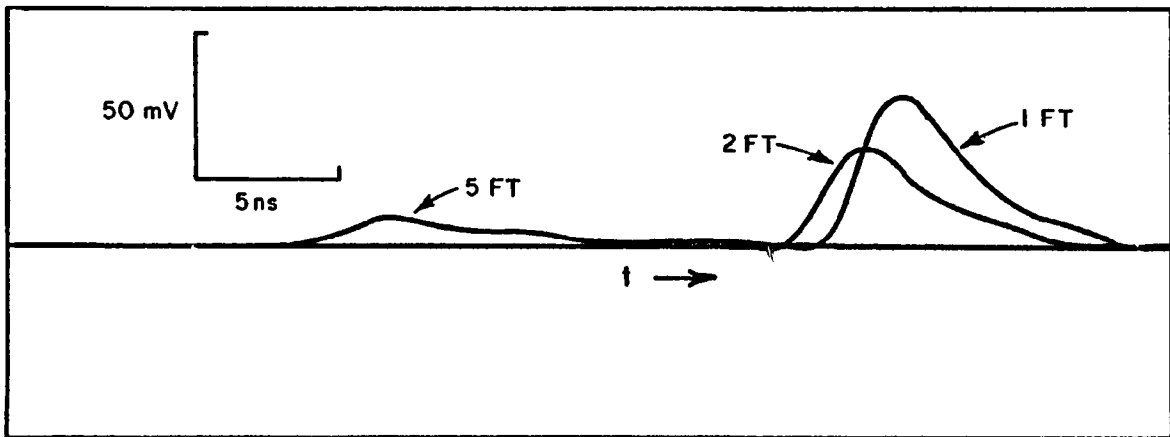


Fig. 29. Reflections from the end of the test cell seen through tap water columns of length 1 ft, 2 ft and 5 ft.

average magnitude of the reflection coefficient was nearly constant at 0.805 and the attenuation was constant at 2 dB/ft over the 20-500 MHz range.

For the remaining three materials (sand, sifted dirt and unsifted dirt), distilled water was added to a dry sample and the effect on the time-domain waveform and the reflection coefficient were noted as a function of time after the addition of the water. The amount of distilled water added was 200 mL in each case and the tube was sealed so that the amount of water present was constant.

The sand proved to be most informative because its small reflection coefficient and low attenuation made possible a study of the effect on both reflected pulses. Figure 30 shows the effect on the time-domain waveform of the addition of 200 mL of distilled water to 7 ft of dry sand. The immediate effect is evidenced (see 4 min. curve) by the sharp increase in the top surface reflection (most of the water being near this surface) and the corresponding decrease in the shorted-end reflection. The water permeates the sand rapidly with largest changes in the reflected pulses occurring within the first hour. After four hours from the time the water is added, little change in the pulse shapes is noted.

The effect of the percolation of the distilled water through the sand on the reflection coefficient from the front interface of the sample can be seen from Figs. 31 through 38 for the range of frequencies 20-500 MHz. This reflection coefficient is equal to $\sqrt{\mu/\epsilon}$ where μ and ϵ are the complex permeability and permittivity of the medium respectively. The moisture content influences the permittivity ϵ whereas the permeability is, in the absence of magnetic materials, that of free space. Notice from Fig. 31 that the magnitude of the reflection coefficient over the given frequency range is nearly constant for dry sand, while soon after the addition of water (as shown in Fig. 32) the reflection coefficient shows large variations over the same range of frequencies. These variations result from the presence of a water density gradient and hence a dielectric constant gradient. The reflections thus no longer occur at a single sharp boundary. Figures 32 through 38 give an indication of the percolation process. It can be seen that after 4 hrs (Fig. 35) the large variations have essentially vanished; and after 24 hrs (Fig. 38) the variation over the 20-500 MHz frequency range resembles the initial dry sand variation (Fig. 31) although the magnitude of the reflection coefficient is slightly larger. The attenuation for dry sand and for water saturated sand (after 24 hrs. percolation) are plotted in Fig. 39 over the frequency range 20-360 MHz.

No attempt has been made to correlate these data to those obtained by other experimenters because of the wide range of variables as has been noted in the summary.

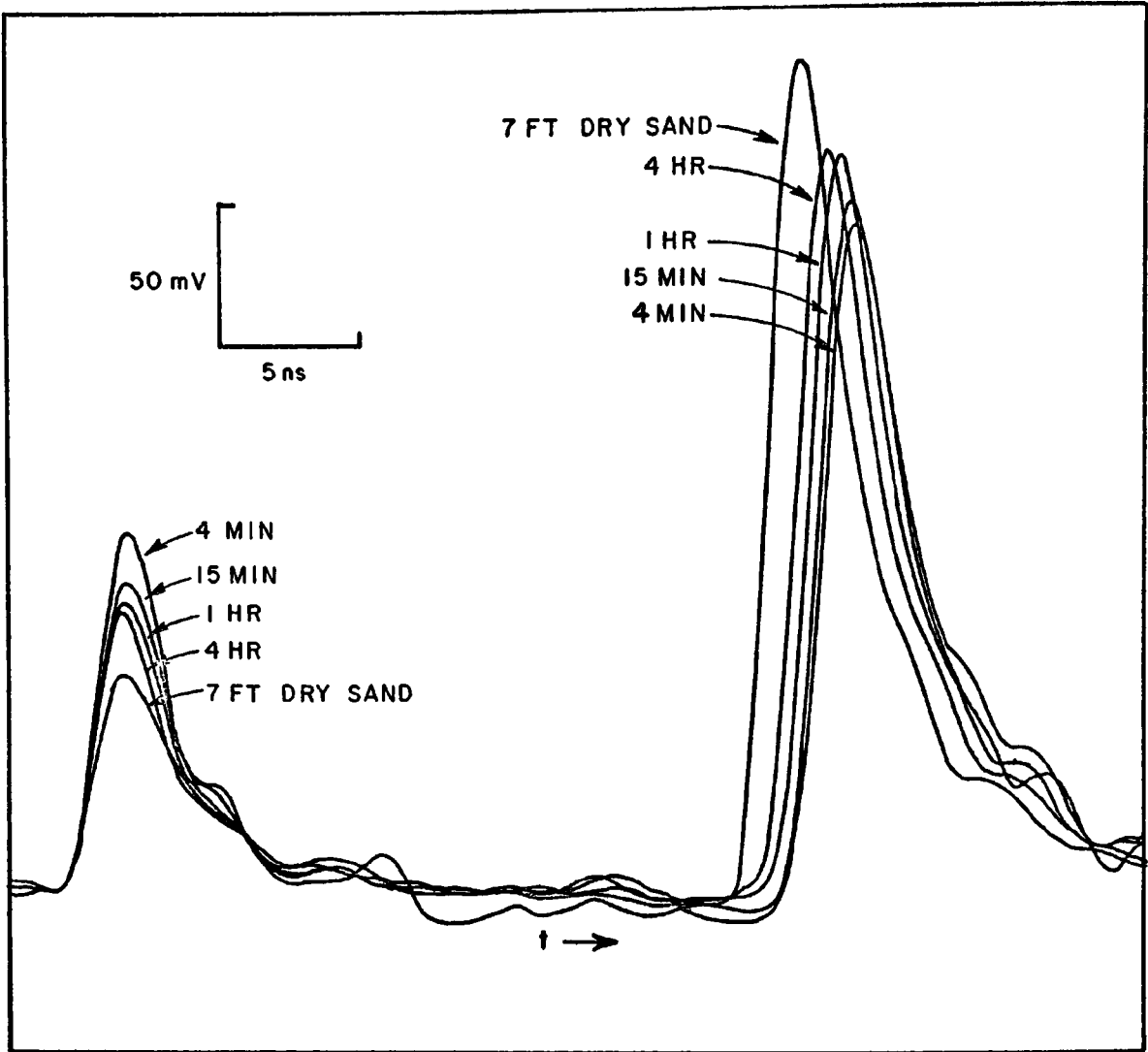


Fig. 30. Time domain waveforms for 7 ft of sand as a function of time after the addition of 200 ml of distilled water.

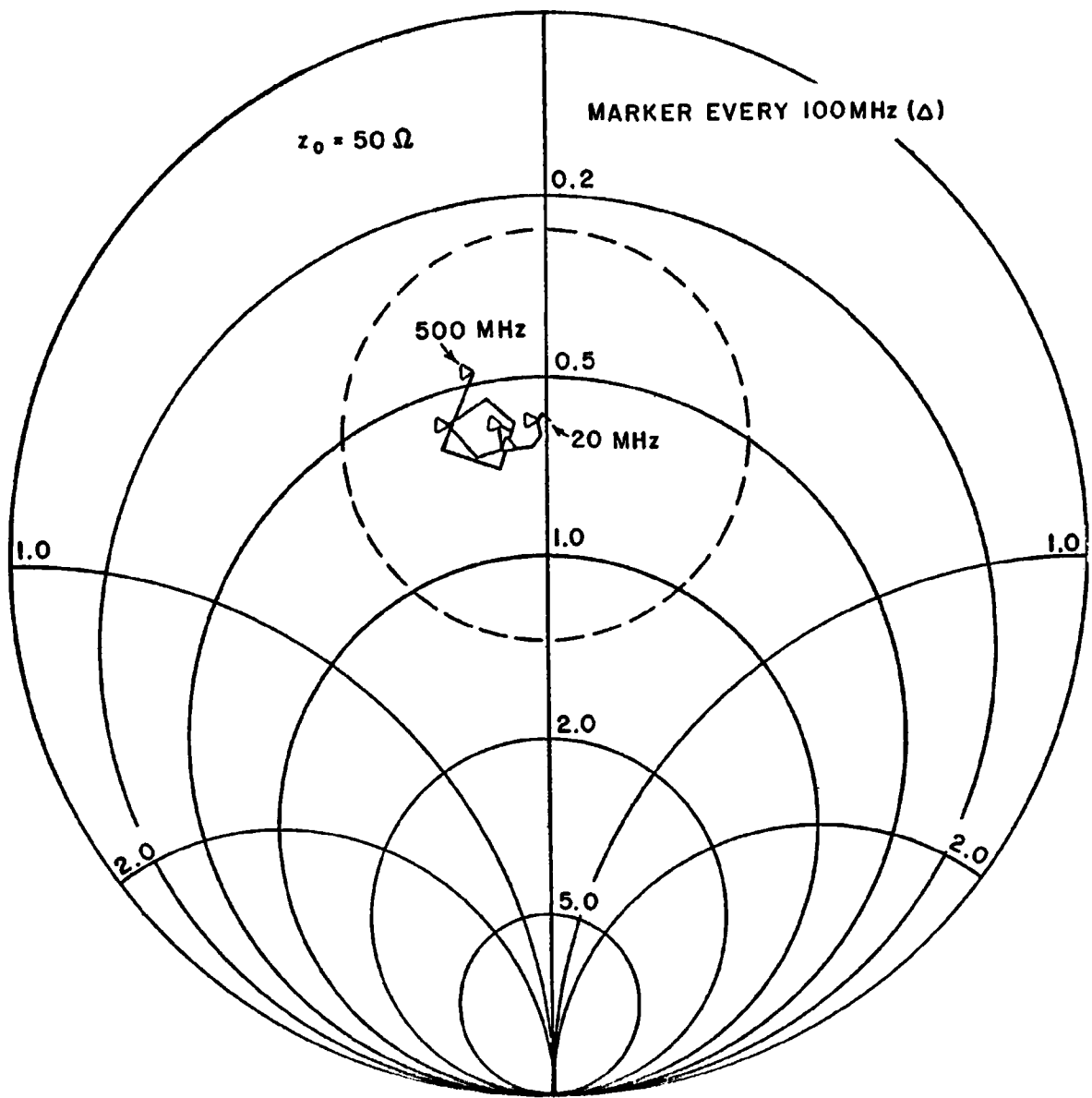


Fig. 31. Reflection coefficient from sand surface (dry).

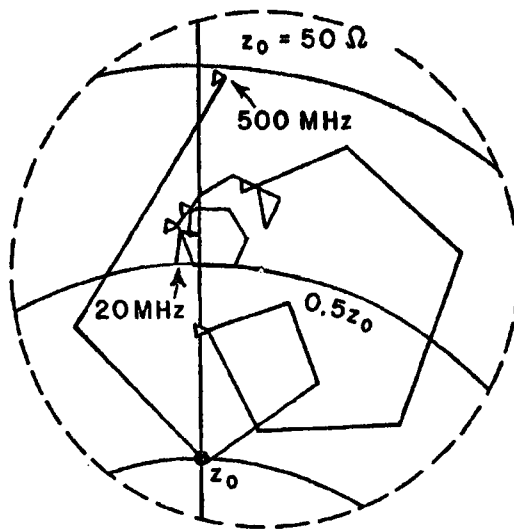


Fig. 32. Reflection coefficient from sand surface 4 min after adding 200 ml of water.

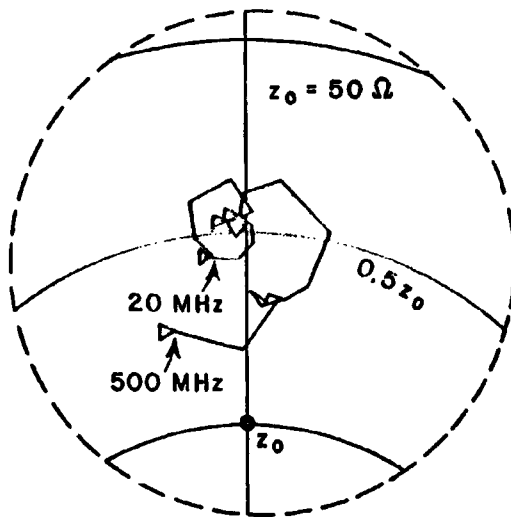


Fig. 33. Reflection coefficient from sand surface 15 min after adding 200 ml of water.

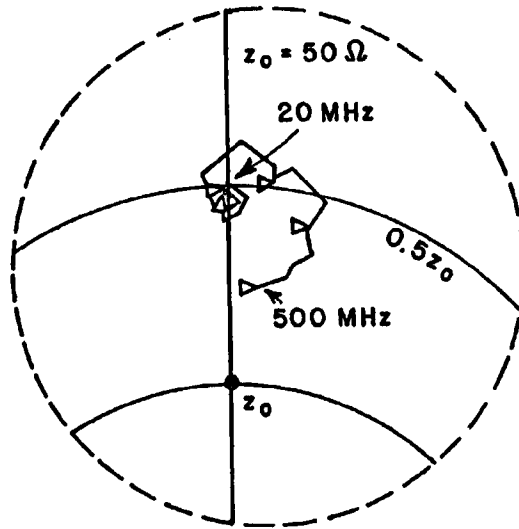


Fig. 34. Reflection coefficient from sand surface 1 hour after adding 200 ml of water.

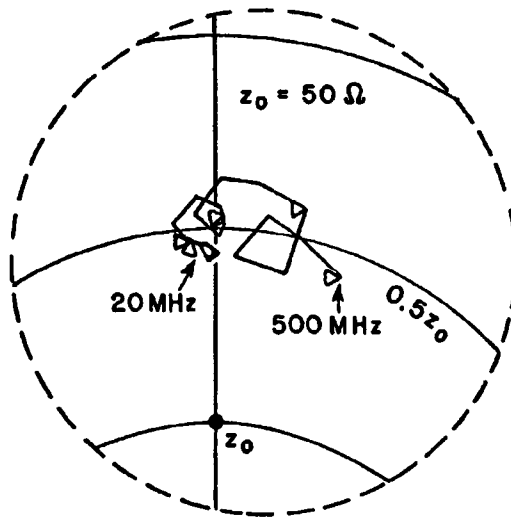


Fig. 35. Reflection coefficient from sand surface 4 hours after adding 200 ml of water.

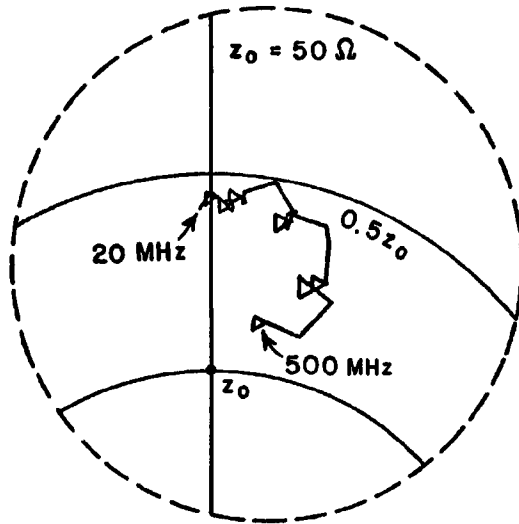


Fig. 36. Reflection coefficient from sand surface 16 hours after adding 200 ml of water.

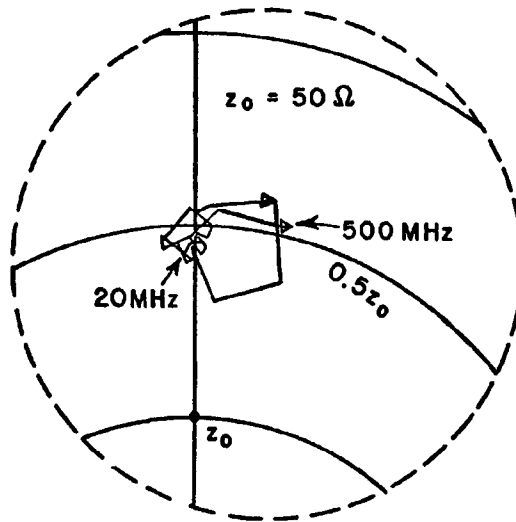


Fig. 37. Reflection coefficient from sand surface 19 hours after adding 200 ml of water.

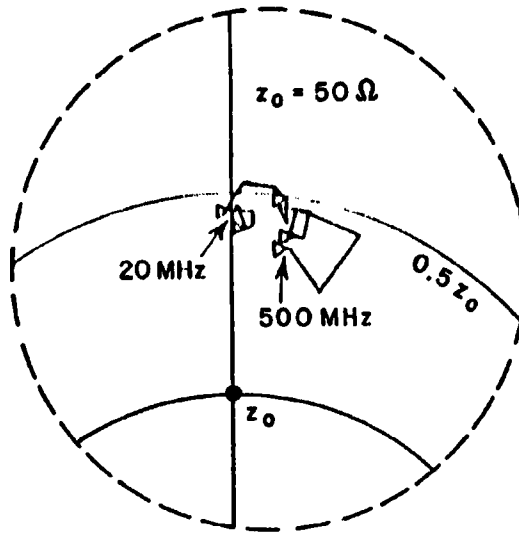


Fig. 38. Reflection coefficient from sand surface 24 hours after adding 200 ml of water.

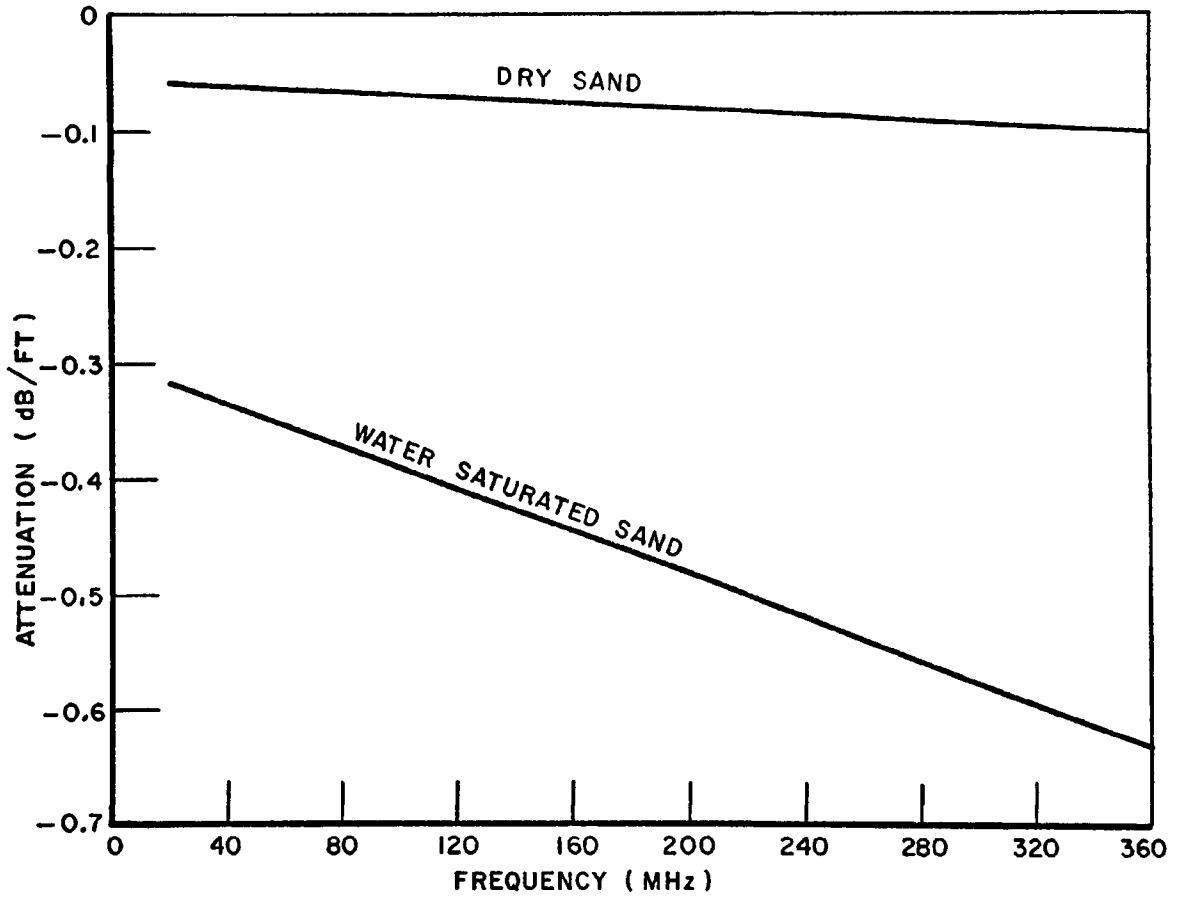


Fig. 39. Attenuation of dry and wet sand as a function of frequency.

Two dry potting soil samples were tested. One sample was sifted to form a powder while the other was only ground sufficiently to allow the soil to be placed in the tube with no attempt to sift out irregularities. (These samples had been open to the air in the laboratory for some time but had not been baked. Thus they undoubtedly contained some moisture initially.) As seen in Fig. 40 with 6 ft of dry sifted dirt in the test cell, the transmitted wave was able to penetrate the material and a reflection at the shorted-end was obtained. Using the frequency-domain procedures mentioned before, the attenuation for dry sifted dirt was relatively constant at 2.8 dB/ft over the range of frequencies 20-400 MHz.

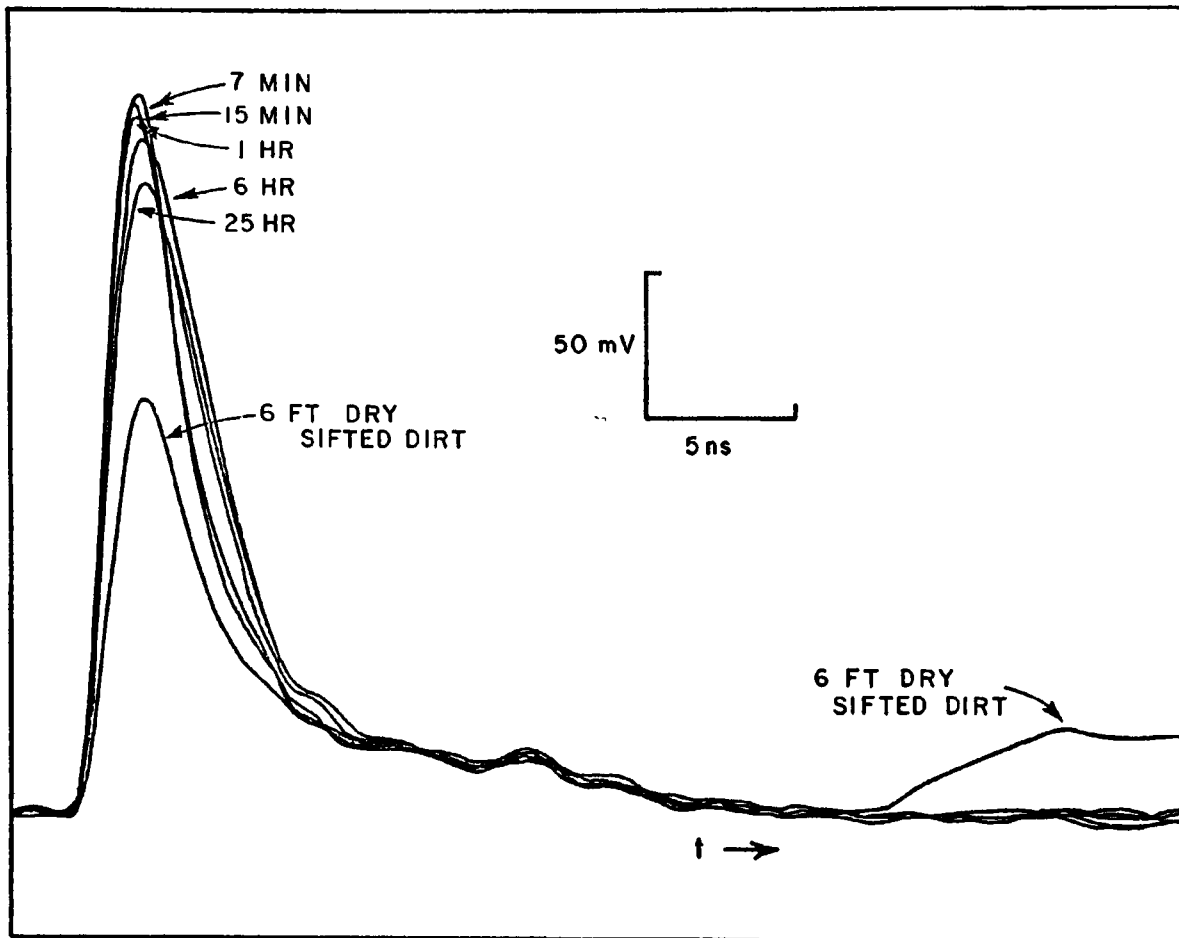


Fig. 40. Time domain waveform for 6 ft of finely sifted dirt as a function of time after the addition of 200 ml of distilled water.

Once the 200 mL of distilled water was added, the reflection at the shorting plate vanished, indicating the transmitted wave in the sample is greatly attenuated. Figures 40 and 41 show the time-domain waveform at different times after the addition of 200 ml of distilled water to finely sifted dirt and unsifted dirt samples, respectively. The variations of the reflection coefficient over the percolation time for the two dirt samples show similar changes as were noted in the case of the sand although the variations were not as regular. The general indication appears to be that the bulk of the water remained near the upper surface in the short time span of these measurements.

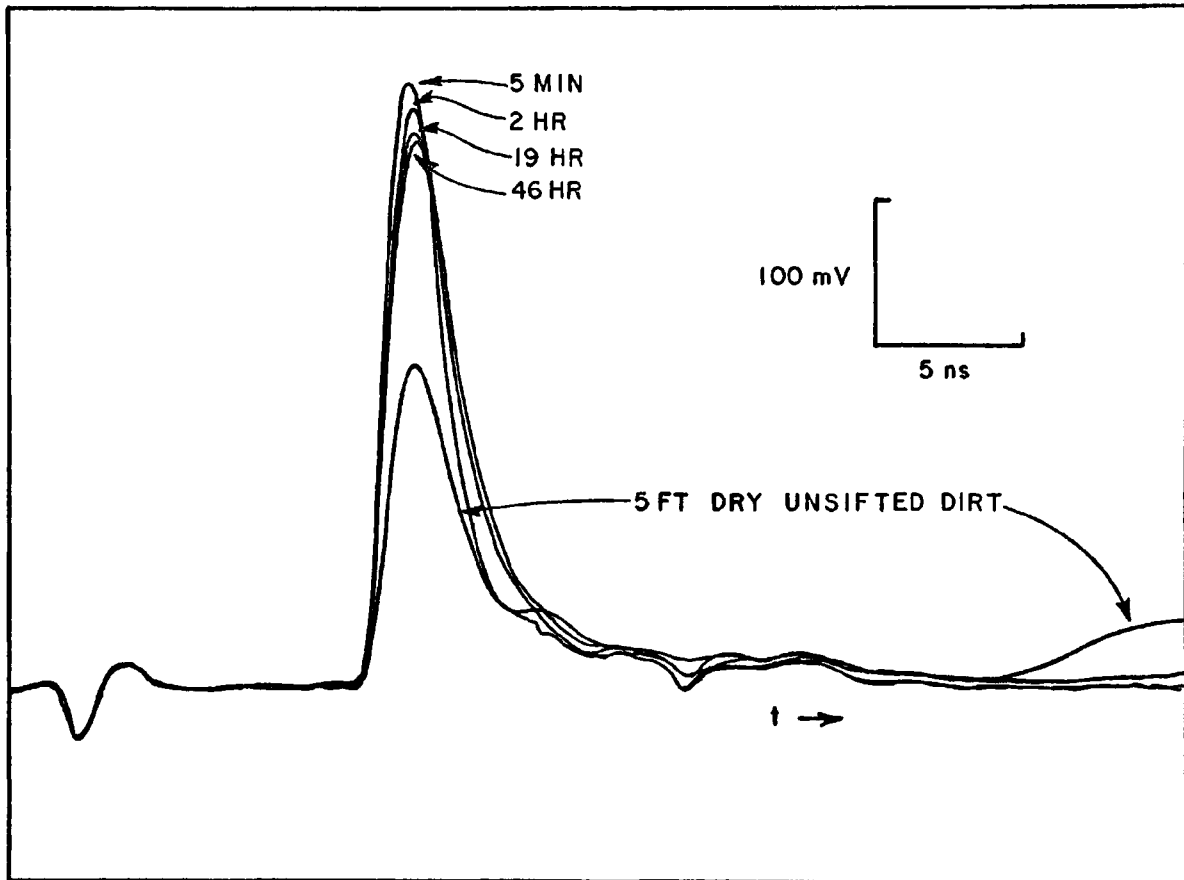


Fig. 41. Time domain waveforms for 5 ft of unsifted dirt as a function of time after the addition of 200 ml of distilled water.

In conclusion, a system has been developed that makes it possible to evaluate the electrical properties of the soil as a function of moisture content. These measurements in conjunction with the measured data of the preceding section and the theoretical analysis of the following section would make it possible to obtain the moisture content of the soil using either the scattered fields from buried cylinders or the attenuation caused by the lossy ground between antennas.

7. Propagation Calculations

A comprehensive analysis and computer program for all types of wire antennas and arrays of wire antennas in a homogeneous dissipative medium has been developed.* Linear dipoles, V-dipoles, rectangular loops, circular loops as well as arrays of such antennas can be handled by the program. The wire antenna can have a finite conductivity and certain arbitrary portions of the antenna can be enclosed by a thin dielectric sleeve. The output from the program provides a complete analysis of the system including self impedance, mutual impedance, current distributions, near-zone fields and far-field patterns. Briefly, the solutions are obtained via a piecewise-sinusoidal expansion for the unknown current distribution and Galerkin's method for reducing the integral equation formulation to a system of simultaneous linear equations. Because the present program will handle any type of finite wire antenna in an arbitrary homogeneous dissipative medium, it is felt to be a significant advance in the state of the art.

For the present purpose, the programs have been used to calculate the coupling between two parallel linear wire dipoles as a function of frequency, separation and the constitutive parameters of the homogeneous dissipative medium in which the antennas are embedded. It could also be converted to compute the scattered fields from a buried finite cylinder. Before presenting the results of these calculations it is appropriate to discuss in somewhat general terms the electromagnetic properties of the medium.

The propagation of electromagnetic waves in a homogeneous dissipative medium is governed, of course, by the constitutive parameters σ , μ and ϵ of the medium. Assuming an absence of magnetic material, the medium is characterized electromagnetically by a relative dielectric constant, ϵ_r , and conductivity, σ . For any real medium, these parameters are frequency-dependent. For rock and soil media, this frequency dependence can be grossly summarized as follows;¹ the relative dielectric constant is most strongly dependent upon frequency at low frequencies, i.e., frequencies less than 100 MHz, and displays rather slow changes at higher frequencies.

*The analysis and computer programs were developed by Prof. J. Richmond on several different contracts, and were not exclusively the result of studies on this grant.

In general, the relative dielectric constant increases with decreasing frequency and several orders of magnitude change between 1 MHz and 100 Hz is not unrealistic. Conversely, the conductivity is nearly constant at low frequencies (< 1 KHz) and displays a greater frequency dependence at higher frequencies. Conductivity generally increases with frequency, but it is possible at lower frequencies (< 1 MHz) to observe a decrease with increasing frequency over a limited frequency span.

Both the relative dielectric constant and the conductivity of a soil medium depend quite strongly on the moisture content of the medium. The moisture content of a soil medium obviously depends upon many factors, e.g. porosity, grain size, density gradient etc., but it is customary to lump these various parameters under moisture content for a given soil type. Measurements on prepared soil samples of silt loam and clay² have demonstrated that for frequencies above 300 MHz, both the conductivity and relative dielectric constant display roughly a linear dependence upon moisture content. Orders of magnitude increases in both parameters with moisture content increases from 10 to 40 or 50% (by volume) have been measured² at frequencies from 300 MHz to 35 GHz. Below 300 MHz, order of magnitude changes with moisture content are also possible, but at least below 1 MHz the parametric variations with moisture content are no longer linear.¹ In this frequency range, moisture content variations at low percentages are more noticeable. That is, a moisture content change from say 1 to 3% can produce an order of magnitude change in the conductivity and relative dielectric constant whereas a change from 20 to 25% cannot. The measured data discussed in this report that can be correlated to moisture content are in general above 1 MHz. It should be noted that the moisture content discussed above assumes a normal ion content for the water in the soil, i.e., the water contains salt or other possible contaminants. Scott¹ has noted that for a soil which has a heavy annual rainfall a leaching action can actually produce a decrease in relative dielectric constant and conductivity with increasing moisture content. It follows that the same effect could occur for either laboratory or in situ measurements of near surface soil taken some time after a heavy rainfall. We consider this effect to be anomalous since it does not conform to the general statements regarding moisture content, but recognize that in certain locales or possibly at a given locale during particular seasons it may well be necessary to take into account such an effect.

One possible method for deducing the moisture content of a given soil medium is to monitor the transmission between two antennas buried in the medium at a particular depth. Alternatively, one antenna might be at the surface of the soil and the other buried at some depth. We restrict ourselves here to the former case simply because the necessary modifications of the analysis and computer programs to account for the air-soil interface have not been completed. Pulse transmission, where the pulse has as broad a spectral content as possible, is suggested in order to obtain data, via fast Fourier transform procedures, over as wide a frequency range as possible. Using a comparison of measured data and theoretical calculations based on the experimental configuration and assumed constitutive parameters for the soil, the constitutive parameters and hence the moisture content

of the soil could be deduced. Certain disadvantages are obvious; the medium must be disturbed in order to install the antennas and a calibration of this perturbation would be required,* ground-truth data relating relative dielectric constant, conductivity and moisture content at a particular time over frequencies spanning the spectral content of the pulse are needed, and the constitutive parameters and moisture content deduced would be effective values averaged over some range of depths and the transmission path length.** The theoretical analysis assumes a homogeneous dissipative medium but this assumption does not preclude realistic computations of the pulse transmission. By reconstructing the pulse via a Fourier synthesis procedure³ using theoretical calculations at discrete frequencies, any desired frequency dependence of the constitutive parameters can be obtained. The method has the advantage that the installation can be permanent, and the measurements can be automated and remotely controlled. Field site visits could be eliminated and any desired time sampling rate of the moisture content obtained. The fact that the deduced moisture content must be correlated with constitutive parameter variations over a large range of frequencies would virtually eliminate the erroneous conclusions possible from measurements at one or two spot frequencies. Finally, for a specific soil type, it should ultimately be possible to tailor the spectral content of the transmitted pulse to exploit specific spectral characteristics of the medium.

Consider the single frequency cw transmission between two identical, parallel linear dipoles in a homogeneous dissipative medium. Assume that at each specific frequency, the sinusoidal input voltage to the transmitting antenna has a peak magnitude of 1 volt and that the receiving antenna is terminated in say a 50 ohm load. The magnitude of the received voltage across the fixed load as a function of frequency can be qualitatively deduced. At very low frequencies, the received voltage will be independent of the relative dielectric constant and determined strictly by the range and the conductivity of the medium. To deduce the dependence of the received voltage upon conductivity at low frequencies, one must carefully consider the physical situation being simulated by the analysis. If the ambient medium fills all of space including the gaps at the feed points of the dipoles then the d.c. and very low frequency received voltage should be inversely proportional to the conductivity. However, if the vicinity of the feed points is insulated from the medium (as would certainly be the physical situation since the feed point and feed cable at the feed would be encapsulated in an epoxy to withstand moisture deterioration) then the received voltage is proportional to the conductivity. Our analysis and

*For buried antennas as proposed in Fig. 24, this effect would be calibrated out of the system if attenuation per additional path length is the quantity to be measured.

**Again, the experiment of Fig. 24 would resolve these difficulties.

computer programs properly assume the latter situation. Over a span of lower frequencies the received voltage will remain relatively constant. Note that these idealized calculations assume frequency independent constitutive parameters. The attenuation constant of the medium therefore increases with increasing frequency. It does not necessarily follow however, for finite antenna elements, that the received voltage will uniformly decrease with increasing frequency. The input impedance of the antenna is a function of the size and shape of the antenna and the constitutive parameters of the medium. It is possible then, for a fixed load on the receiving antenna, to obtain a maximum received voltage at some finite frequency where the antenna impedance best matches the load. At still higher frequencies, the medium attenuation will again dominate. Gabillard et al⁴ have suggested a second "window" at still higher frequencies, but our calculations do not encompass this range.

Examples of the calculated received voltage under the above discussed limitations, i.e., a constant input voltage of 1 volt and frequency independent constitutive parameters, are shown in the following figures. In each case the antennas are identical 20 ft. linear dipoles (10 foot arms) made of 3/8 in. diameter perfectly conducting rods. The transmitting and receiving dipoles are oriented parallel to each other and the receiving dipole is terminated in a fixed 50 ohm load. In Fig. 42 the received voltage is shown as a function of frequency for a relative dielectric constant of 9.0 and conductivities of 0.003 and 0.1 mhos/meter. The effect of a dielectric sleeve ($\epsilon_r = 2.56$) with a diameter twice that of the conducting rod is also shown for a conductivity of 0.003 mhos/meter. Note that the theoretical calculations shown in Fig. 42 display a qualitative agreement with the measured attenuation curves shown in Figs. 16-19. A quantitative agreement would not be expected until the air-soil interface is included. It is interesting to note that the input admittance of the transmitting dipole is a maximum at the same frequency as that for which the received voltage is a maximum. The effect of the dielectric sleeve is apparent at low frequencies, but is barely noticeable in the region of maximum received voltage. Similar results are shown in Fig. 43 for the same configuration and conductivities of 0.1, 0.05 and 0.01 mhos/meter. In Fig. 43, the assumed relative dielectric constant is 15.0 and the dipoles are bare. Figure 43 also shows (dashed curve) the effect of changing the assumed relative dielectric constant to 9.0. This change only affected the 0.01 mhos/meter conductivity case and then only for frequencies above 1 MHz. This curve for $\sigma = 0.01$, $\epsilon_r = 15$ can be made to exhibit the resonance behavior shown in Fig. 43b simply by increasing the load resistor to 100 Ω . Altering this impedance would be difficult in practice but this calculation indicates the sensitivity of the experiment to the parameters of the system and emphasizes the need for careful design. Figures 42 and 43 both illustrate that as the conductivity of the soil is increased, the frequency for which the received voltage is a maximum becomes less distinct. Note also that the received voltage maximum increases with increasing conductivity and that the frequency of maximum received voltage decreases with increasing conductivity. In Fig. 44, results similar to those in Fig. 42 ($\epsilon_r = 9.0$, $\sigma = 0.003$) are shown but the separation of the dipoles has been doubled,

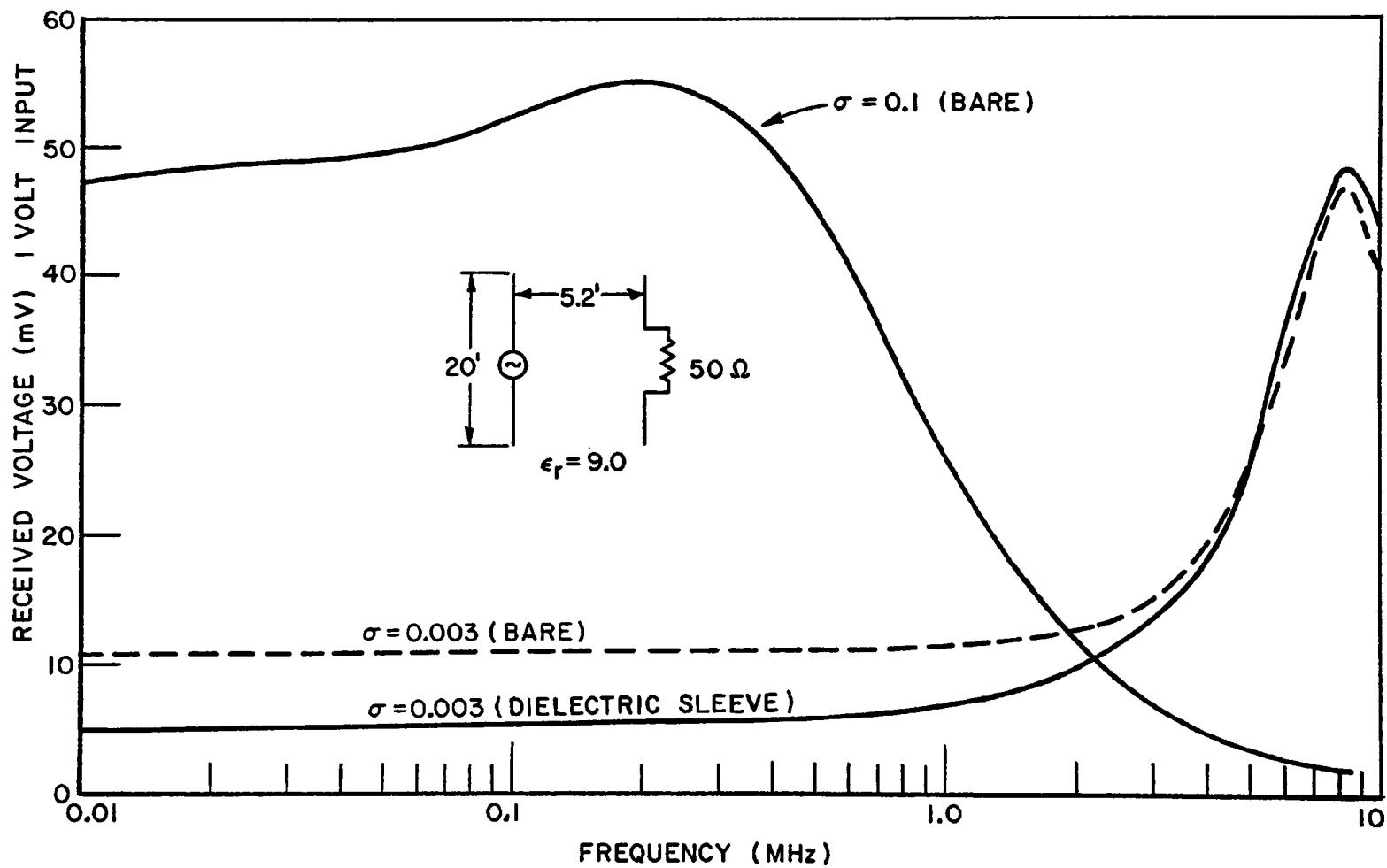


Fig. 42. Received voltage for transmission between two linear wire dipole antennas in a homogeneous conducting medium, 1 volt input.

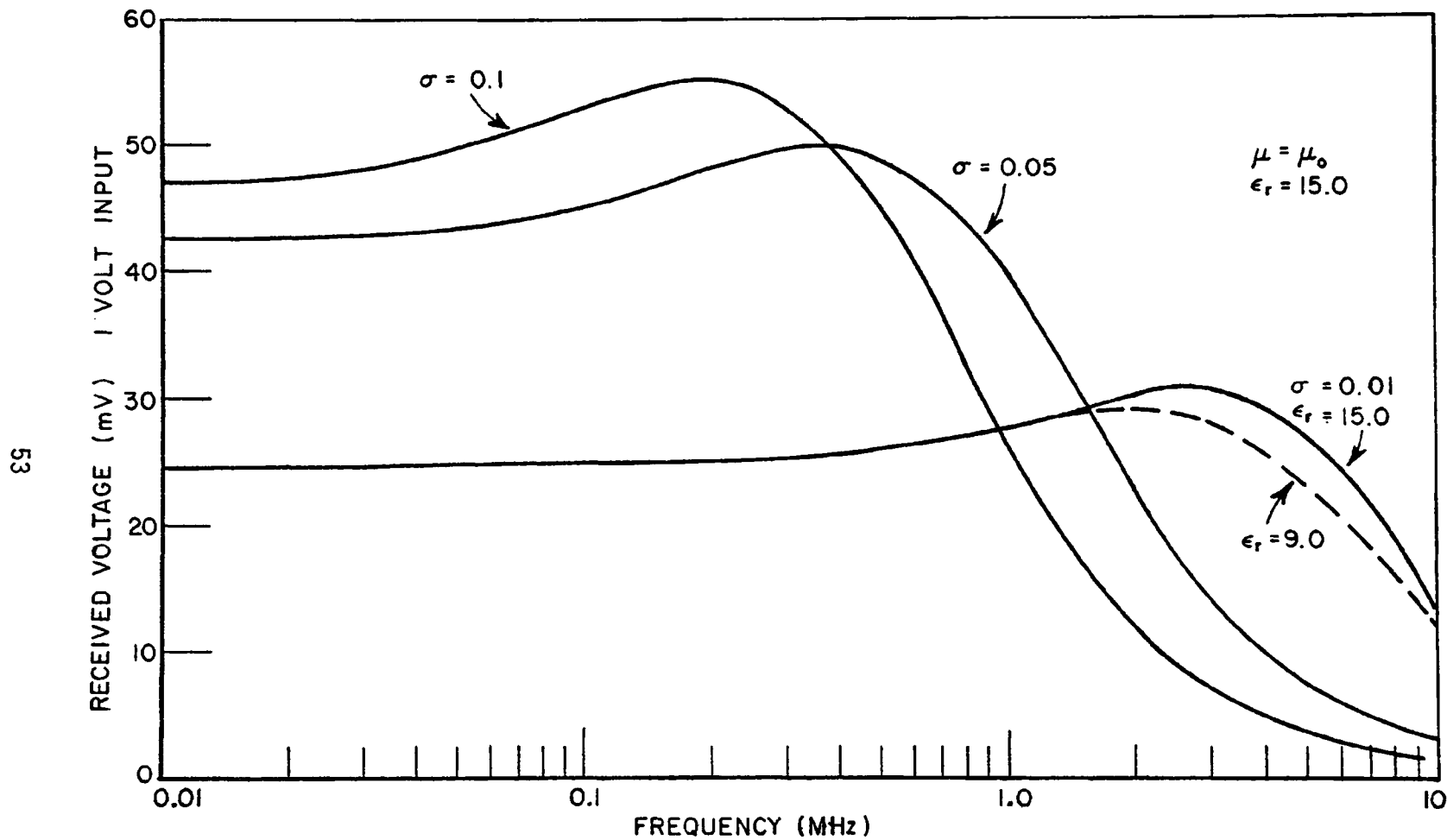


Fig. 43a. Received voltage for transmission between two linear wire dipole antennas in a homogeneous conducting medium, 1 volt input.

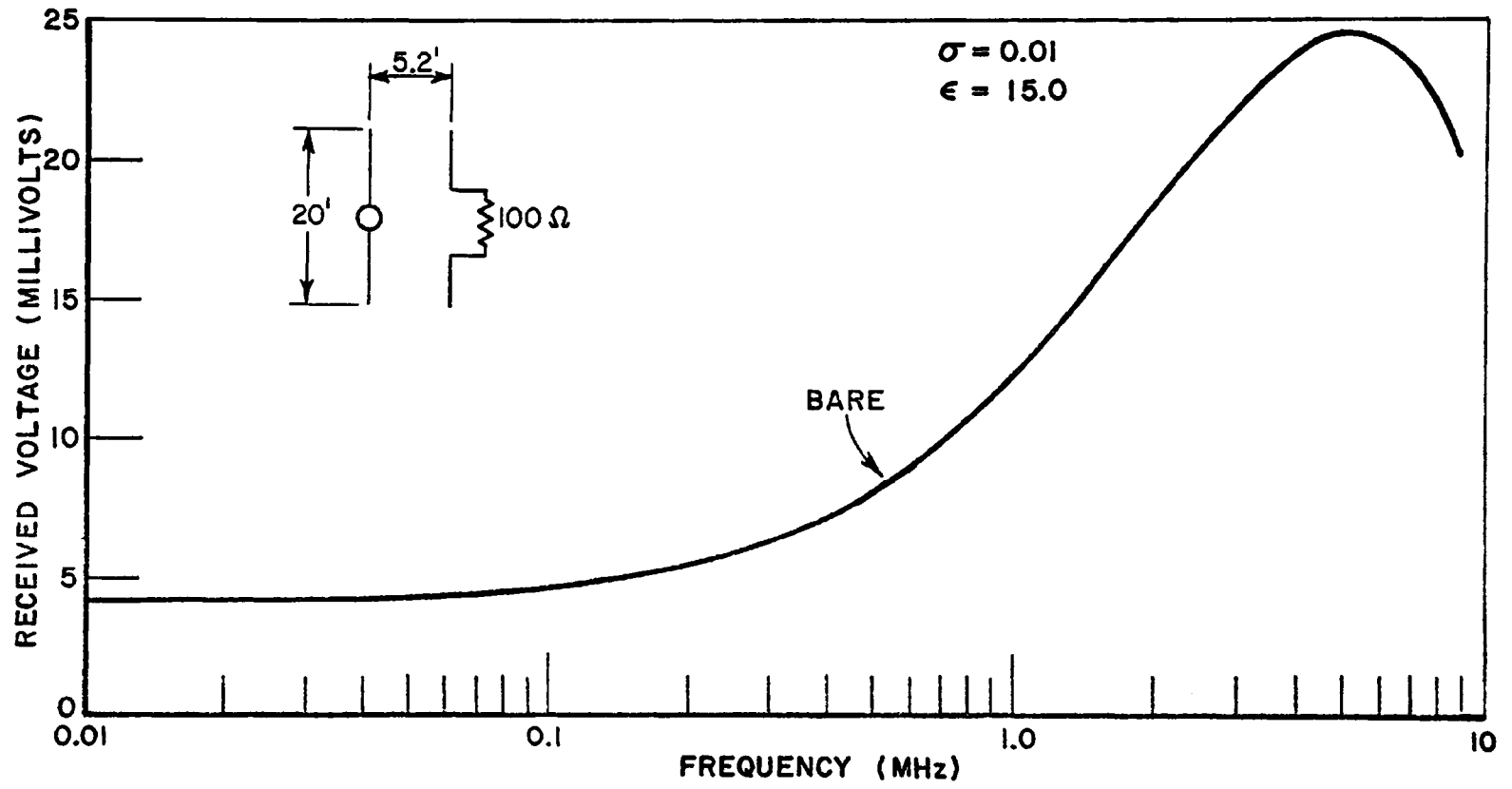


Fig. 43b.

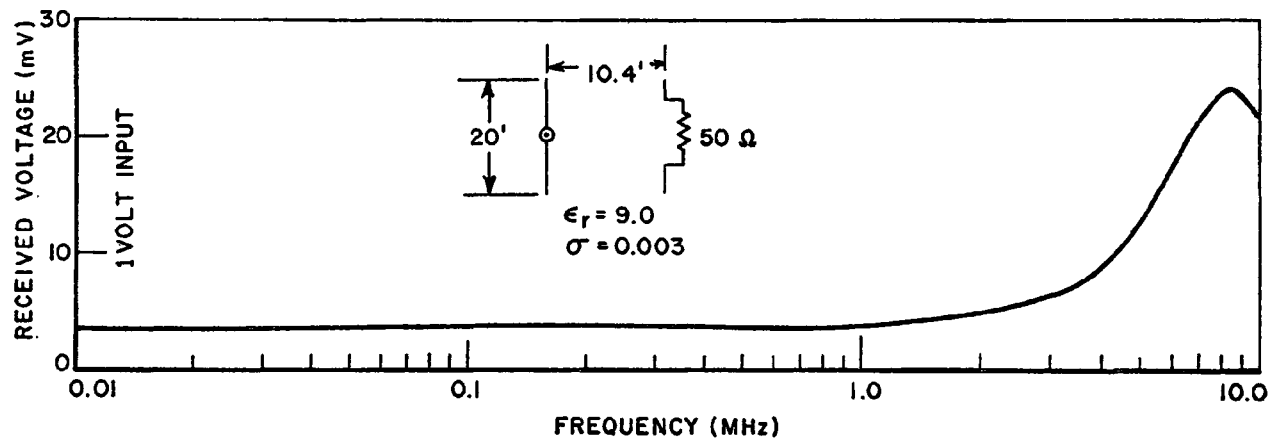


Fig. 44. Received voltage for transmission between two linear wire dipole antennas in a homogeneous conducting medium, 1 volt input.

i.e., from 5.2 feet to 10.4 feet. The frequency of maximum received voltage is unchanged, and the reduced magnitude at the frequency indicates an inverse dependence on range. In Fig. 45 predicted values of attenuation in dB per foot are shown for a soil medium with a relative dielectric constant of 15.0 and conductivities of 0.1, 0.05 and 0.01 mhos per meter. Note specifically the qualitative agreement between these curves and the measured attenuation given in Figs. 16-19. As noted previously, quantitative agreement would require modifications to include the air-soil interface or use of the antenna system of Fig. 24.

These computed results illustrate that the pulse transmission between two embedded dipole antennas in a soil medium contains numerous diagnostic tools for deducing the constitutive parameters and thereby the moisture content of the soil; the magnitude of the received voltage in the frequency range between 10 KHz and 1 MHz, the frequency of maximum received voltage, the "bandwidth" in the vicinity of maximum received voltage, etc. It is also clear that in the frequency range between 10 KHz and 10 MHz, where reasonable penetration is feasible, that the conductivity of the medium is more easily deduced than the relative dielectric constant. Thus moisture content diagnosis should be based on conductivity measurements. The calculated data demonstrate that the accuracy with which the conductivity and hence the moisture content can be determined is directly related to the magnitude of the conductivity. It follows that soils with large moisture contents will be most difficult to diagnose. Finally, it is postulated that the characteristics of the received pulse waveform such as rise time and decay rate may possibly provide even simpler tools for deducing the moisture content of the medium.

CONCLUSIONS

1. Electrically measurable quantities were observed which appear to correlate well with ground moisture content, at least for the one site and time period (a few months) which could be evaluated under this grant.

2. The experiments concentrated on field conditions, so that the preceding evaluation would be realistic in a practical sense. However, this approach precluded obtaining quantitative information for widely varying conditions, since conditions in the field cannot be controlled and are difficult to monitor.

3. The observed correlations were achieved by use of data processing possible only with pulsed signals. The utility of this approach is thus demonstrated.

4. Time and funds limited the investigation to reflections from a limited arrangement of objects (cylinders) and transmission between a single class of antennas (horizontal dipoles), and did

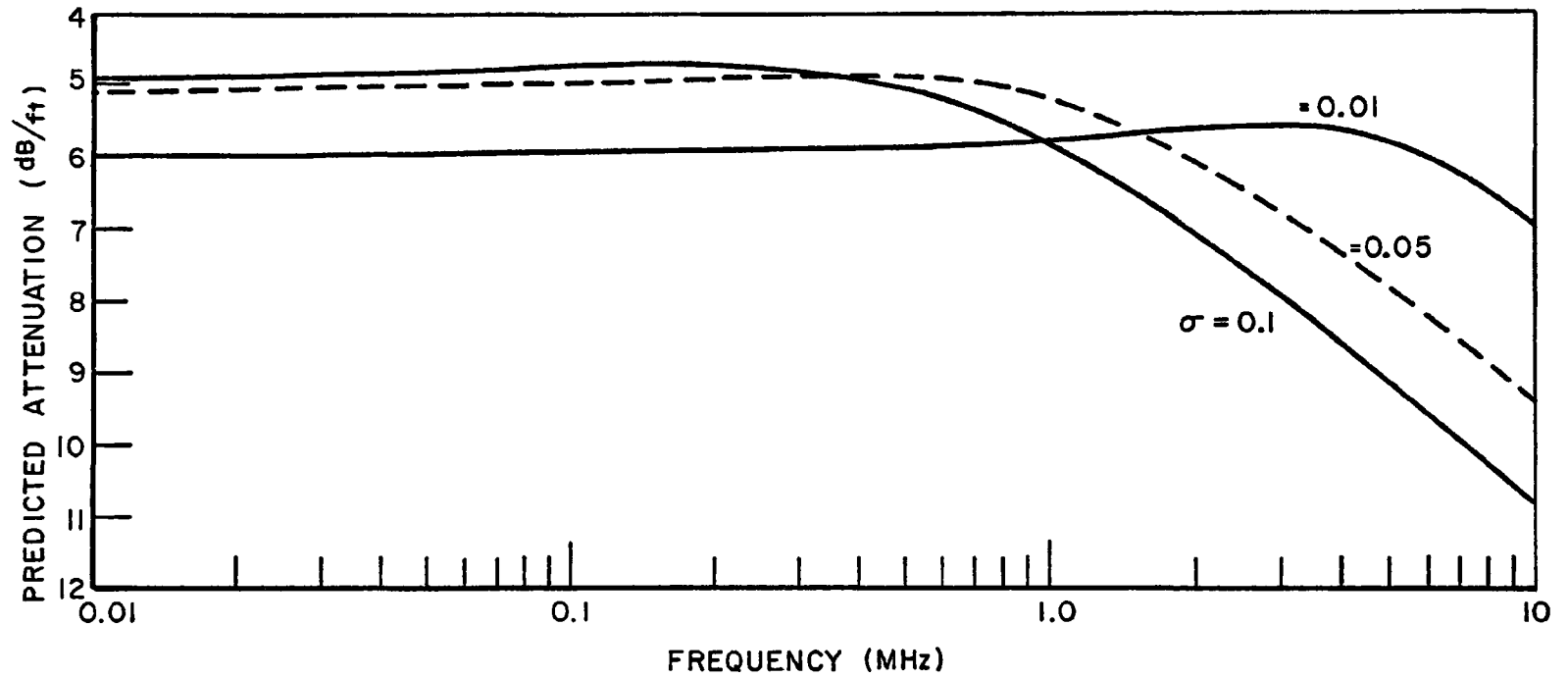


Fig. 45. Predicted attenuation for a homogeneous conducting medium.

not allow optimization with respect to clutter even within these arrangement restrictions. Thus there should be much room for improvement on these initial encouraging results.

RECOMMENDATIONS

1. The measurements which have shown reasonable correlation with moisture content should be continued in the field for at least one full year in order to observe as large a variety of conditions as possible.

2. Quantitative relations between the observables and moisture content need to be established. These can best be obtained by calculations and by laboratory measurements under controlled conditions. For example, the scattering from cylinders imbedded in lossy media should be calculated and the analytical results processed in the same way as the experimental results to obtain quantitative correlations. The transmission between antennas buried in a lossy medium should be analyzed and processed similarly. Calculations for other scattering and antenna configurations should be used to see whether better sensitivity can be obtained.

3. Calculation and measurement of the electrical effects of moisture in a medium consisting of a suspension of relatively lossless dielectric solids (such as silicates) in an electrolyte should be made as functions of the properties of the suspended material, the solute, and the water content.

4. Improvements in the sensitivity of the field-measurement apparatus should be continued as inventive ideas occur to the investigators.

5. While a sophisticated computer-controlled system is useful for the research, in which many different approaches are being considered, the goal should be to simplify the instrumentation once useful quantitative relations have been established. The end result should be a simple, rugged, and dependable instrument for field use.

6. Since the achievement of this goal depends on the interaction of calculations, laboratory experiments, field measurements, and instrumentation, this goal should not be expected to be realized from a short-term effort. A three-year period seems reasonable for the purpose. Of course, evaluation of progress on an annual basis and modifications of the proposed program and of funding on the basis of such evaluations would be quite in order.

REFERENCES

1. Scott, J. H., "Electrical and Magnetic Properties of Rock and Soil," AFWL Electromagnetic Pulse Theoretical Notes, Vol. 1, Note 18, May, 1966.
2. Lundien, J. R., "Terrain Analysis by Electromagnetic Means," Technical Report No. 3-693, U. S. Army Engineer Waterways Experiment Station, Corps of Engineers, Vicksburg, Miss.
3. Kennaugh, E. M. and Moffatt, D. L., "Impulse and Transient Response Approximations," Proceedings of the IEEE, Vol. 53, No. 8, August 1965.
4. Gabillard, R., Pierre Degaugue, and J. R. Wait, "Subsurface Electromagnetic Telecommunication - A Review," Transactions on Communication Technology, Vol. Com-19, No. 6, December 1971.

APPENDIX I - TRANSMISSION MEASUREMENTS USING A BURIED ANTENNA

The complete sequence of measurements made during the propagation path or transmission measurements is outlined. At the onset it is realized that only the transmission measurements are of sufficient accuracy largely because of the calibration system discussed in the text which could not be adapted to the reflection measurements.

The complete sequence was performed both with the 3 nsec pulse generator and with the Hewlett-Packard 214A adjusted for its shortest pulse width of 40 nsec. In addition the pulse transmission test was repeated with the Hewlett-Packard 214A with a pulse width of 2 sec. For the surface antenna measurements, the short circuit reference was a wire shorting the terminals of the twin lead. For the buried antenna measurements the short circuit was another four cable feed line identical to the one used to feed the antenna but with all four center conductors shorted together at one end. This made possible placement of the reference short the same electrical length down the cable as the buried antenna.

The data were processed to yield three quantities. The impedance of the underground antenna vs frequency, the impedance of the surface antenna vs frequency, and attenuation through the soil from the underground antenna to the surface vs frequency. Each of these quantities was calculated using data obtained with both the 3 ns pulser and the Hewlett-Packard 214A to yield information over different frequency ranges.

The impedance was calculated by dividing the Fourier transform of the reflected signal from the antenna terminals by the Fourier transform of the pulse incident on the antenna terminals. The result is the reflection from an incident impulse with magnitude one, which is the true reflection coefficient of the antenna. It may then be plotted on a Smith chart and interpreted as input impedance where the characteristic impedance is that of the cable feeding the antenna.

The exact process is shown in Fig. 46 through Fig. 50 for the buried antenna with the short pulser. Figure 46 shows the reflection from the antenna and from a reference short circuit at the antenna terminals. Note that in addition to the primary reflection there are some secondary echoes present. These are the result of multiple reflections between the balun transformer and the antenna. In Fig. 47 these multiple reflections have been range gated out so they will not affect the final result for both the antenna and short circuit termination. In Fig. 48 the short circuit reflection has been shifted in time to coincide with the initial antenna reflection thus eliminating the effect of slight differences in cable lengths. The antenna reflection is now converted to frequency domain via FFT and stored temporarily. Since the reflection coefficient of a short circuit is -1, the short circuit reflection is inverted to yield the incident pulse on the antenna terminals. This is also converted to the frequency domain and stored. Both frequency domain quantities are shown in Fig. 49. The last step is dividing the antenna

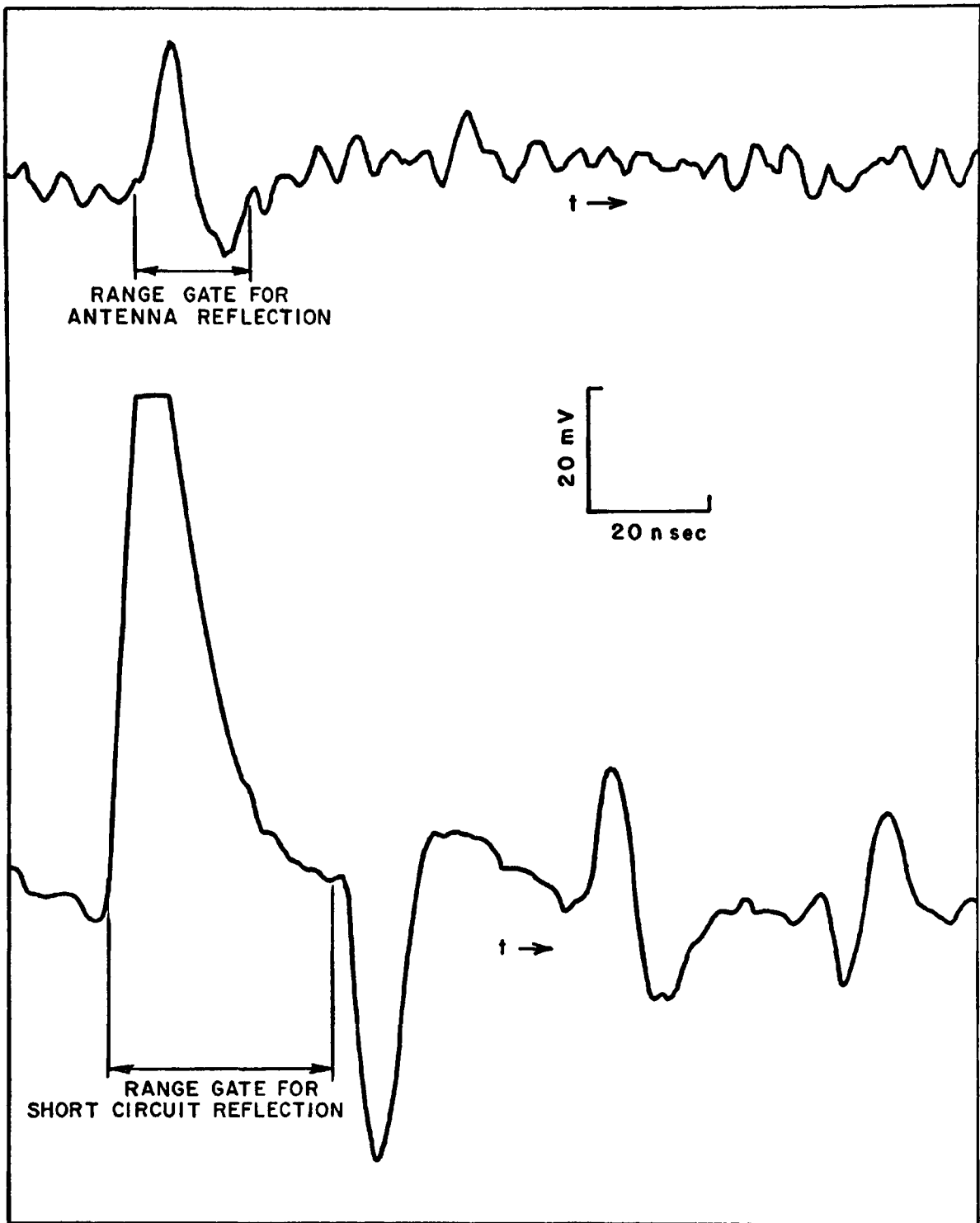


Fig. 46. Antenna and short circuit reflections before range gating.

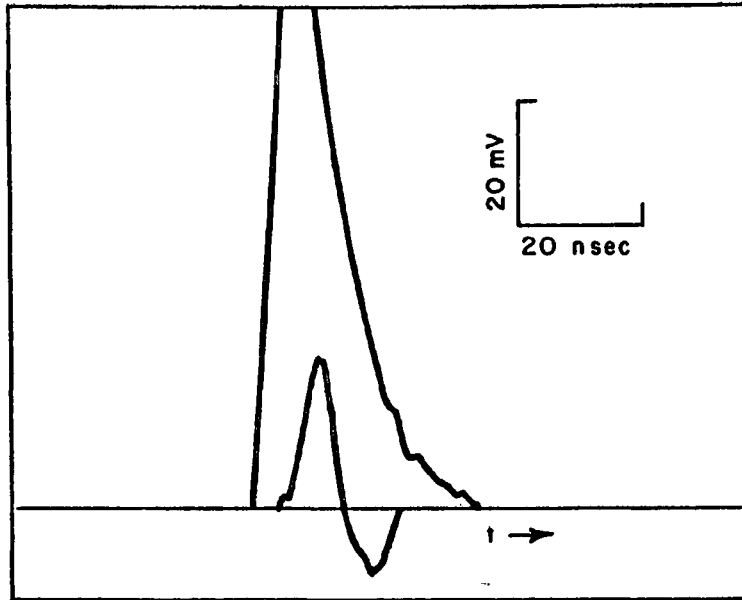


Fig. 47. Antenna and short circuit reflections after range gating.

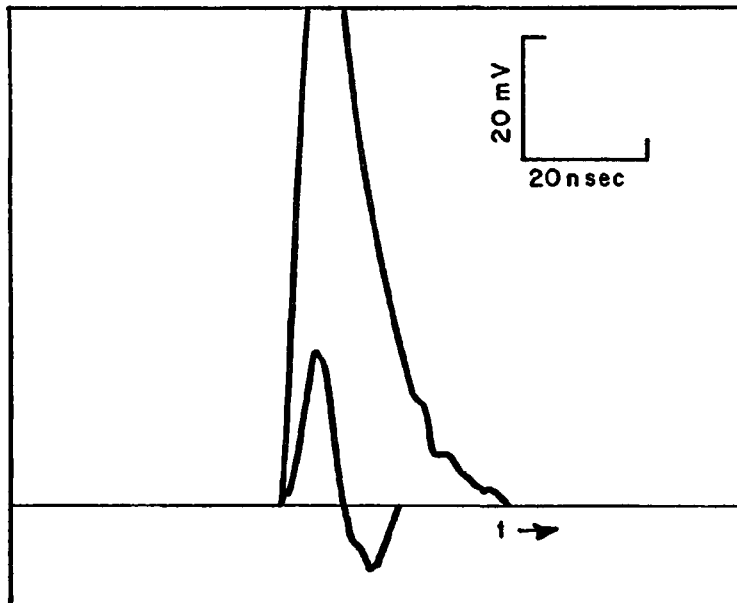


Fig. 48. Antenna and short circuit reflections aligned in time.

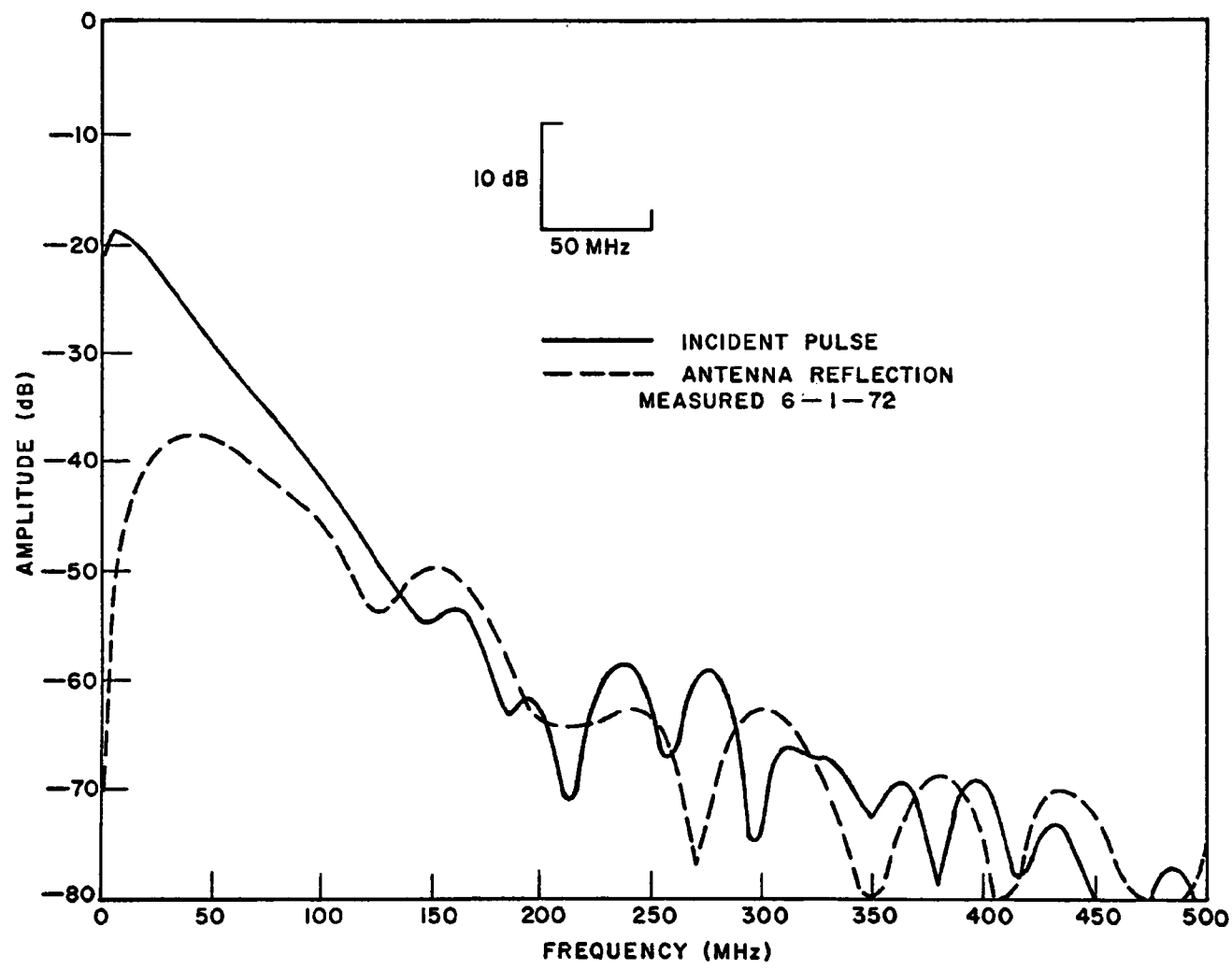


Fig. 49. Incident pulse and antenna reflections in frequency domain.

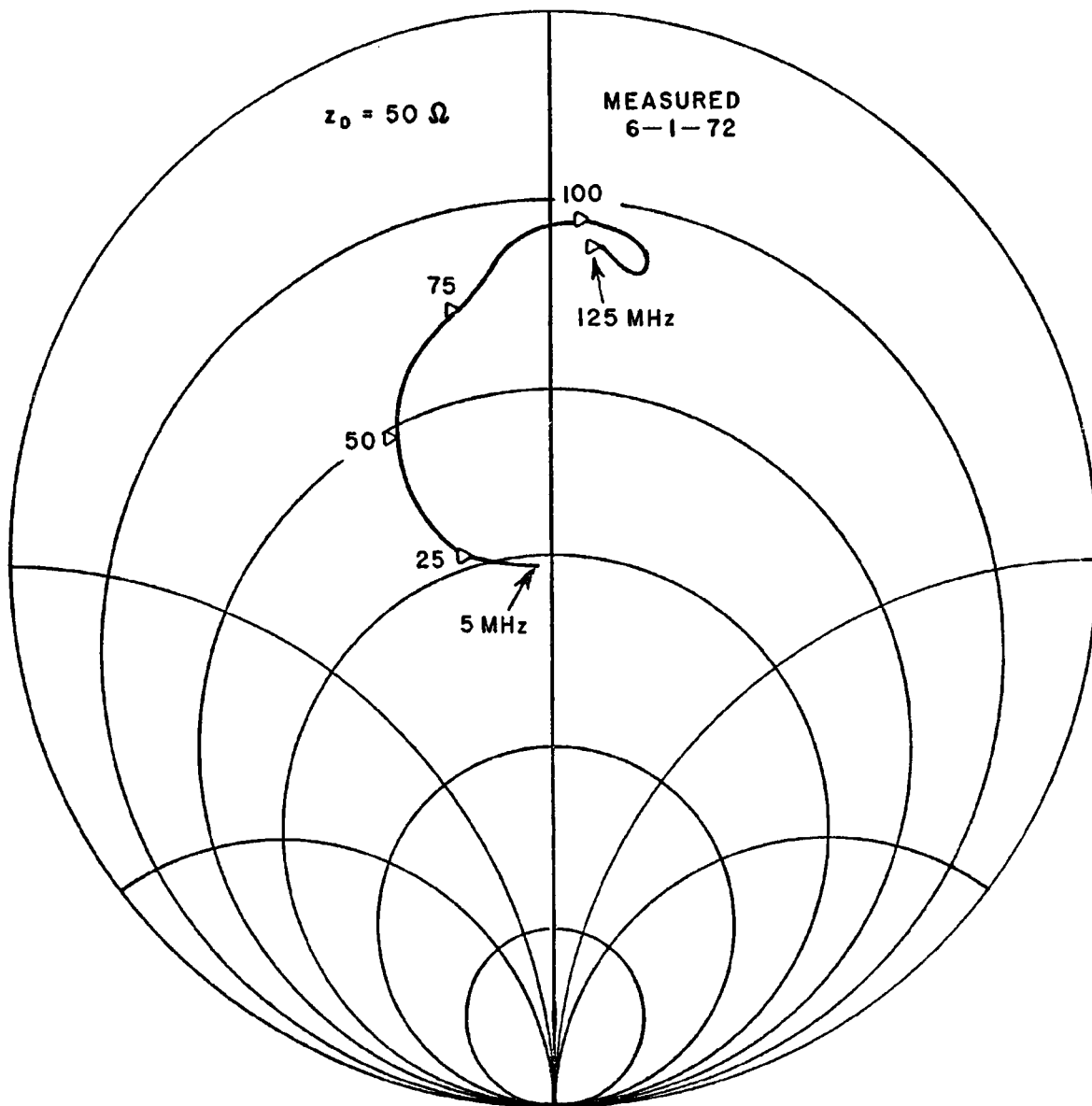


Fig. 50. Underground antenna impedance.

reflection spectrum by the incident pulse spectrum to get the true reflection coefficient of the antenna vs frequency. This is plotted on a Smith Chart as shown in Fig. 50. The characteristic impedance of the chart is 50 ohms the impedance of the line feeding the antenna. The impedance plot shown begins at 5 MHz and has markers every 25 MHz. In all cases the upper limit for valid impedance data was taken to be the point where the spectrum dropped into the noise or where the magnitude of the antenna reflection spectrum exceeded that of the incident pulse spectrum. This would have resulted in a reflection coefficient greater than one which is invalid.

There are several sources of error in this measurement including the different length of range gate used for the short circuit reference measurement and the antenna impedance measurement. Because of these errors, consistent correlation of antenna reflection coefficient and moisture content could not be obtained either for the buried antennas or the surface antennas. The Smith Chart plot of Fig. 50 is one of the better antenna impedance measurements made in this study. The others are not included because they contain no additional information.

The transmission data were taken over the three paths of 5, 7.5 and 10 ft. as shown in Fig. 51 for the short pulser. The three measurements were then converted to the frequency domain via FFT giving the spectra of Fig. 52. Now taking the difference between the 5 ft and 7.5 ft path transmission or the 7.5 ft and 10 ft. path yields attenuation in dB/2.5 ft. Likewise taking the difference of the 5 ft and 10 ft path transmission yields attenuation in dB/5 ft. These are shown in Fig. 53. These measurements were repeated using the Hewlett Packard 214A at its 40 nsec pulse width setting. An example is shown in Figs. 54-56. Note the frequency scale is half that of the short pulse measurements. A third set was taken with the 214A with a pulse width of 2 μ sec and these are illustrated in Figs. 57-59.

It is clear from these data, that reliable information is contained in the frequency band below 20 MHz. Because of the design of the antenna, reliable information is also restricted to frequencies above 1 MHz.

The transmission data exhibited some unusual effects and a definite trend as discussed in the report. The noise level of the transmission data taken with the short pulser began to rise steadily after the month of March for unexplained reasons. Thus the short pulsed data over the last two months of the program is considered unreliable. No apparent trends could be observed in this data.

The data taken with Hewlett-Packard pulser exhibited one unusual effect noticed only in this series of measurements which recurred several times. Generally in a homogeneous dissipative medium attenuation would be directly proportional to path length; thus in our case the same increase in attenuation would be expected when comparing the 5 ft path with the 7.5 ft path as when comparing the 7.5 ft path with the 10 ft path.

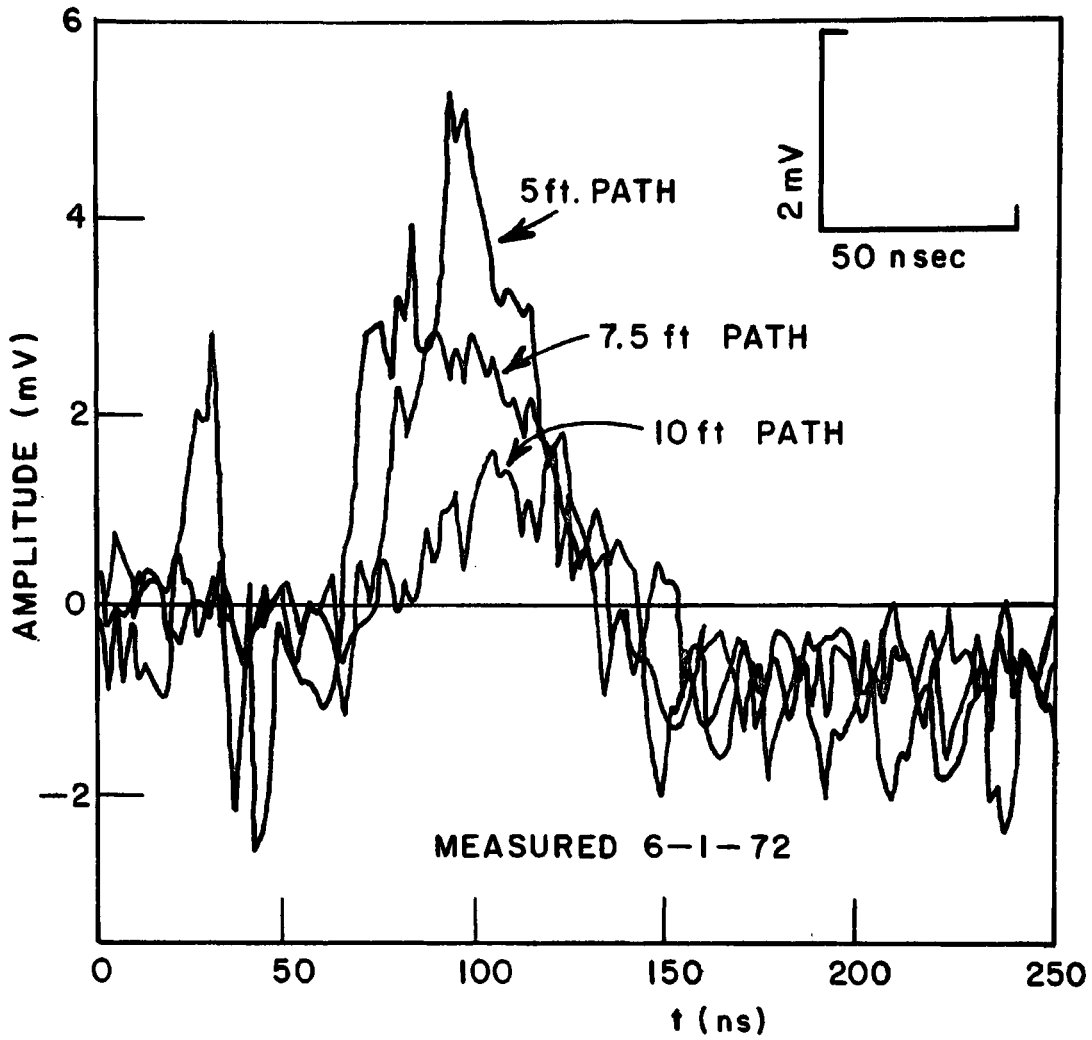


Fig. 51. Pulse transmitted from the buried antenna to the three surface antennas.

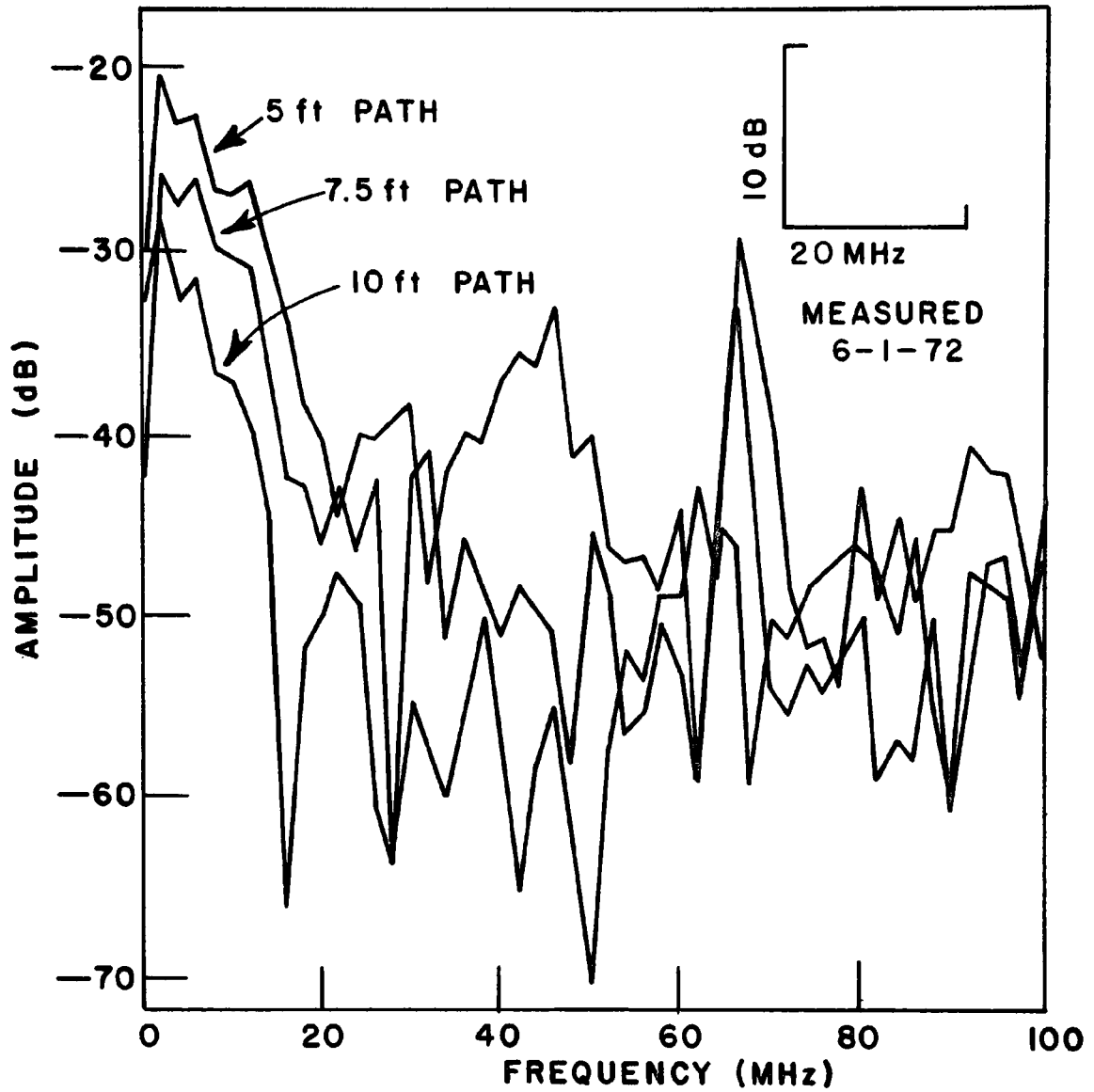


Fig. 52. Pulse transmitted from the buried antenna to the three surface antennas (frequency domain).

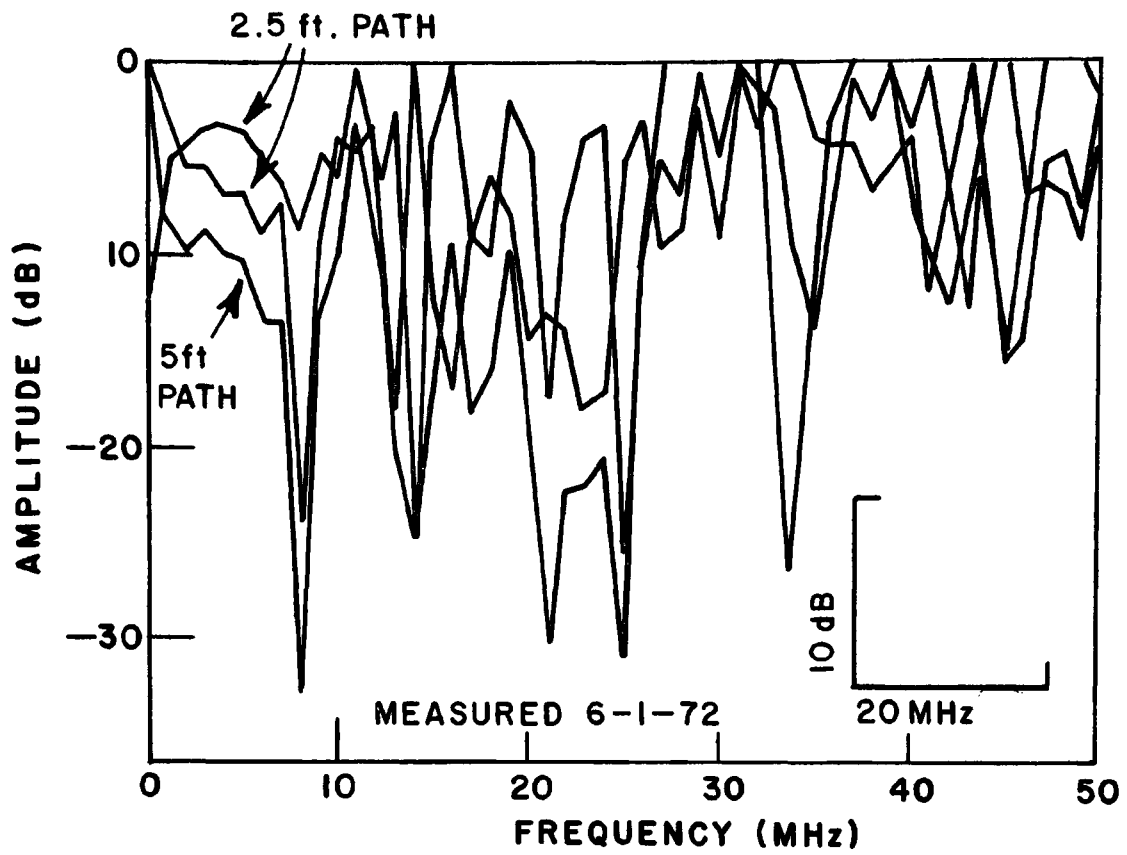


Fig. 53. Attenuation vs frequency for 2.5 ft and 5 ft path differences.

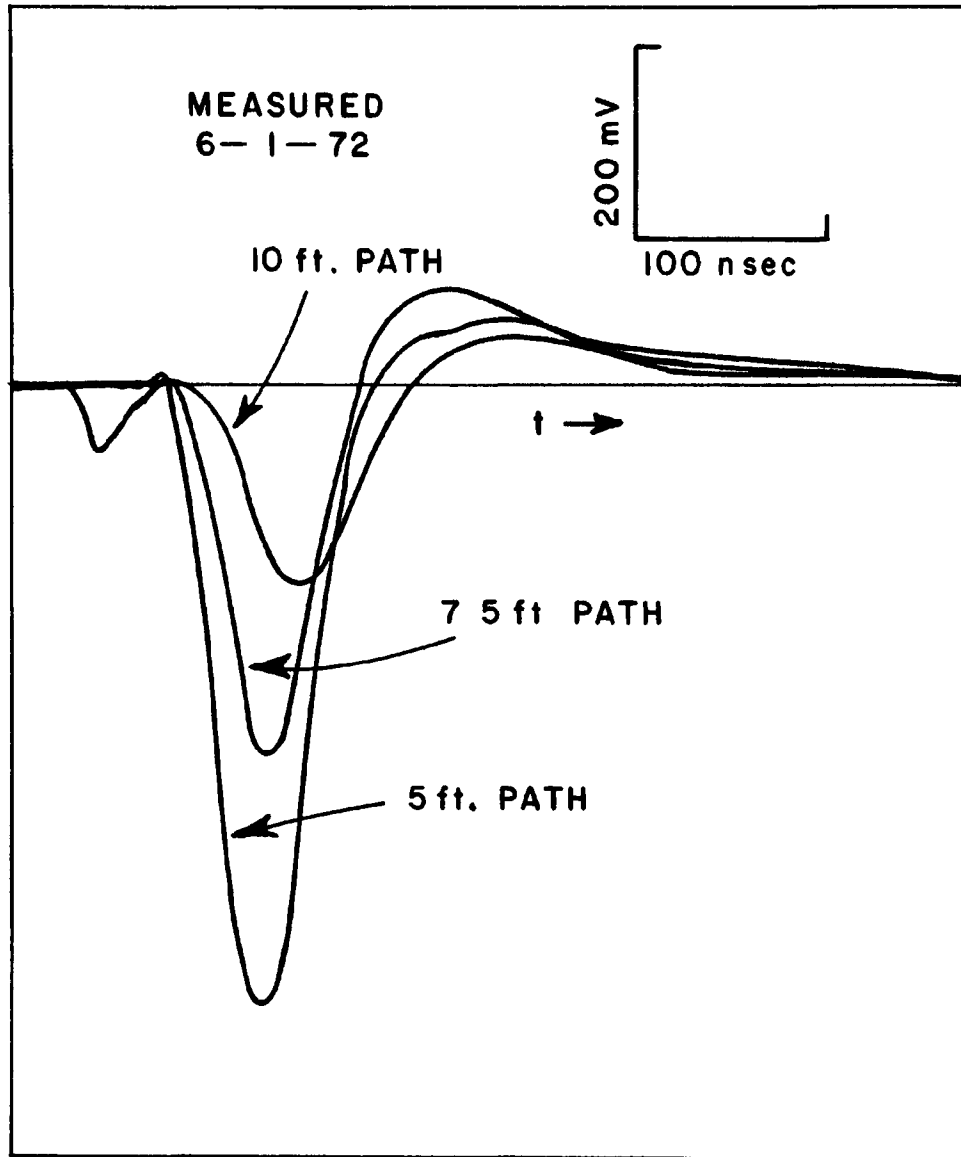


Fig. 54. Pulse transmitted from buried antenna to the three surface antennas (H.P. pulser).

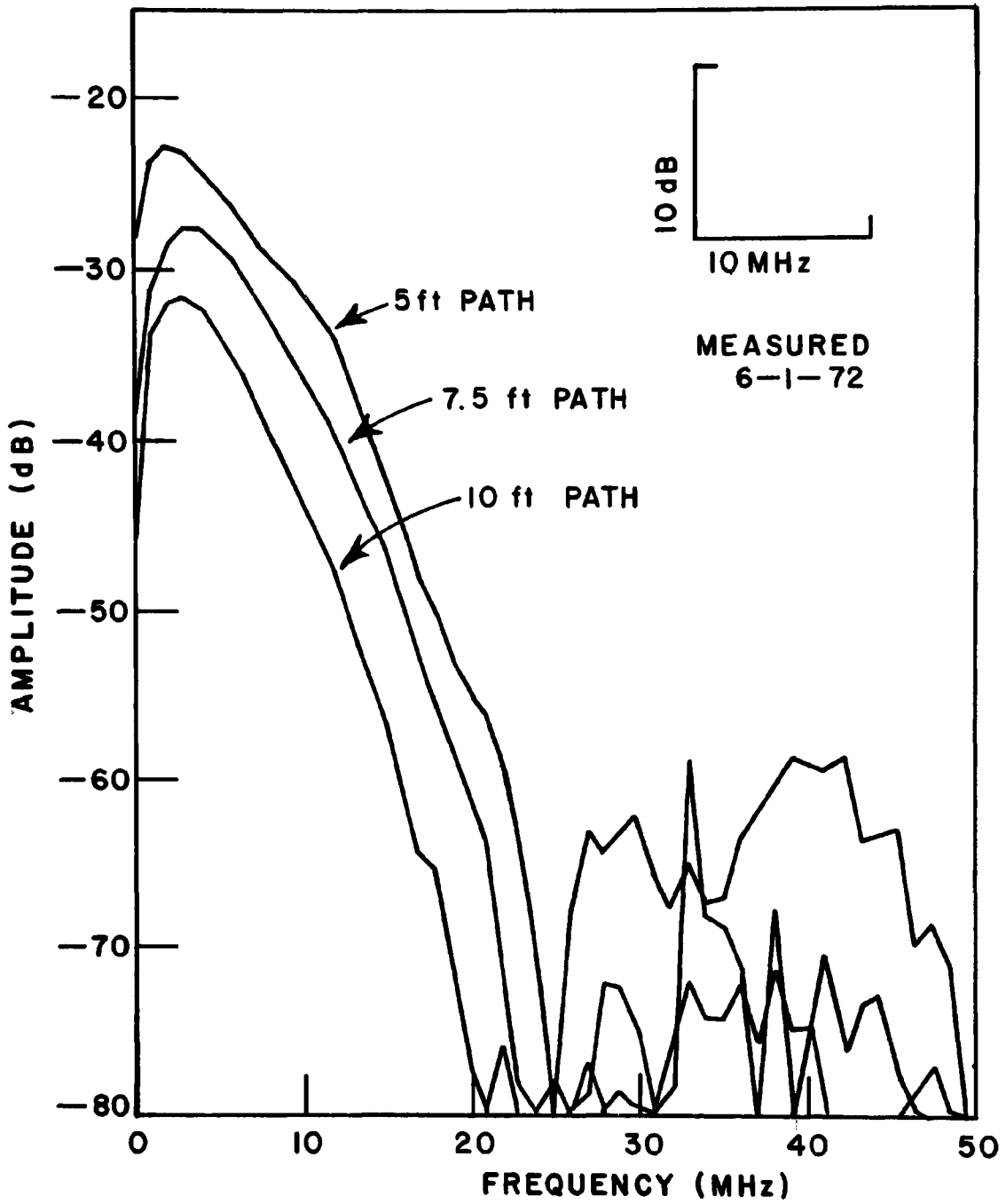


Fig. 55. Pulse transmitted from buried antenna to the three surface antennas (H.P. pulser, frequency domain).

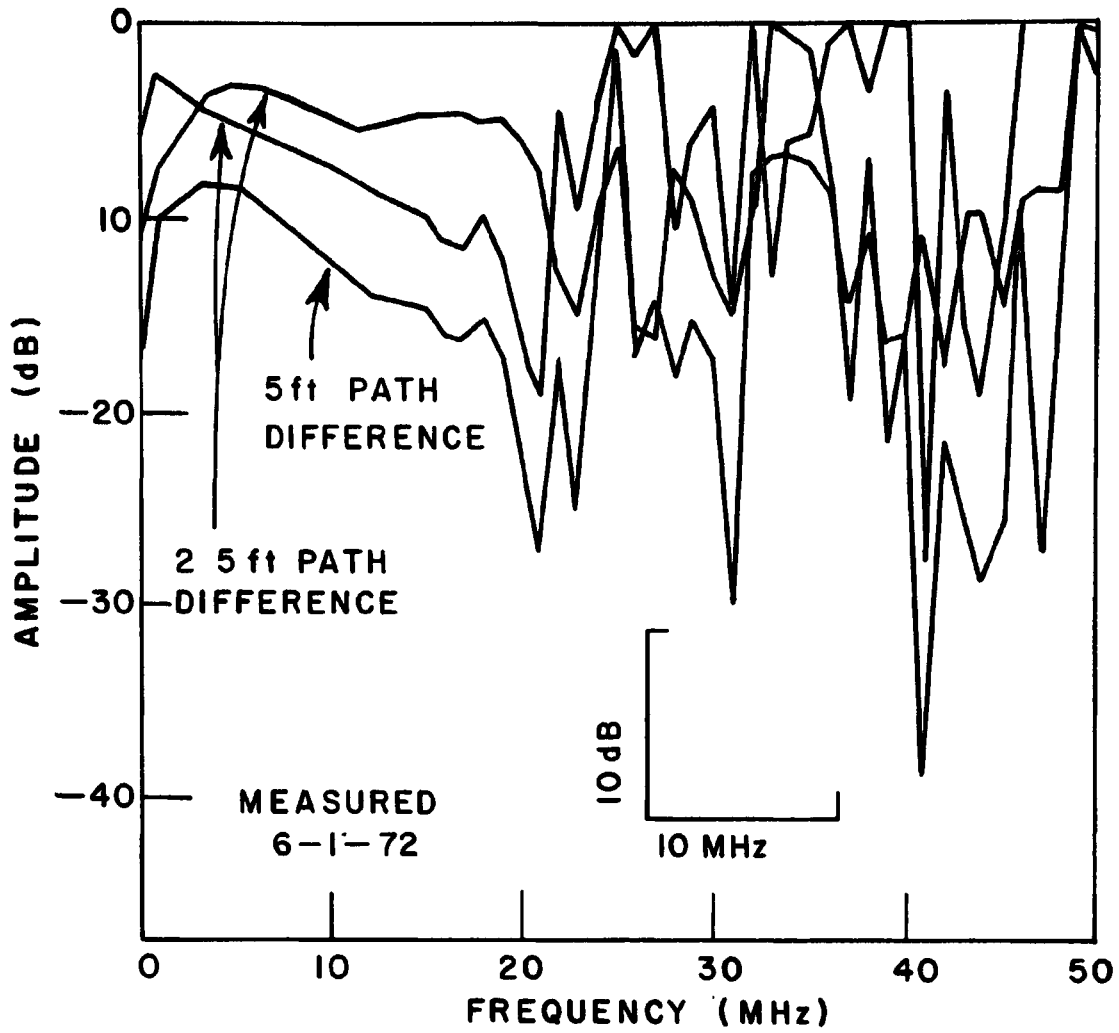


Fig. 56. Attenuation vs frequency for 2.5 ft and 5 ft path differences.

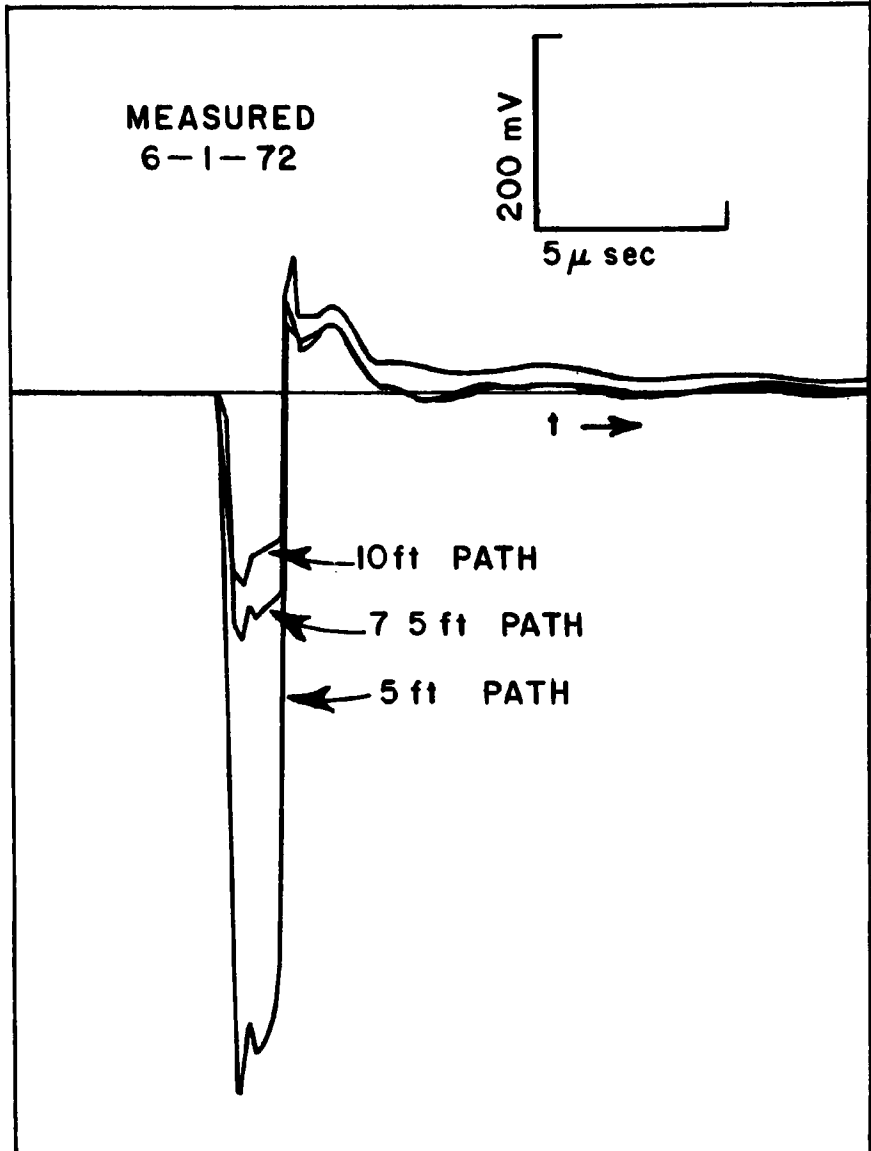


Fig. 57. Pulse transmitted from the buried antenna to the three surface antennas (H.P. pulser, low frequency).

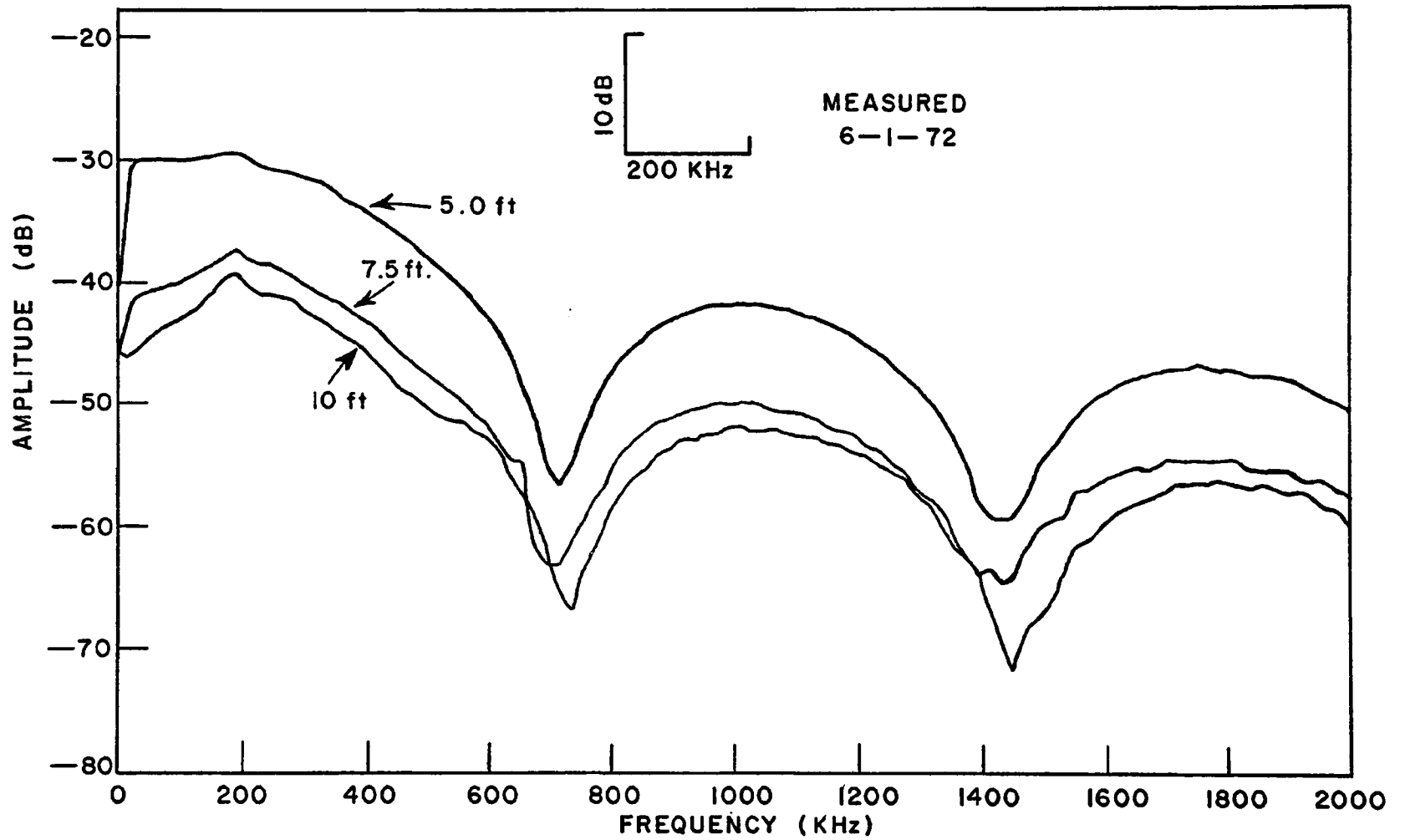


Fig. 58. Pulse transmitted from the buried antenna to the three surface antennas (H.P. pulser, low frequency, frequency domain).

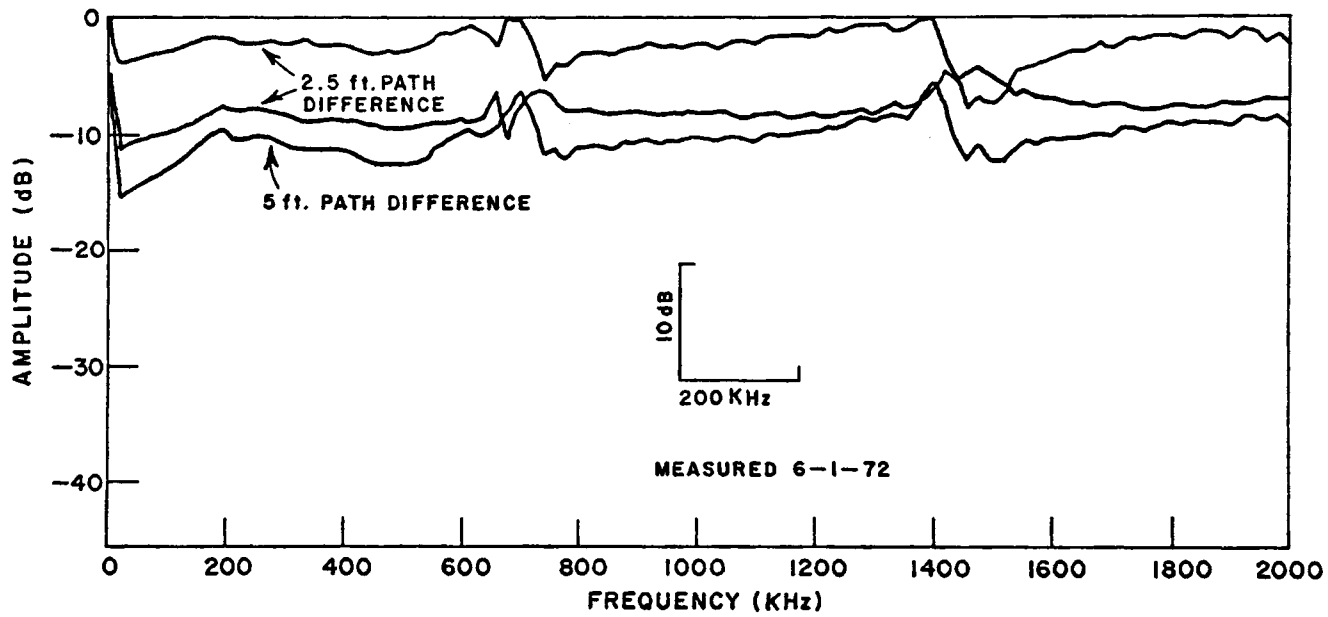


Fig. 59. Attenuation vs frequency for 2-5 ft and 5 ft path differences (low frequency).

However in some cases it was observed that there was little or no increase in attenuation going from the 7.5 ft path to the 10 ft path while there was significant attenuation going from the 5 ft path to the 7.5 ft path. An example is the data of Figs. 60-62. Note the waveforms from the 7.5 ft and 10 ft paths are nearly the same amplitude in Fig. 60, and both are several dB below the transmission of the 5 ft path in spectral amplitude as shown in Fig. 61. Thus in Fig. 62 the change in attenuation going from the 7.5 ft to 10 ft path is much less than the change from the 5 ft to 7.5 ft path. Compare Fig. 60 with Fig. 54, a case in which the increase in attenuation is more nearly uniform. The occurrence of this anomalous attenuation effect is tabulated in Table III. Note that it appears predominantly as a low frequency effect. This is probably because the antennas are poorly matched at this low frequency band and any minor perturbations could significantly alter the measured data.

Another possible explanation of this effect is that at least part of the time the medium under investigation is in fact not homogeneous. A further possibility is illustrated in Fig. 63. Remembering that the buried antenna was implanted by digging a five foot deep trench and repacking the fill after placing the antenna on the bottom, the placement of the antennas relative to the trench is shown in the figure. It is known that no amount of care in refilling a trench of this sort will be sufficient to return it exactly to its original state, particularly over a span of less than a year. The disturbed soil of the trench may either collect or reject water relative to the surrounding soil and this effect is known to last for years. Thus the trench walls may form a boundary between two dissimilar media. The 7.5 ft path and 10 ft path pass through the walls of the trench. If this boundary condition is the predominant effect on propagation along these paths then they will exhibit more nearly equal attenuation relative to the 5 ft path which travels straight up the trench. The fact that the effect comes and goes may indicate that soil conditions were changing in or around the trench. Much more careful investigation is needed before this explanation can be confirmed. It should be noted that there were some anomalous effects which could not be explained by the aforementioned theory. Figure 64 shows a case where the low frequency transmission is almost the same for the 5 and 7.5 ft paths. No explanation can currently be offered for this result.

After these effects were studied the data were analyzed for any long term trends which could be detected. The attenuation path length vs frequency data were all converted to dB/ft. and plotted over suitable frequency scales: 1-25 MHz for the high frequency measurements and 20 KHz to 2 MHz for the lower frequency measurements. These data have been discussed in the body of this report. The later data with the short pulse were not used.

The lower frequency impedance data for the buried antenna taken with the Hewlett-Packard 214A were rather consistent. The impedance of the buried antenna as a function of frequency did not change significantly over the four months period of measurements. This would indicate that the ambient medium (soil at a depth of 5 ft) was not changing significantly. This was confirmed via the 2 ft. soil sample discussed earlier where the moisture content was almost equal the most moist case at a one foot depth.

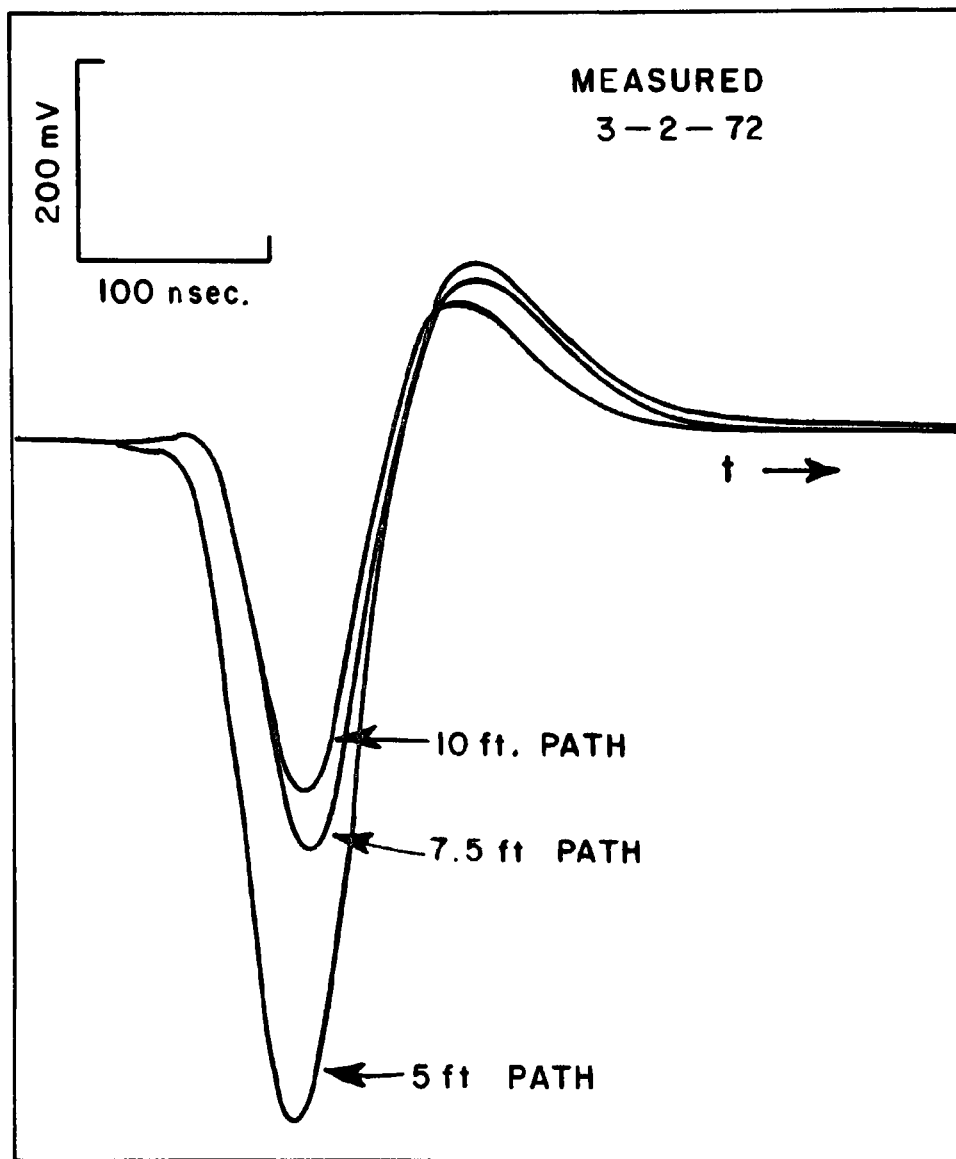


Fig. 60. Anomalous propagation (high frequency, time domain).

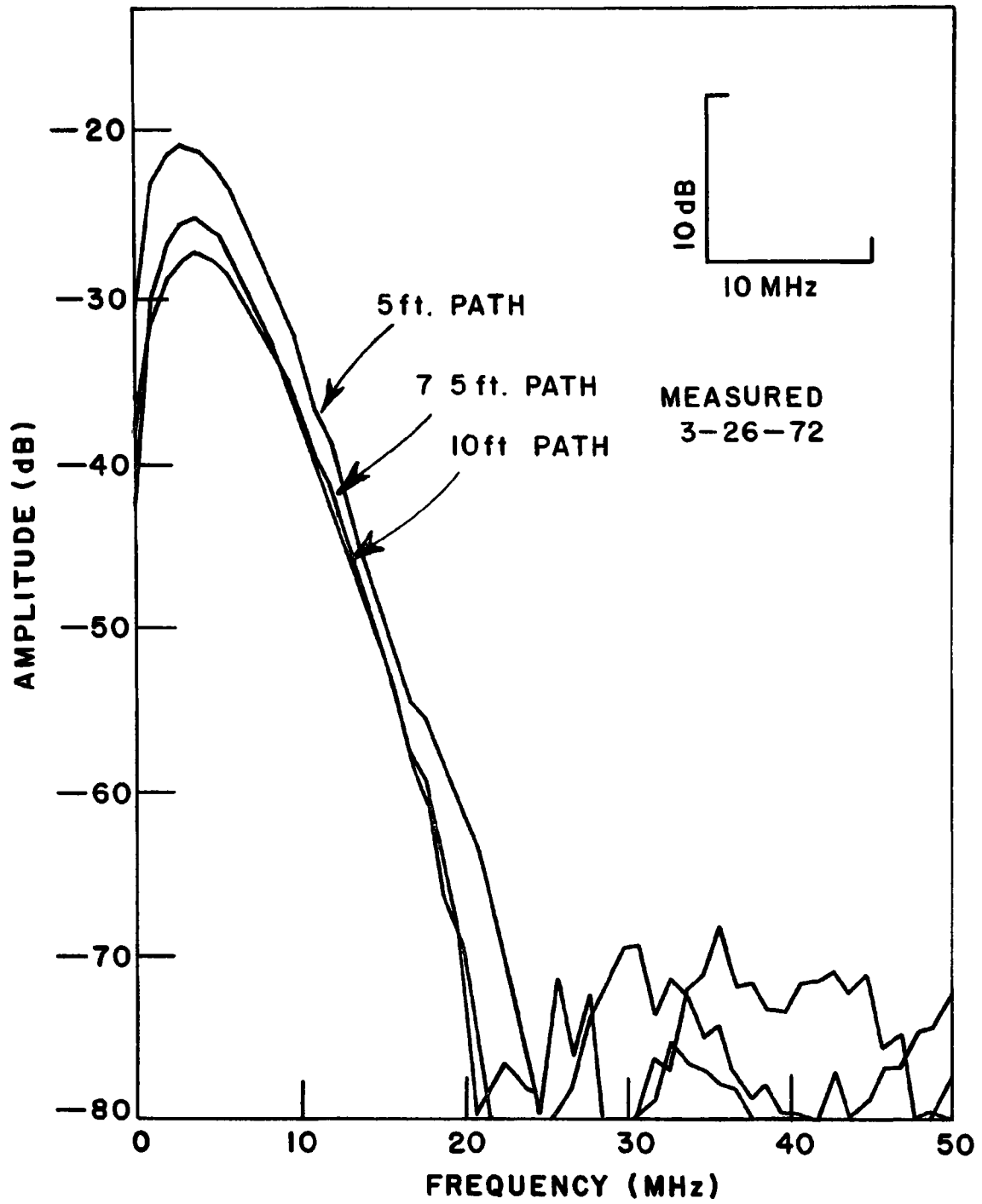


Fig. 61. Anomalous propagation (high frequency, frequency domain).

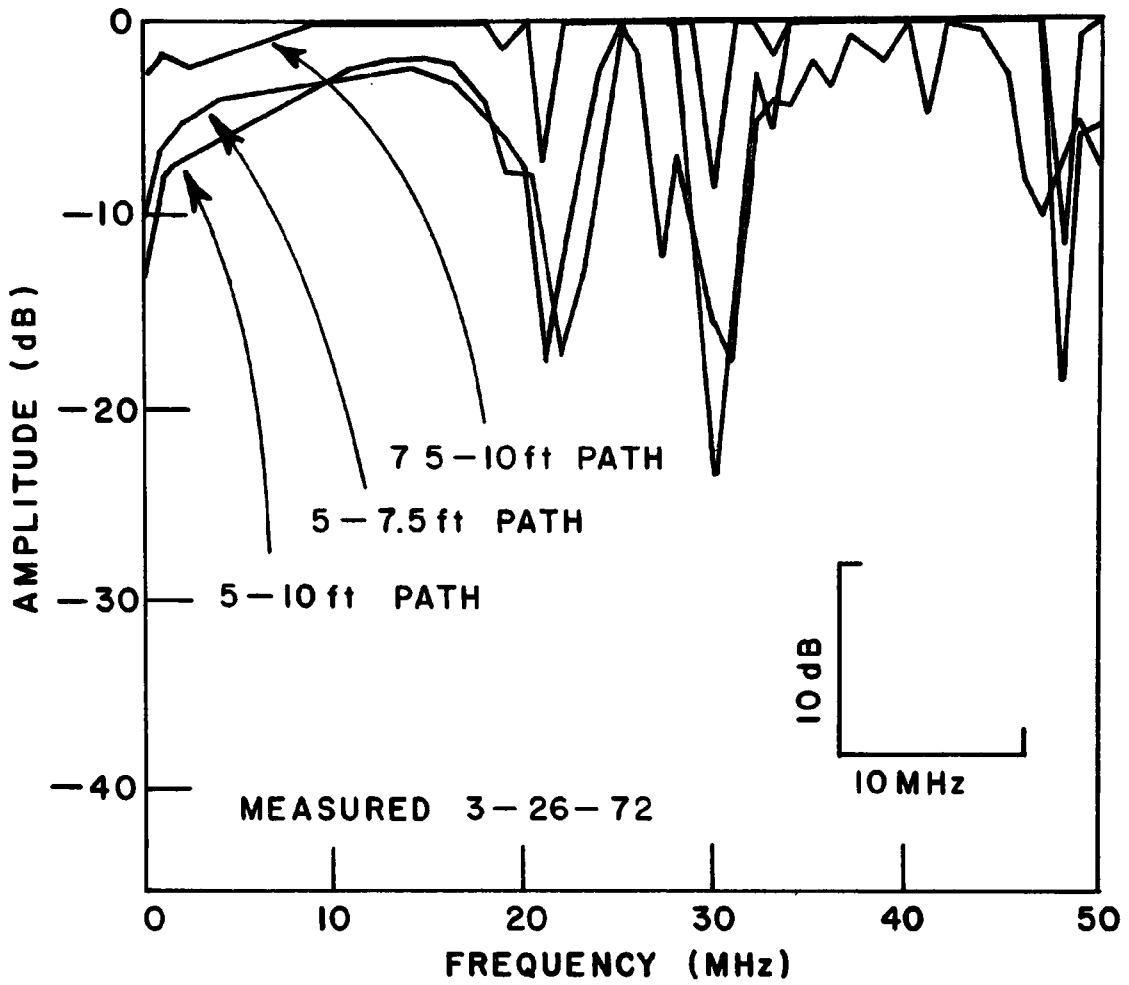


Fig. 62. Attenuation for 2.5 ft and 5 ft path differences (anomalous propagation).

TABLE III
Occurrence of Anomalous Propagation

Date	High Frequency	Low Frequency
11-12-71		
11-16-71		
11-17-71		x
11-23-71		x
12-11-71		
3-7 -72		
3-20-72		x
3-22-72		x
3-28-72	x	x
3-31-72		x
4-12-72		
4-20-72		
4-24-72		x
4-28-72		x
5-9 -72		x
5-12-72	x	
5-19-72		
5-22-72		
6-1 -72		x
6-6 -72		x

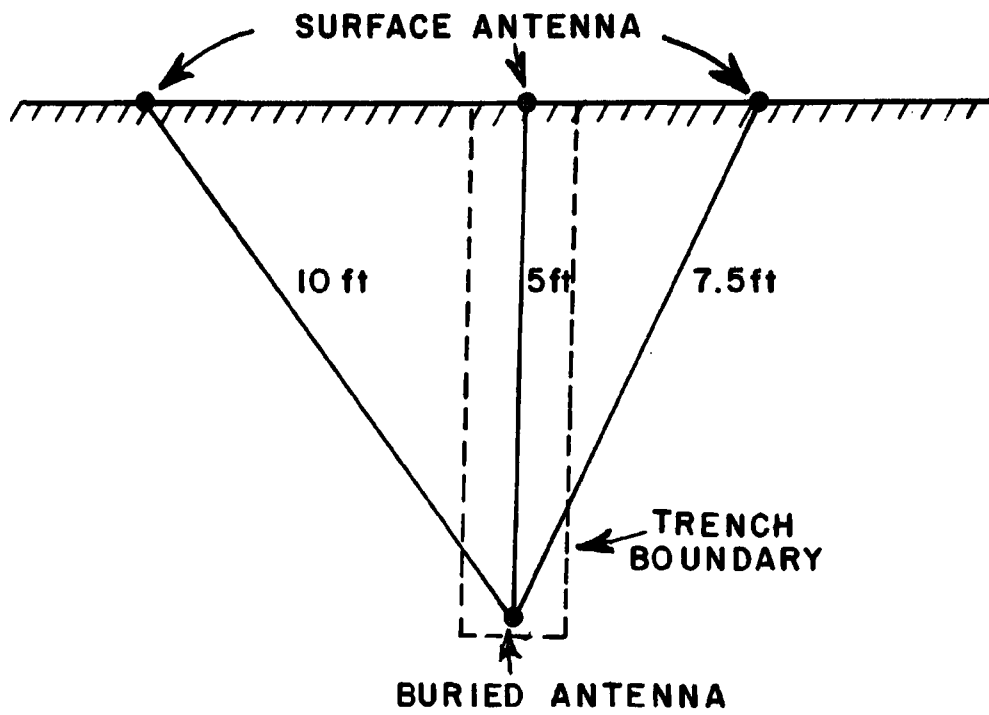


Fig. 63. Trench geometry.

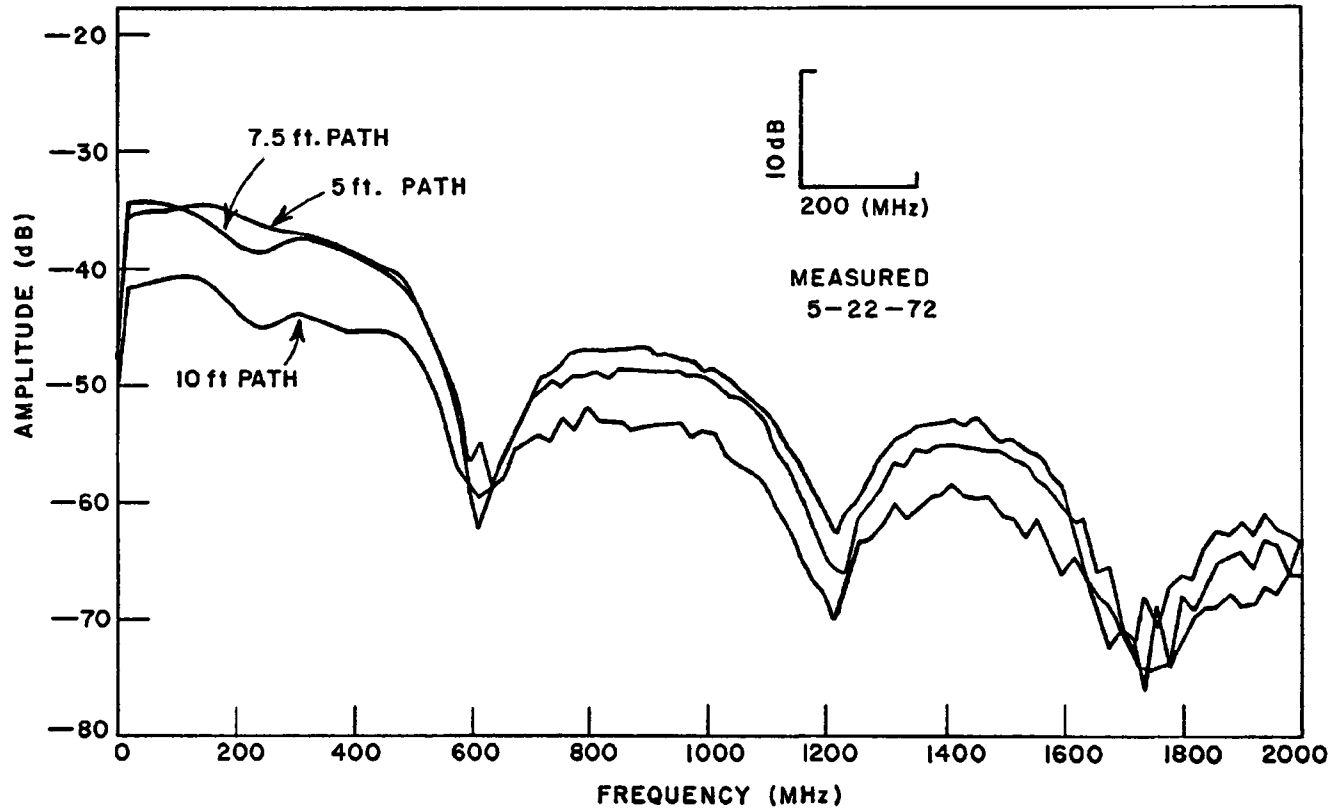


Fig. 64. Anomalous propagation not explained by trench effect.